An Investigation of the Cellular and Molecular Mechanisms of Stem Cell Regulation in Schmidtea mediterranea

BY

ELLEN ABOUKHATWA
LADY MARGARET HALL

Thesis submitted in partial fulfillment of the requirements for the degree of Master of Science by Research

University of Oxford
Department of Zoology

2015

OSS Student No. 617586

THIS THESIS IS DEDICATED TO MY BELOVED FAMILY AND FRIENDS

‘Never doubt that a small group of thoughtful, committed citizens can change the world; indeed, it’s the only thing that ever has’ – Margaret Mead

“I like the cold weather. It means you get work done’ – Noam Chomsky

Table of Contents

Acknowledgements

I would like to thank Aziz for taking me on as a graduate student and, for his support and critical insight over the last years. I am extremely grateful to all the other members of the Aboobaker lab, Damian, Belen, Natasha, Sujai and Nobu for their collaboration, friendship, and for the many hours of enlightening scientific conversation. I would like to give a special thanks to lab member Yuliana who has made a selfless and considerable commitment to my training.

I would like to thank Mark Hill and James Thompson from the Gray Institute for Radiation Oncology for all their help and expertise in designing the shield, and for their continued support and facilitation over the past years. I must also thank Tony and John in the Zoology workshop for making the shield and for always being available to have impromptu discussions about projects.

I am also thankful for the friendship and support of many zoology researchers including Suzie Ford, Michelle Taylor, Crystal Vincent, Tom Hart, Amr Aswaad, Catherine Head, Jesse Van Der Grient, Anni Djurhuus, Vanessa Lovenburg, Philip Boersch – Supan, Nicolai Roterman and Caitlin Black.

I would like to thank Professor Peter Holland for his belief in me, and for his pastoral support during my time at Oxford.

Finally this work would not have been possible without the generous financial support from the Elizabeth Jenkinson Fund, the Warr Goodman Scholarship and The Department of Zoology at The University of Oxford.

Declaration

I hereby declare that the work presented in this thesis was conducted by myself under the supervision of Dr. Aziz Aboobaker, with the exception of those instances where the contribution of others has been specifically acknowledged. I have clearly indicated the presence of all material and information I have quoted, paraphrased or referenced from other sources, including any diagrams, charts, tables or graphs.

Ellen Nadia Aboukhatwa

OSS Student No. 617586

2015

Abstract

The planarian *Schmidtea mediterranea* discovered by Benazzi, Baguñà, Ballester, Puccinelli & Del Papa, 1975 is a classic model organism for the investigation of regenerative processes. The source of new tissues is a population of proliferative cells called 'neoblasts'. The level of heterogeneity among this population of cells is unknown. However at least a proportion of neoblasts are pluripotent stem cells, and these are sometimes referred to as clonogenic neoblasts (cNeoblasts). Although the *Schmidtea mediterranea* genome has been sequenced, and RNAi techniques are well established, our knowledge of the molecular regulators of neoblast behaviours such as migration *in-vivo* remain limited.

This thesis presents an assay for tracking spatio-temporal processes such as stem cell migration and division. Data presented herein supports the assays potential as an adjunct method for functional testing of molecular regulators of stem cell biology. Moreover this thesis demonstrates the effect of various gene knockdowns on cell migration *in vivo*. The matrix metalloprotease MTMMPA has been shown herein to inhibit stem cell and progeny migration. Conversely the serine threonine kinase and tumor suppressor SMG-1 has been shown to positively effect cell migration and regeneration time frames.

This ‘over activity’ in SMG RNAi has also been demonstrated to ultimately result in the formation of ectopic growths, analogous with tumor masses seen in cancer.

The characterisation of the Methyl-CpG-binding domain protein MBD 2/3 has been expanded upon to include a migration effect. MBD 2/3 RNAi animals exposed to shielded irradiation fail to regenerate as previously published by Jaber 2014[1] and through the use of Fluorescent Insitu Hybridisation (FISH) visualisation we can confirm that this phenotype is in part attributable to cell migration failure.

This body of work also demonstrates the ability of the developed assay to uncover otherwise undetectable phenotypes. Knockdown of the well-known cancer implicated zinc finger protein SNAIL has previously failed to give rise to regeneration defects in planarians. However in the shielded irradiation paradigm SNAIL RNAi does result in a lethal regenerate defect. SNAIL RNAi animals are able to maintain their stem cell and progeny populations, suggesting SNAIL does not have a role in cell maintenance and differentiation. However, investigations using a Fluorescent *In situ* Hybridisation technique (FISH) show that the cells of SNAIL RNAi animals fail to migrate, supporting the broadly proposed role for SNAIL in the promotion of cell migration.

Four additional genes selected using the Oncomine web-based microarray database have been identified as having a role in planarian biological processes. Knockdown of gene UDP-N-acteylglucosamine pyrophosphorylase 1 (UAP1) caused homeostatic animals to regress their heads. Further investigations using FISH to visualise underlying cell behaviours is required, however head regression is associated with stem cell defect in the planarian model[2].

Knockdown of ribosomal biogenesis protein (WDR12), thyroid hormone receptor interactor 13 (TRIP13) and Bystin (BYSL) resulted in regeneration defects. To the best of our knowledge these genes have never before been investigated in planarians. The phenotypes, all characterised by a failure of animals to regrow a head, were only observable in shielded irradiation experiments. Detailed characterisation of the underlying cellular and molecular mechanisms of these defects is required. However the observations presented herein are adequate to propose that the assay developed has significant potential as a novel technique for the planarian community to investigate important cell behaviours, particularly cell migration, which has a key role in disease, specifically cancer metastasis.

List of Figures

List of Tables

1. An Introduction to Planarian Regeneration

1.1 Planarian Phylogeny and Anatomy

Planarians are soft bodied, unsegmented flatworm acoelomates of the order Tricladida (possessing a gut of three major branches), within the phylum Platyhelminthes, a group within the protostome super phylum Lophotrochozoa[3, 4]. (Figure 1.1).

Figure 1.1 Live brightfield images of five planarian species
Courtesy of Katerina Jonhson, unpublished are images of various planarian species from left to right *Dugesia benazzi, Dugesia tigrina, Polycelis tenuis, Polycelis felina* and *Schmidtea mediterranea*. Scale bar represents 100µm and images were acquired using Zeiss Discovery V8 (Carl Zeiss) and recorded using AxioCam software. Scale bar represents 1mm.

They are widely distributed ecologically, and can be found in marine, freshwater and terrestrial environments[5, 6]. As triploblastic bilaterians, planarians have tissues derived from ectoderm, mesoderm and endoderm. Together these tissues give rise to a nervous system comprised of a cephalic ganglion (CG) (bi-lobed brain) and two ventral nerves cords (VNC's) that run longitudinally [7, 8] (Figure 1.2). Transverse

neuronal fibres that run the length of the animal connect the VNCs [7, 8]. Planarians also have a variety of sensory receptors for detecting light (photoreceptors), chemical (chemoreceptors) and pressure changes (mechanoreceptors) [9, 10]. A centrally located pharynx is used for both feeding and waste expulsion from a blind gut with three major branches, two posterior and one anterior, excretory organs and osmoregulation are facilitated by a network of ciliated organs called protonephridia [11-13](Figure 1.2, G). Ventral and dorsal motile cilia aid gross locomotion (Figure 1.2, G), while a combination of longitudinal and circular muscles aid turning and obstacle avoidance [14-16]. For those animals which are asexual, reproduction occurs via fission. Sexual strains are cross-fertilizing hermaphrodites. These animals have paired ovaries and testes that are accessible through a ventrally located gonadophore[11].

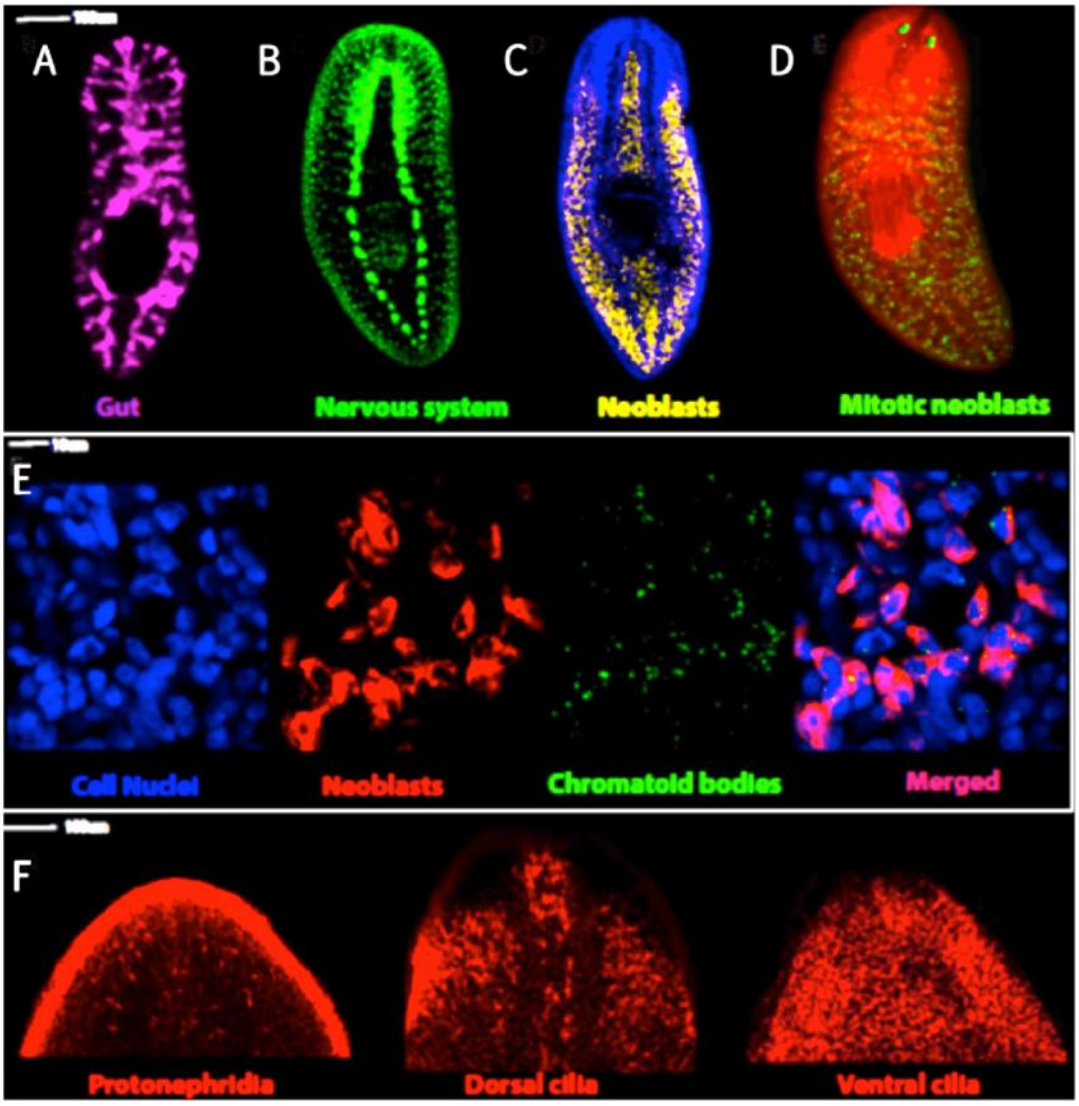

Figure 1.2 A Panel of FISH and Immuno images showing key planarian structures and cell populations.

A) Live imaging of planarian gut structures in purple showing primary, secondary, tertiary anterior and posterior branches using acetyl-pentafluorobenzene sulphonyl fluorescein (which is converted to its fluorescent form when exposed to H_2O_2) **B.** Monoclonal anti -3C11 antibody in green shows the nervous system structures cephalic ganglia, ventral nerve cords and transverse fibres **C.** RNA probe for neoblast marker *histone 2b (h2b)* in yellow, nuclear stain DAPI in blue **D.** Monoclonal anti-H3P antibody labels mitotic cells in green against red autoflourescence. The antibody recognises Histone H3 when phosphorylated at Serine 10 during mitosis **E.** Genes required for neoblast maintenance are often associated with chromatoid bodies. Cells are stained with anti-tudor antibody labelling the perinuclear CB structures of neoblasts in green and neoblasts are also labelled in red by marker *h2b* **F.** Courtesy of Yuliana Mihaylova, unpublished, is Anti- a tubulin in red. The antibody recognizes acetylated

tubulin and labels planarian protonephridia cilia as well as dorsal and ventral cilia. Scale bars represent 100um for A-E and 10um for F.

1.2 An Introduction to Regeneration

Historically, freshwater triclads have been of particular interest to biologists because of their ability to regenerate any missing tissue after injury[17]. Regeneration in planarians begins with rapid closing of a wounded surface, achieved by the protective spreading of existing epithelial cells [18]. The early stages of regeneration involve two peaks in stem cell proliferation. The first peak occurs globally throughout the whole organism 6 hours after wounding, and the second more localised to the wound site between 48 and 72 hours. During these early stages of regeneration (within 24hrs) an unpigmented structure known as the regenerative blastema is formed at the wound site [19, 20] (Figure 1.3). Planarian stem cells, called neoblasts, are a group of undifferentiated adult somatic stem cells that are distributed throughout the animal's mesenchyme (Figure 1.2). As the only mitotic cells within the planarians they are widely considered to be the sole source of all new tissues produced during regeneration [21, 22](Figure 1.4 & 1.5). It is the post-mitotic progeny of these stem cells that migrate to form the blastema, where they subsequently differentiate into missing distal tissue types [19-22] (Figure 1.4 & 1.5).

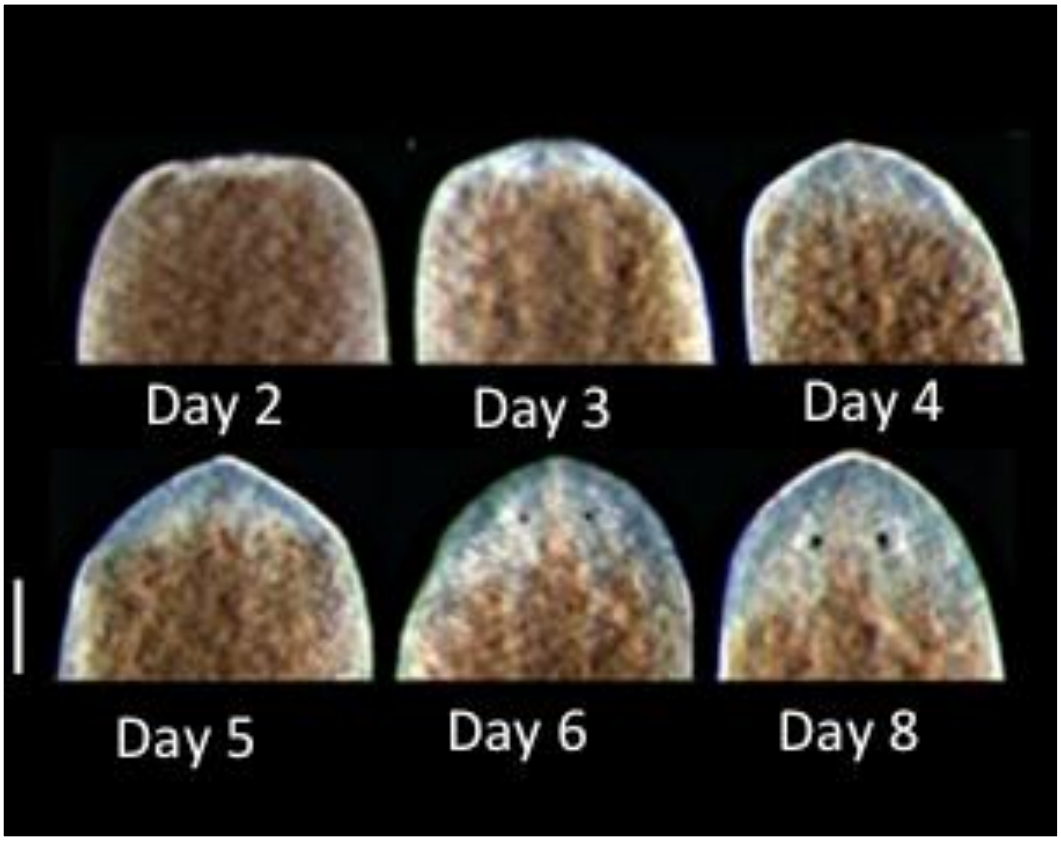

Figure 1.3. Live brightfield images of anterior regeneration

Live bright field images show the time course of anterior regeneration in *Schmidtea mediterranea*. Wound closing and the first mitotic peak of stem cells is proceeded by the formation of an unpigmented regenerative blastema and a second localised mitotic peak at approximately 3 days. Over the subsequent days, stem cells give rise to post mitotic progeny, which move into the blastema, and give rise to all necessary tissue types. By day 8 the bi-lobed brain and photoreceptor (eyes) are fully regenerated. Image was acquired using Zeiss Discovery V8 (Carl Zeiss). Scale bars represent 100µm and the image is **modified from Solana *et al.*, 2012**

However, planarians do not complete the regeneration process solely by new tissue production. Fragments of animals are able to regenerate in full due to the accompanying remodelling and rescaling

of pre-existing tissues in a process traditionally referred to as morphallaxis [15].

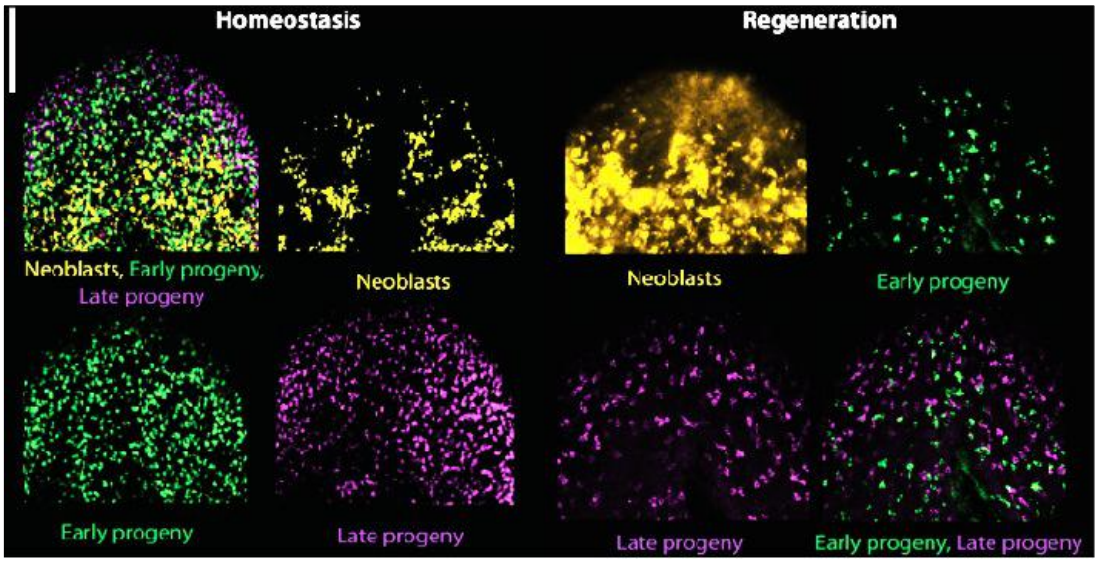

Figure 1.4. FISH images showing stem cell and progeny distribution during anterior regeneration
Triple FISH *h2b+, NB21.11.e and AGAT-1* distribution during homeostasis **D.** Courtesy of Yuliana Mihaylova, unpublished single FISH (yellow) showing *h2b+* accumulation at post-blastema region in a 5-day regenerate. Double FISH shows *NB21.11.e+* cells (green) and AGAT-1 (purple) distribution, within the blastema proper at day 5 of regeneration. Scale bars represent 100**µ**m.

1.3 Neoblasts

Neoblasts are small cells with large cytoplasmic peri-nuclear ribonucleoprotein (RNP) granules called chromatoid bodies. These are both morphologically and biochemically likely to be similar to germline granules, germplasm or nuage seen in other animals [21-23] (Figure 1.5). They divide, giving rise to post-mitotic progenitor cells that differentiate in order to become any required cell types during normal

homeostasis or regeneration. They also have an indefinite capacity to self-renew, in order to maintain a basal population of pluripotent stem cells and at least some individual cells are known to be pluripotent, as shown by experiments in which a single neoblast transplant was able to rescue a lethally irradiated host [24]. Neoblasts are also acutely sensitive to irradiation, and doses over 30Gy ablate all cycling cells within 24 hours of exposure [25, 26]. It is possible to determine if genes are expressed in neoblasts by observing if their expression patterns persist after irradiation exposure using RNA-seq and *in situ* hybridization techniques [25]. Recent research compared the global gene expression profiles of animals post i) irradiation and ii) genetic ablation of neoblasts (RNAi) [27]. RNAi of the gene Histone 2B, when cross referenced with irradiation data, allowed noise reduction in both data sets and improved efforts to identify neoblast enriched genes [27]. The results suggested the caveat that whole organism irradiation causes many expression changes not related to the neoblast population.

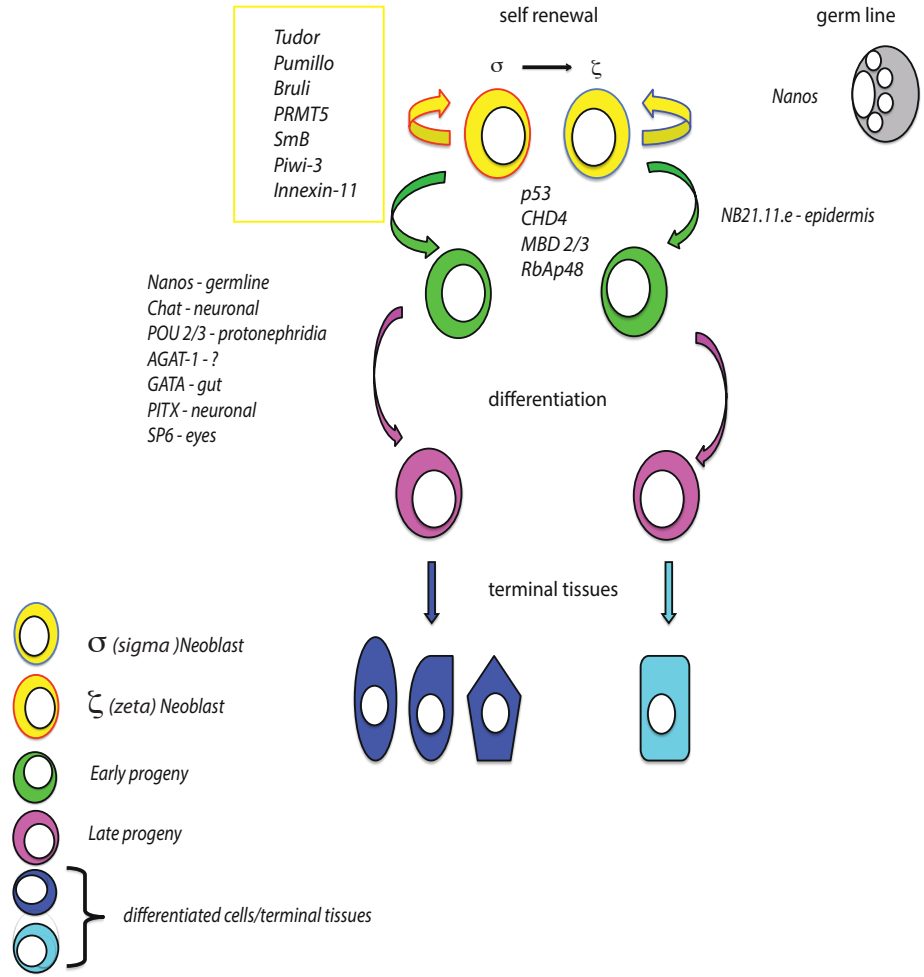

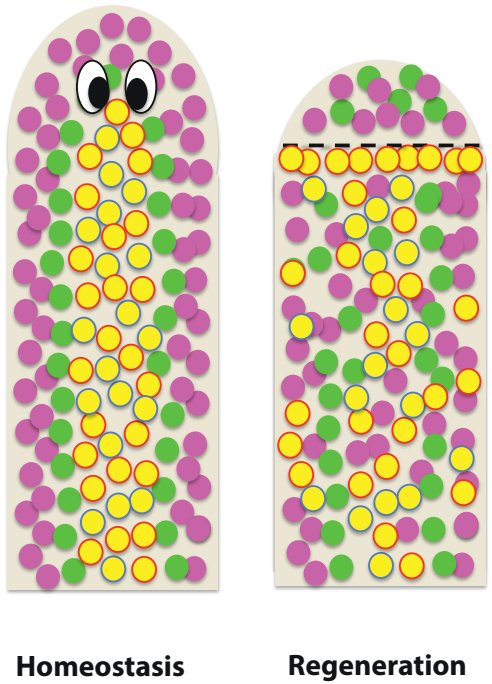

Figure 1.5 overleaf

Figure 1.5 Schematic overview of gene functions in stem cell renewal and progeny production

A. An overview of selected genes required for the maintenance/self-renewal and differentiation of 2 discrete neoblast populations (s and z). Boxed in orange are several genes known to be necessary for neoblast maintenance. *Nanos* is required for formation of the germline. *p53*, *CHD4*, *MBD 2/3* and *RbAp48* are not initially required for stem cell maintenance, but are necessary for the proper production of progeny and ultimately for production of new differentiated tissues as required during regeneration and homeostasis. All these genes are expressed in neoblasts and p53 is also expressed in early post mitotic progeny. Boxed in green are selections of genes, which are used as markers of different progenitors types. Each is associated with a specific lineage choice/tissue fate, except the category marker *AGAT-1* which labels a transitioning progenitor cell based on their expression dynamics after irradiation but are of unknown lineage **B.** Cartoon representation of neoblasts in yellow (*h2b+)*, with their subpopulation (s and z) illustrated with a red and blue outline respectively. Early progenitors in green (*NB21.11.e+)* and late progenitors in purple (*AGAT-1+)* are shown to have different spatial distributions during homeostasis and regeneration. The *h2b+* cells are located within the mesenchyme with *NB21.11.e+* cells radiating more peripherally*,* and *AGAT-1+* cells expressing the most peripheral expression*.* During regeneration the normally distinct spatial compartments o*f h2b+, NB21.11.e+* and *AGAT-1+* as seen in homeostasis, break down . Consequently these cells types are seen to share spatial regions. Mitotic s *h2b+* accumulate at the post blastema region, with post mitotic *NB21.11.e+* and *AGAT-1+* cells located with the blastema proper.

An alternative method of neoblast gene enrichment is fluorescence assisted cell sorting [28]. In this scenario cells are sorted in order to give rise to three populations including proliferating cells (X1), cells with large nuclei relative to cytoplasm (X2), and differentiated cells which are irradiation insensitive (Xins) [28]. A recent study using this method provided insight into neoblast pluripotency mechanisms [29]. Onal *et al. 2012* analysed the neoblast enriched (X1) fraction and were able to identify a large number of genes that regulate embryonic stem cells (ESCs) and germline pluripotency in mammals. The homologs in their data set included i) 4 major chromatin-modifying complexes shown to be essential in mammalian stem cell regulation and 107 other putative chromatin regulators ii) 67 epigenetic regulators known to be highly expressed in the ESCS of mice, a list which overlapped somewhat with genes found in the previous set and iii) 40 RNA binding proteins that are homologous with germ granule components associated with germline pluripotency across metazoans. The take home message of this and other neoblast enrichment studies has been to confirm that the genetic determinant of pluripotency may well be deeply conserved across phyla [27, 30].

1.4 Population Heterogeneity

As the only cells able to give rise to new tissues, the total irradiation of all constituent neoblasts is lethal for planarians [31]. However, animals can be rescued by a receiving a transplant of just one healthy neoblast [24]. These experiments demonstrate that at least some neoblasts are *bona fide* pluripotent, able to generate progeny that in turn can replace all damaged tissues. These neoblasts have been called clonogenic neoblasts (cNeoblasts) [24]. However in other animals there is often heterogeneity among stem cell populations, with some populations of stem cells being lineage restricted [21, 22, 31]. In planarians, although the existence of cNeoblasts has been established, the extent to which they represent the general neoblast population is unknown, and it is possible that subpopulations of multi potent neoblasts are also involved in planarian homeostatic turnover and regeneration. Although the proposition of heterogeneity has been considered, the lack of evidence and markers to support cell – cell differences has resulted in them historically being considered a uniform population [21-23]. However, recent work has shown that some differentiated tissue marker genes are also expressed in both post-mitotic progenitors and sub populations of cycling neoblasts, providing

preliminary evidence that there are subpopulations of cycling cells with potentially restricted fate [13, 32, 33] (Figure 1.4 and 1.6)

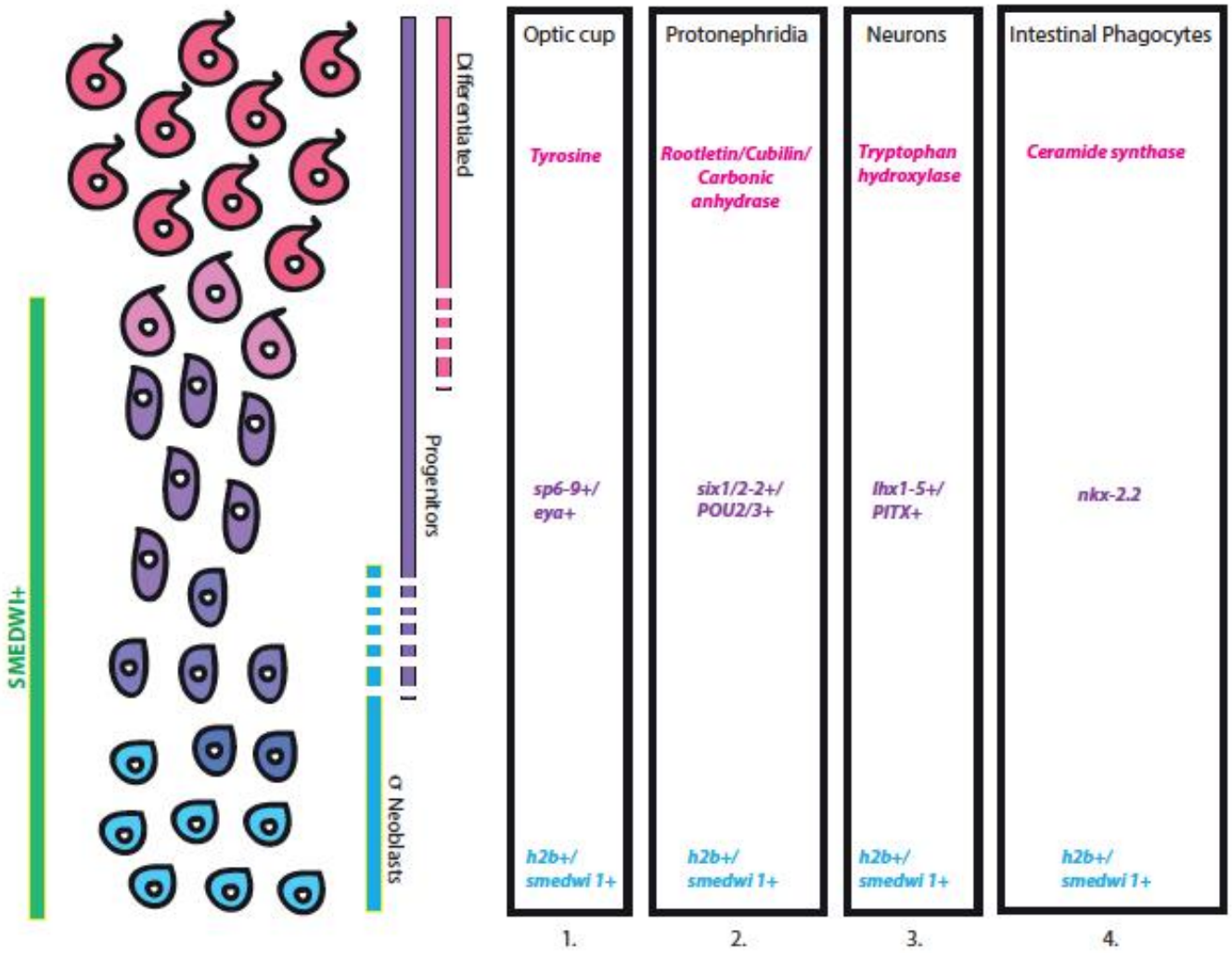

Figure 1.6: overleaf

Figure 1.6 Diagram showing the dynamics of lineage restriction in planarian stem cells and progeny
Lines indicate cell types that express the adjacent gene, and the overlapping of lines represents co expression overlaps between cell types. Models propose that a large s neoblast population produce **1.** Optic cup **2.** Protonephridia **3.** Serotonergic progenitors, and **4.** Intestinal phagocytes, and that the production of these post-mitotic progeny are all specified from the cycling neoblast population (*H2b+ and smedwi+* mRNA). Different groups of neoblasts have been shown to co express either **1.** *h2b+/smedwi+* and *sp6-9+/eya+* (**optic cup progenitors**) **2.** *h2b+/smedwi+* and *six1/2-2+/POU2/3+* (**protonephridia progenitors**) **3.***h2b+/smedwi+* and *lhx1-5+/PITX* (**serotonergic progenitors**) **4.** *h2b+/smedwi+ and nkx 2.2* (**intestinal phagocyte progenitors***)*. Progenitors subsequently undergo changes in gene expression which include the loss of neoblast markers *h2b/smedwi-*, the retention of existing tissue specific expression and the additional expression of differentiated markers. SMEDWI protein produced in neoblasts, but persistent in progenitors has also been used to show lineage related differentiation **1.** Optic cup progenitors that are *h2b-/smedwi-* retain *sp6-9+/eya+* expression and additionally express *tyrosine+* as they are incorporated into the eye. **2.** Protonephridia progenitors that become *h2b-/smedwi-* remain *six1/2-2+* (tubule associated cell fate) or *POU2/3+* (tubule cell fate) and additionally express *carbonic anhydrase+ or rootletin/ cubilin+* respectively **3.** Serotonergic precursors that are *h2b-/smedwi-* retain *lhx1-5+/PITX* and co express differentiation marker *tryptophan hydroxylase+* once differentiated. **4.** Finally intestinal phagocytic precursors that are *h2b-/smedwi- retain nkx 2.2 expression, and co expresses the terminal marker, ceramide synthase.*

These observations provide evidence that there are subpopulations of cycling cells with potentially restricted fate (see Figure 2 and Figure 3). An extensive study of the expression profiles of nearly 100 different stem cell enriched genes in 1,000 neoblast stem cells suggested the existence of two major populations of neoblast cells [34]. One of these (zeta) is thought to give rise to a large post-mitotic lineage of cells giving rise to planarian epidermal cells. The second class (sigma) is required during regeneration to replace all other tissues and lineages and gives rise to the zeta class. Conveniently these two populations can be marked by expression of the genes z*fp-1* (zeta) and *sox-P2 (sigma)*. It is perhaps not surprising, given the anatomy of "flatworms" that the two major categories discovered by profiling would be those stem cells committed to becoming epidermis and those cells becoming everything else. Nonetheless single cell expression profiles also suggested further sub-divisions within the sigma class. For example an expression profile for a potential stem cell lineage for intestinal structures (gamma) was observed as a potential sub class within the sigma population. The markers of the gamma class, h*nf4*, *gata4/5/6*, and *nkx2.2*, have been implicated in controlling gut regeneration and homeostasis [35].

1.5 Gene Expression and Fate Specification

Currently our mechanistic understanding of how stem cells are regulated in planarians to produce different lineage progenitors is limited. It has been shown in other animals that temporal and spatial changes in gene expression can drive lineage choices. The first detailed analyses of planarian progenitor spatiotemporal dynamics began with the identification of several so called 'category marker genes' [25]. These marker genes are hypothesized to label transient progeny cells (early and late) produced by dividing stem cells.[25]. *Eisenhoffer at al.* hypothesised that genes down regulated by 24 hours were likely to be stem cell specific, whereas those down regulated over the subsequent 7 days could instead be associated with differentiating post-mitotic progeny. Early progeny were classed as category 2 cells and were marked by two novel genes NB.21.11e and NB.32.1g. And late progeny were classed as category 3 and markers included L- arginine glycine aminotransferase 1,2 and 3 (Agat -1,2 and 3), Mitochondrial carrier protein (MCP), and Cytochrome p450 1A1 (CYP1A1) among others [25] (Figure 1l4). Despite these markers being useful for understanding stem cell dynamics the terminal tissue type(s) to which cat 2 and cat 3 cells contribute ultimately remains for the most part unknown.

More recent findings have however identified several tissue specific progenitor markers (Figure 1.4 and 1.6) including those associated with optic cup and photoreceptors. Transcription factors (TFs) such as *SP6-9* have been used to show that progeny and cycling neoblasts begin expressing TF's required for photoreceptor regeneration before they i) terminally differentiate and ii) reach the anterior site of eye regeneration [32]; and the spatially distinct subset of stem cells appear to consistently be responsible for eye regeneration. Another set of Transcription factors including *POU2/3* and *Six 1/2 -2* are associated with the planarian excretory protonephridia system [13]. Both TF's are frequently co-expressed with the neoblast marker, *Histone H2b* in cells within the blastema. In the case of *POU2/3* it has been shown that these cycling cells will go on the form protonephdrial tubule cells [13]. A similar phenomenon, of stem cell commitment, determined by co-expression has been reported in relation to the production of serotonergic neurons using genes lhx1/5-1 and Pitx [33] and for gut with genes nKX-2.2 [35] (Figure 1.6).

Finally an ortholog of the gene *Nanos*, required for germ cell differentiation in *Drosophila*, has been identified in Planarians, as a presumptive germ precursor marker [36, 37]. Planarian neoblasts are interestingly able, as adult somatic stem cells, to produce replacement

germ line cells. Researchers showed that the gene *Nanos* is required for regeneration of both gonads and primordial germ cells. *Nanos* positive cells can also be detected in juveniles that lack developed reproductive structures, which have resulted in *Nanos* being considered a progeny marker for gonad and germ cell fated cells. [37].

1.6 Proliferative Control

Our understanding of the mechanisms that control neoblast and progenitor dynamics during regeneration is growing [21, 38, 39]. Genes implicated so far in the proliferation, self-renewal and differentiation of neoblasts are generally highly conserved, and often their function in planarians mirrors their role in the development of other animals [21, 22, 40] (Figure 1.4). It is worth mentioning that the field has focused on selecting candidate genes for investigation based on their conserved roles in other animals, which in part represents a bias toward the confirmation of conserved roles. In the case of neoblast proliferation, the process must be tightly regulated to prevent uncontrolled growth [41-43]. The knockdown of two orthologs of the conserved tumour suppressor, PTEN, results in hyper proliferation [42]. This is proposed to occur through an interaction with TOR signalling that is well characterised across many phyla [43, 44]. However, a more recent example of a proliferation phenotype in planarians is SMG-1, a

member of the PIKK family of kinases, which was found to have a regulatory role in neoblast proliferation [41]. SMG-1 is shown to have multiple functions in other species. It is associated primarily with genome surveillance and is activated in response to DNA damage and oxidative stress [45, 46]. Its knockdown in planarians leads to hyper proliferation, hypertrophy and hyperplasia. Post-mitotic cells accumulate ectopically forming outgrowths and basement membrane disruptions. A novel interaction between SMG-1 and mTOR signalling was suggested by [41] and supported by i) the partial rescue of SMG-1 animals with the pharmacological mTORC1 inhibitor Rapamycin and ii) the concomitant knockdown of TOR in SMG-1 (RNAi) animals. In both cases the SMG-1 associated hyper proliferation was dampened. This research has been the first to suggest an interaction between the two kinases in stem cell proliferation regulation.

1.7 RNA Processing and Chromatin Remodelling

During regeneration and homeostasis, planarian neoblasts must maintain a balance between self-renewal and a-symmetric division, which results in the production of differentiated progenitors [21-23, 25, 31] (Figure 1.3). Interestingly, during starvation planarians are able to de-grow and thereby reducing size while maintaining regenerative capacity

[47]. Research investigating how this is regulated on a cellular level showed that de-growth was achieved by a reduction in absolute cell number (not size) [47] and that normal basal mitotic rates were accompanied by a reduction in asymmetric division.

Related research has collectively identified two potential regulatory hubs. Self-renewal (symmetric division) has been linked to RNA metabolism in peri-nuclear chromatoid bodies (CB's) [21, 27, 48-52] and differentiation (a-symmetric division) with the nucleosome remodelling deacetylase (NuRD) complex [53-55].

CB's are morphologically similar to granule structures seen in the germ line of other species and are rich in RNA binding proteins (RNP) [21, 52, 56] (Figure 1.5). Several RNPs have been shown in planarians to have RNAi phenotypes that impair regeneration through effects on neoblast maintenance. The PIWI-class of proteins has been broadly implicated in the regulation of germ cells through a production of piRNAs that in turn repress transposable elements in the germ line. Planarian orthologs of the PIWI/Argonaute family smedwi-1, 2 and 3 are expressed in neoblasts with a suggested association to CBs [50, 51]. RNAi knockdown of smedwi-2 results in a decrease in piRNAs, a failure of progenitor cells to properly differentiate, and a reduction in the overall number of neoblasts [50, 51]. In other species the best understood

role of piRNAs is to repress transposable elements suggesting that the failure in neoblast maintenance may be the result of transposon initiated mutagenesis [50, 51].

An ortholog of protein arginine methyltransferase PRMT5, an enzyme responsible for symmetrical dimethyl arginine functional modifications (sDMA) to RNPs; was very recently identified in planarians [57]. Knockdown of PRMT5 showed a decrease in functional smedwi3 and a concomitant increase in transposon transcripts [57]. The result was an overall reduction in the number of CB's and a failure of animals to maintain a neoblast population. A similar effect is seen when the BRUNO homolog, smed-bruli is abrogated using RNAi. In *Drosophila* BRUNO represses RNA helicases with an inhibitory effect on germ plasm assembly [58]. In neoblasts Bruli RNAi animals are able to mount a proliferative response to wounding, form an early blastema, and are also capable of producing progeny cells [49]. However, despite the ability to divide and differentiate, the overall numbers of neoblasts decrease over time; suggesting that smed-bruli is essential for neoblast maintenance. LSm (like-Sm), another RNP is known to be involved in the i) splicing of pre-mRNA and ii) the degradative decapping of mRNA [48, 59]. A planarian ortholog, Smed-SmB is expressed in both neoblasts and neurons, and its knockdown results in a

reduction in the number of dividing cells, the disorganization of CBs structural integrity, and a reduction in the mature spliced version of CyclinB, and an increase in the unspliced transcript version. This has lead researchers to suggest that Smed-SmBs role in neoblast maintenance may be associated with its conserved transcript splicing processes in the species.

The PUF family of RNA-binding proteins, including Pumillo, are required for germ-line and stem cell renewal in various species.[60] Although the mechanisms by which this occurs are largely uncharacterized, it has been suggested that they interact with different proteins to i) repress translation or ii) enhance the degradation of target mRNAs [60, 61]. The planarian DjPum is necessary for regeneration, and its knockdown results in a failure to develop a regenerative blastema, a decrease in stem cell proliferation and a reduction in the number of stem cells [61]. The Tudor domain containing Spoltud-1 gene is expressed in neoblasts, germ line cells, the central nervous system, and also during embryonic development [62]. Believed to be enriched in planarian CBs, Spoltud-1 RNAi results in animals losing the ability to regenerate by week 7 post-knockdowns. The latency of effect seen in Spoltud-1 (RNAi) animals may be associated with a slow rate of clearance from the cell of genes protein product [62, 63].

Decisions of differentiation and lineage fate in stem cells and their progeny are linked to transcription factor activation, and chromatin structure remodelling, which in turn regulates the extent to which a given gene is accessible for transcription [64-66]. A family of transcription factors, including p6, p73 and p53, have known functions as tumour suppressors, but are also involved in processes of cell proliferation and stem cell renewal [40]. *Smed-p53* is the only member of the family present in planarians. It is expressed predominantly in sub-epithelial post-mitotic progeny, but also found in mesenchymal neoblasts [40]. The knockdown of *Smed-p53* results in an initial expansion of neoblasts, a reduction in differentiating progenitor cells, and as the phenotype progresses, a depletion of stem cells leading to the conclusion that it is necessary for lineage specification and differentiation in planarians[40].

The NuRD complex is required for epigenetic control of cell fate, and several genes associated with NuRD have been identified as having a role in controlling the differentiation of stem cells [66]. NuRD complex remodelling usually results in transcriptional repression. The planarian ortholog of Mi-2, *Smed-CHD4*, is necessary for neoblasts to successfully produce differentiating progeny [55], and hence *Smed-CHD4* RNAi animals fail to regenerate despite neoblast numbers remaining

steady relative to homeostatic controls. However when researchers analysed the 'progeny enriched' FACS compartment (X2) they found a significant depletion of progeny number, leading to the proposal that *Smed-CHD4* is not required for neoblast maintenance, but it necessary progeny production [55].

The *Retinoblastoma-associated protein 48* (*RbAp48*) is a chromatin remodelling factor associated with several chromatin remodelling complexes, including NuRD and polycomb repressive complex 2 (PRC2) [67]. Planarian *RbAp48 (DjRbAp48)* regulates progeny differentiation through influencing chromatin architecture [53]. Without *DjRbAp48*, neoblasts continue to proliferate and accumulate at the wound site, but there is an absence of differentiated cells. A final member of the NuRD complex, and the only one exclusively associated with NuRD is the protein Methyl-CpG Binding Domain (MBD) protein, *Smed-MBD2/3.* Expressed in neoblasts, *Smed-MBD2/3* like *Smed-CHD4* and *DjRbAp48,* does not affect stem cell maintenance, but instead is necessary for the differentiation of progenitor cells [54]. *Smed-MBD2/3* is the first planarian gene to be associated specifically with the differentiation of late progeny, while markers of early progeny production remain unaffected. Interestingly, efforts by Jaber-Hijazi *et al.*[68] to find methylated DNA in planarians were unsuccessful, leading

to their suggestion that *Smed-MBD2/3* may function to epigenetically regulate stem cell differentiation by a method other than cytosine methylation. However a separate published work by Geyer *et al.* 2013[69] used, amongst other techniques, enzyme-linked immune absorbance assay (ELISA), and did propose that *Schmidtea mediterranea* genome contained methylated cytosines [69].

Resolving how these two potential stem cell regulatory hubs interact and identifying and detailing others will shed light on how much planarian stem cells have in common with both adult stem cells and germ line stem cells in other animals. One current hypothesis is that neoblasts may in fact have an evolutionary origin that was more recently germline than somatic [52].

1.8 Future Perspectives

Research using the planarian model system is still very much in its infancy compared to other model organisms. For the continued development of the system a robust method for systematic generation of transgenic animals is urgently required so that greater mechanistic detail can be acquired by direct experimentation. Key molecular details regarding exactly how stem cell self-renewal and differentiation are regulated remain almost entirely unknown and solving these problems

will require combining biochemical approaches with existing genetic and cell biological approaches.

1.9 Project Objectives

The work contained in this thesis was planned with the over arching objective of establishing a robust method for the high throughout screening (in vivo) of potential novel genetic regulators of cancers. Specifically our aim was to aid the cancer research community in the investigation of RNA-Seq data which is currently being harvested and stored in databases such as Oncomine. The community intends for these datasets to be analysed and for any genes with interesting expression profiles to isolated be investigated experimentally. We saw the planarian model as a potential opportunity for these investigations to be done in vivo cheaply, and quickly. Consequently we planned an approach which was 4 fold.

1. We aimed to develop an assay which would allow researchers to observe key cellular behaviours associated with cancer progression. We elected to develop a shielded irradiation assay which would allow among other things, for researchers to

observe cell motility – a key factor in cancer metastasis (Chapter 3).

2. Secondly we wanted to both establish robust controls for the migration assay and to demonstrate that the assay could clarify our understanding of complex RNAi phenotypes. Specifically we were interested is testing genes which were previously hypothesised to be migration related, but could not be tested due to the absence of an assay (Chapter 4).
3. Thirdly we wanted to test if the assay could unveil gene functions which were masked in typical RNAi experiments. In particular we hypothesised that the sheer abundance of stem cells throughout the animals body mass may mean that it was able to compensate for that lack of a genes function through redundancy. In this paradigm the knockdown of a gene may not affect processes normally measured such as regeneration. Conversely we hypothesised that the shielded irradiation assay, through the depletion of a large proportion of the animals stem cell population may result in a reduction of the animals ability to compensate for gene knockdowns, and as a result could unveil new phenotypes previously not observable (Chapter 5).

4. Finally we aimed to test the assays ability to handle large experiments where multiple gene knockdowns were simultaneously undertaken. The aim here was to demonstrate that the assay could be used for screening experiments. In particular we wanted to test the assays usefulness in analysing the biological function of those genes contained within RNA- seq datasets harvested from cancer patients. We were eager to select genes which were poorly/under investigated generally in order to test if the assay had the potential to aid researchers in identifying novel regulators of cancer processes such as metastasis (Chapter 6).

2. Materials and Methods

2.1 Planarian Culture

An asexual strain of *Schmidtea mediteranea* was used for all experiments. Animals were kept in a light safe (dark) environment at 20 °C. Animals were maintained in a milliQ ddH2O salt solution containing 1.6mM NaCl, 1.0mM $CaCl_2$, 1.0mM $MgSO_4$, 0.1mM $MgCl_2$, 0.1mM KCl, 1.2mM $NaHCO_3$.

Animals were fed organic veal liver 3 times per week for 3 to 6 hours and were cleaned after each feeding event. Animals were starved for 1 week prior to experiments, and were kept in 10µg/µl of Gentamicin throughout experiments to stave off possible infections.

2.2 Live Brightfield Imaging

For the purpose of phenotypic characterisation, live planarians were imaged using a Zeiss Discovery V8 and Axio Cam MRC.

2.3 Irradiation

Individual irradiation experiments used size-matched animals with identical feeding and culturing histories. Animals were immobilized by incubation in chilled 0.2% Chloretone (Sigma-Aldrich) as described in [70] and transferred to a 3mm petri dish and placed upon a custom lead shield device (Figure 2.1). Irradiation was delivered to animals at a dose of 30 Grays per 1 minute 18 seconds using 225 Kv and 17mA

of X-rays. Irradiation source was positioned below the specimens. For survival experiments, irradiated animals were maintained in 14 cm Petri dishes (20 worms/dish) in the dark; water and dishes changed every 48 hours. For dose distribution calculations Gafchromic EBT3 (Vertec Scientific) radiographic film was used, and scanned with the Epson Expression 10000XL using the optional transparency unit. Dose distribution was then calculated from the films, using the scanned pixel intensity.

2.4 *In situ* Hybridization

Fluorescent whole-mount *in situ* hybridizations (FISH) were performed and RNA probes prepared as described in [71]. For double and triple labelling, Peroxidase quenching was performed between labelings using 100mM sodium azide for 45 minutes.

2.5 Phylogenetic Analysis

Sequences for 3 unpublished members of the 'Snail gene superfamily' for 100 cancer-implicated, poorly characterised genes (Table 2.1. and 2.2.) were found by blasting protein sequences from different organisms to find planarian homologs in the consolidated *S. mediterranea* transcriptome (unpublished) and genome database

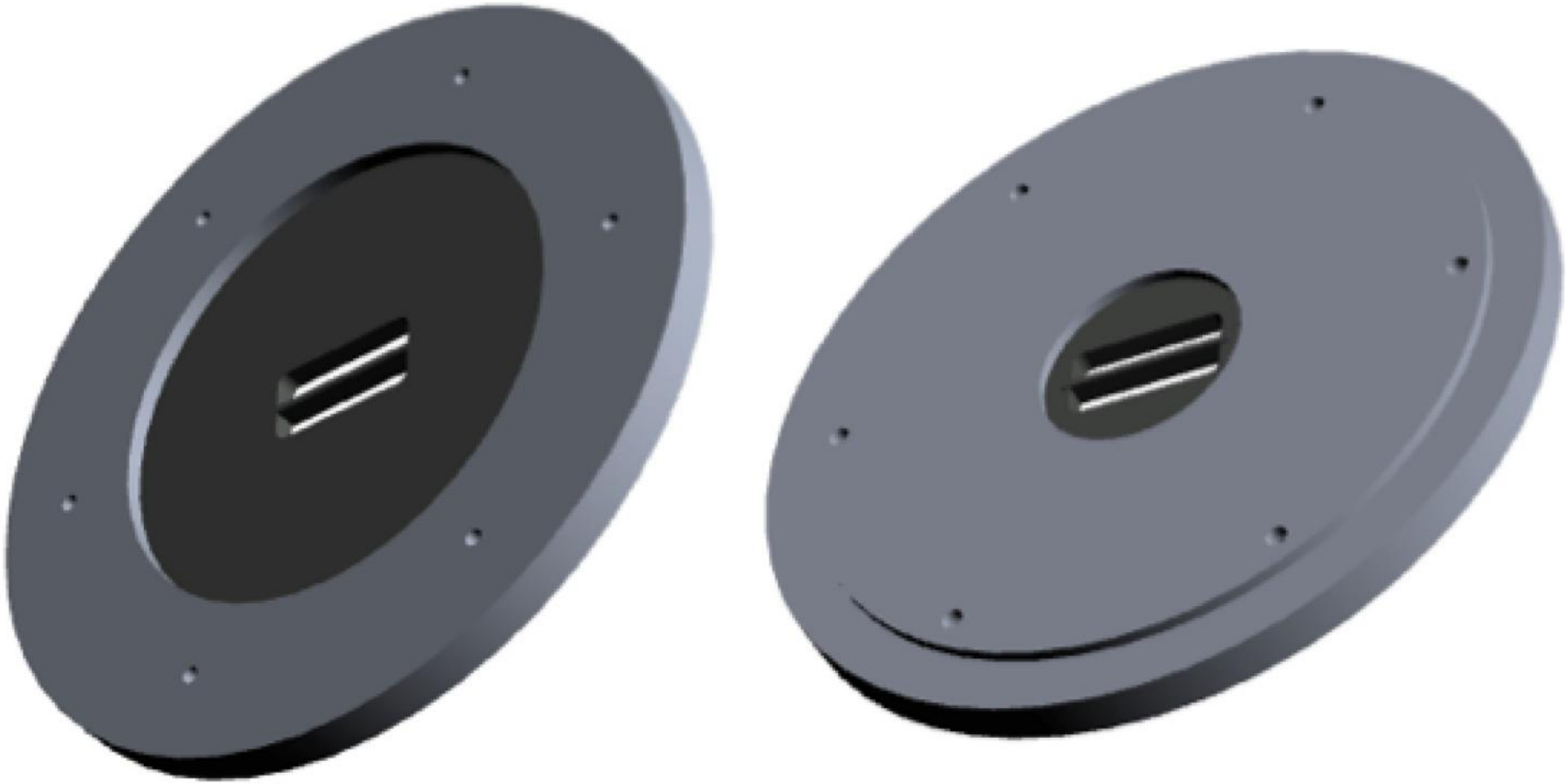

Figure 2.1. Computer aided design (CAD) image of bespoke shielded irradiation assay
A CAD representation of the proposed shielding assay design which shows on the left the underside of the shield which laid on top of the x ray source. The image to the right is the top side of the shield onto which the animals contained in a petri dish and anaesthetized are placed.

Planarian homologs were then used for reciprocal BLAST to verify homology. Conserved characteristic domains were extracted using ClustalW default settings [73]. Extracted planarian sequences were putatively named based on the outcome of their alignment with representative sequences from other species.

For Snail superfamily genes a neighbourhood-adjoining tree was generated using ClustalW default settings and 1,000 bootstrap replicates to support name selection and putative *Smed-SNAIL*, *Smed-SNAIL like* and *Smed-SCRATCH* sequences were identified.

For Oncomine generated candidates rooted neighbour-joining trees were generated in Geneious tree builder. The Jukes-Cantor model of sequence evolution was used and 1,000 bootstrap replicates to support name selection of *Smed-WDR12*, *Smed-TRIP13*, *Smed-BYSL* and *Smed-UAP1.*

2.6 Primers

Primers were designed in order to synthesize DsRNA for RNAi experiments and to produce RNA probes for *in situ* hybridisation experiments (Table 2.1.). Primers were designed using the following criteria: primer length 22 – 26 nucleotides, amplicon length between 300 to 900 base pairs. Melting temperature (50 to 60 °C) and GC content (40 to 60%) were checked using Oligo Calc: "Oligonucleotide

Properties Calculator" online. Primers from which DsRNA and probes were to be made directly from cDNA were designed with T7 universal linkers to mediate secondary PCR reactions.

Table 2.1. List of primers used to generate DsRNA and RNA probes

List of primers used to generate DsRNA, RNA probes and for gene cloning. The T7 linker sequences (F' and R') were added to primer sequences only when reactions were not going to be cloned.

Gene ID	Forward primer	Reverse Primer
MBD 2/3	5'-CCTCCTGGTTGGAAACGCGAAGAAATT-3'	5'-CAATGGCTGATTGGCTGTGATAAGTAGG-3'
SMG-1	TGGCTGGAATTTGTTACGCATCACT	GTCGCATTTTTGGTTCGTTCAAGAA
MMP	ATCCTGATTACGGCTT	TTTATTGGGGGTGCAACTGT
SNAIL	ACGTTCCCGTCGTTGTTAAA	TGCAAACATATGGCCTTTCA
H2B	TCTGTTAAGAAGATTTCAAAGG	TCCTGTGTATTTTGTAACAGC
NB21.11E	TGATTGCGTTCGCGTATATT	ATTTATCCAGCGCGTCATATTC
AGAT-1	CACCTAAGCCTTTAATGTTG	TGCCAATTGTCACCGTCTTAT
T7 linkers	GGCCGCGG	GCCCCGGC
CHAT	CATCCCTTGCACTAAAATTTCC	ATAAGGTTGTTGGTGTGATTGC
P53	Nobuyoshi Kosaka stocks	Nobuyoshi Kosaka stocks
BYSL	GATTTGGCTGATGTTGAAGG	GCAACAGTAAATGGGTCATG
UAPI	GAGCAATTTACTTTACCGGC	TTCCGGACAATCTGATACAC
TRIP13	GCTGAAAATTGGATGCTACC	GGTTAGACTTTCCACTTCGT
WDR12	CTTCTAGCCCACTCAGAATC	GCTGATTTTATGTTCCTGGC
AHNAK	GCAAAGAGATGTTGAGGTTG	TTCTTAGATCCGCCAAATCC
KIF20A	CTCTTTTCTCCATCAGCAGT	CTGTTCGATGAGACTATGCA
FAM21A/21C	CTGAATTGAGAGGTGGTTCA	CCTTTGGAATGTCAGAGTCA
M13	GTAAAACGACGGCCAG	CAGGAAACAGCTATGAC
T7 Universal	GAGAATTCTAATACGACTCACTATAGGGCCG	AGGGATCCTAATACGACTCACTATAGGCCCC

2.7 Gene Cloning

Templates between 350 and 800 base pairs were generated by PCR using cDNA and gene specific primers, which incorporated T7 promoters onto both strands. In a standard 0.2ml PCR tube, 10 to 100ng of cDNA template were mixed with 2nM dNTPs, and 1µM of both forward and reverse primers. Thermopol buffer (NEB), and I unit of Taq polymerase (NEB) in a final volume of 50µl in ultrapure water. In a primary PCR reaction gene specific forward and reverse primers were used. In secondary reaction for DsRNA synthesis T7 universal forward and reverse primers were used, and in RNA probe synthesis PCR reactions, a combination of forward and reverse primers were used. To amplify products from cloned inserts, M13 primers were used. Thermal cycling conditions for primary and secondary PCRs were as follows: 1 minute initial denaturation at 94 °C, 35 cycles of 30 seconds of denaturation at 94 °C, 30 seconds of primers annealing at 50 to 60 °C, and 1 minute of extension at 72 °C. Reactions were carried out used a TECHNE thermal cycler machine.

The TA cloning Kit Dual Promoter (pCR®II, Invitrogen) was used for the ligation and transformation of products. The presence of inserts was verified by colony PCR, using universal M13 primers. Positive colonies were grown up for an additional 16 hours LB broth/Ampicillin

(100µg/ml, Sigma-Aldrich) and plasmids were then purified using the QIAprep Spin Miniprep Kit (Qiagen) as instructed. Purified plasmids were quantified using a Nanodrop spectrophotometer and were sequenced by Source Bioscience (Oxford UK).

2.8 RNA Probes

Hapten-labeled anti-sense RNA probes were generated from *in vitro* transcription reactions containing DIG-12-UTP (Roche), DNP-11-UTP (PerkinElmer), or FAM-12-UTP (Roche) according to the manufacturer's suggested protocol (Roche). Probes were precipitated using LiCl/ethanol according to the manufacturer's suggested protocol (Roche) and resuspended in 50 µl RNAse-free water. Probe quality and concentration were assessed on a 1% agarose gel and using a NanoDrop ND-1000 spectrophotometer. Probe concentration was adjusted to 50 ng/µl by adding hybridization buffer and probes were stored at -20°C.

2.9 RNA Interference

Purified plasmids were used as template for an M13 PCR reaction. The PCR product was used to set up two separate *in vitro* transcription reactions, one with T7 RNA polymerase (37°C for 4 hours, 40 U, Roche) and a second with Sp6 RNA polymerase (40°C for 4 hours, 40 U, Roche). The reactions were then combined and left to precipitate

overnight at -20˚C in 100% ethanol and 5µl of 3M Sodium acetate. Salts were removed using 70% ethanol washes and temperature-controlled centrifugation (4˚C 3 times at 13,000 RPM for 20 minutes). Dried pellets were re-suspended in 20µl of RNAse free water and incubated at 68˚C for 15 minutes to remove secondary structures, and at 37˚C for a further 45 minutes to produce DsRNA. DsRNA was introduced to animals by microinjection using the Nanoject apparatus (Drummond Scientific). Each animals was injected 3 times with 32.2nl of 2µg/µl of gene specific DsRNA. Injections were repeated for 6 days over 2 weeks. All experiments included the injection of *Gfp* DsRNA as a negative control and *Prep* DsRNA as a positive control.

2.10 Microscopy and Spatial Visualization Software

Samples were incubated in 70% glycerol and then mounted for imaging. Confocal imaging was carried out using the Inverted Olympus FV1000 Confocal system. Images were processed using Imaris bitplane 3D analysis software and Adobe Photoshop CS6; with figure composition done using Adobe Illustrator CS6. Live imaging was carried out using a Zeiss Discovery V8 (Carl Zeiss) and recorded using AxioCam software. Quantification of H3P+ cells was done using whole planarian confocal stacks using the Object Counter 3D plugin from

ImageJ. For all graphs, error bars represent standard deviation of the mean (sd) and asterisks indicate $P<0.05$ using two-tailed Student's t-tests. Heat maps and quadrat depictions of cell migration were generating using SPATSTAT, an R package for analysing spatial point patterns[69]. R is free software for statistical computing and graphics, and a pdf format instruction manual on the relevant software/package is available at the following link:

http://cran.r-project.org/web/packages/spatstat/spatstat.pdf

3. Developing a Shielded Irradiation Assay

3.1 Abstract

A shielded irradiation assay has been developed using a 6mm deep and ~1mm wide lead strip which is housed in a universal circular holding disk. The shield is placed on top of a bespoke lead collimator, and a bottom source X-ray machine projects irradiation upward. This allows the selective removal of cycling cells. We have demonstrated that up to 20 animals can simultaneously be exposed to 30 grays (Gy) of irradiation in a ~ 1 minute 30 seconds time frame allowing large partial irradiation experiments to be designed and executed for the first time. These data demonstrate key observations of cell behaviour, and the developed assay will be crucial in broadening our understanding of genes that regulate cell behaviours.

3.2 Introduction

How adult somatic stem cell populations are recruited to carry out tissue repair during regeneration is a fundamental biological question. In the highly regenerative planarian model, research has focused on identifying key molecular regulators of regeneration/stem cell processes including proliferation, differentiation and directional signal integration [31, 63].

However certain processes have to date been understudied despite their probable importance in fully understanding regeneration biology. Specifically, there have only been a handful of published papers that address (stem) cell migration during regeneration[19, 70] because of the absence of a robust assay so that experimental investigations could be designed.

Cell migration is a process that is also known to be important in disease states such as cancer[74]. In particular, the acquisition of migratory capacity is one of the key characteristics of metastasis whereby cells (through a variety of phenotypic changes) are able to detach from a primary tumor mass, and travel to distant sites of secondary implantation. The result of this acquired mobility is that cancers spread, and consequently efforts to target them with treatment are an on-going challenge.

Based on the conserved nature of gene function across phyla, we propose that efforts to identify common molecular regulators of cell migration in planarians could have a broader application in human disease. Specifically, we propose that by using the planarian model in conjunction with a migration assay it will be possible to test large numbers of putative cancer implicated genes selected from expression studies. And further we propose that this form of high throughput *in vivo* testing is itself a novel concept that has the potential to establish planarians as a pre-vertebrate model for early stage investigations into the molecular regulators of human diseases such as cancers.

3.2.1 Study Aims

The aim of this study was to design an assay, based on earlier data published by Guedelhoefer *et al*., [70, 75]. The approach selected was shielded irradiation. In this paradigm the targeted removal of spatially distinct regions of cells using a protective lead shield is used to consequently observe repopulation, and ergo migration.

We hypothesised that in order to repopulate the irradiated tissue regions, stem cells and their progeny would need to first migrate into those areas, where they would begin the familiar regeneration processes of symmetric and asymmetric cell division.

The work published by Guedelhoefer *et al.* [70, 75] demonstrated that a shield could be designed and used to observe cell behaviour post-irradiation. However, the research detailed in this chapter aims to improve upon key limitations in the Guedelhoefer approach (Table 3.1)

Table 3.1. Table listing Guedelhoefer *et al.* 2012 approach limitations and proposed improvements.
List of key limitations to existing shielded irradiation assay published by Guedelhoefer *et al.* 2012, alongside the improvements proposed in this research chapter.

Guedelhoefer *et al.* 2012 approach	Limitations of Guedelhoefer *et al.* 2012	Improvements proposed in this chapter
Animal size > 1cm	Difficult to culture and Not amenable to FISH and IMMUNO techniques due to tissue permeability issues.	Animal size <5mm
Shield width > 4mm	Required large size of animals. Exacerbated by scatter effects of X-rays.	Shield width ~ 1mm Collimation to inhibit scatter
~ 40% of animal mass coverage by shield	A reduction in the migration field size Limiting migration observations	25% animal mass coverage by shield
Single animal capacity shield design	Limited experimental design options (low n numbers)	Multi animal shield design with top source X-ray to allow larger experiments

3.3 Results & Discussion

3.3.1 Lead shielding successfully protects stem cells from otherwise lethal doses of irradiation

X-ray irradiated planarians are known to degenerate over time and eventually die. We subsequently developed a modified method [70], which allows the high throughput (20 animals per run) irradiation of selected portions of the animal, while consistently protecting specific regions using a lead shield. Animals are placed on top of a 1mm lead shield which is in turn placed within a universal housing (see figure 3.1 and 3.2). This housing sits on top of a bespoke collimator which receives x rays from underneath, using a bottom source x ray machine. The outcome was the repeatable production of a defined band of ~1mm within which the stem cell marker *h2b* was detected.

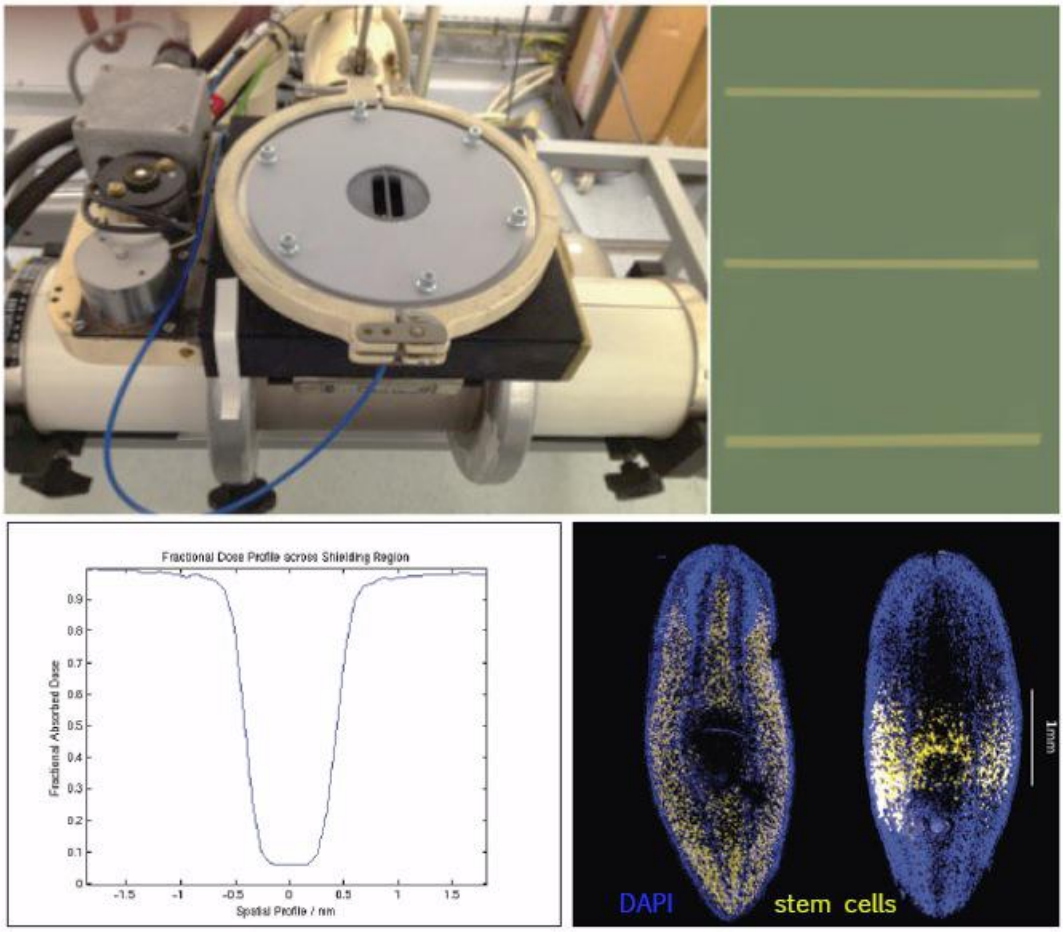

Figure 3.1. A composite image illustrating the bespoke irradiation apparatus

225kV of X-rays were generated and then released from an X-ray tube. X-rays passed through a lead aperture, and exposure time was controlled using a lead shutter, photograph top left courtesy of Mark Hill. The effectiveness of the collimation and relative scatter was measured using standard radiograph film top right courtesy of James Thompson. X-rays which make contact with the longitudinally placed ~1mm shield strip are attenuated by approximately 99% as seen in dose distribution graph bottom left courtesy of Mark Hill and verified by FISH bottom right which clearly shows an absence stem cells outside of the protected shielded region, and retention of the stem cell population within the shielded zone. Scale bar represents 1mm (n=9).

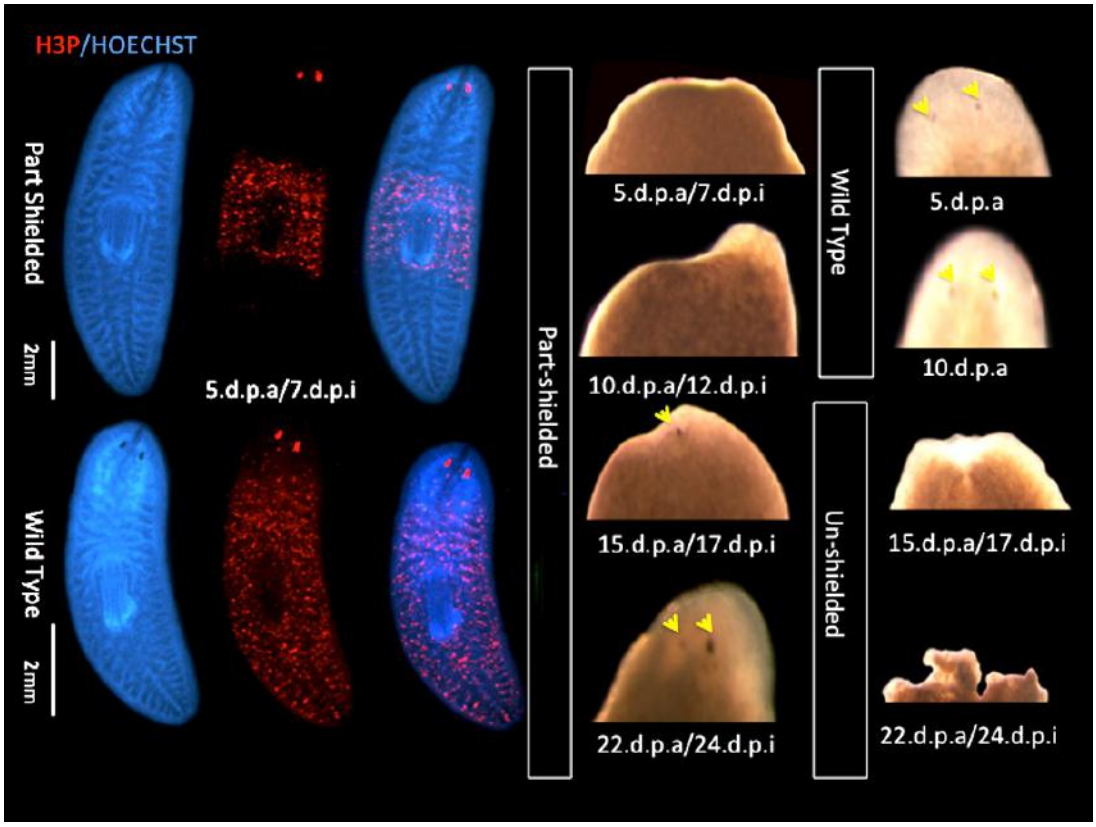

Figure 3.2. Immuno histochemistry showing H3P, cell in M Phase (red).

The image shows that post irradiation mitotic cells are restricted to a central region around the pharynx. Conversely in homeostatic animals cells are distributed throughout the mesenchyme, absent only from the anterior tip of the head and the pharynx. Live brightfield images show that animals that were shielded by the lead assay regenerate at a rate of 24 days for eyespot formation. Conversely wild type animals, subjected to no irradiation regenerate in the expected <10-day time frame. Animal irradiated unshielded, were exposed to a lethal dose, and 100 percent (n= 10) perished by day 30 post exposure. Scale bar is 2mm

3.3.2 Stem cells do not migrate in the absence of a wound

Using the lead shield we investigated whether stem cell ablation was sufficient to trigger stem cell migration. Animals that were partially irradiated were observed over time (see figure 3.3). Their morphology initially appeared normal, but over time head regression occurred as

reported by Guedelhoefer *et al.* and Wolfe and Dubois (1949). Animals did eventually regenerate their heads, and partially irradiated animals survived (*n*=10) the 30 gray dose that was lethal to unshielded animals (*n*=10). The spatial distribution of stem cells was observed using FISH and stem cells marker *h2b+*, and as reported by *Guedelhoefer et.al., 2012*[70] we saw a band of shielded tissue that contained h2b+ cells, and irradiated tissue's which were devoid of stem cells. Observations up to 10 days post irradiation showed no visible changes in the stem cell containing region, and these data suggest that stem cells do not undergo migration into irradiated tissues during this time frame. It has been shown that planarian tissues exhibit significant cellular responses to irradiation, including a variety of gene expression changes in both stem cell and differentiated tissue compartments [27] and measurable increases in apoptotic cell death [76]. However, the findings of this research and that of Guedelhoefer et.al., 2012[70] clearly show that the removal of stem cells from tissue, by irradiation is insufficient to induce stem cell migration.

3.3.3 Wounding (amputation) causes stem cell dispersal and migration

In order to investigate if the migration and dispersal of stem cells was affected by wounding, animals were anteriorly amputated at 2

days post irradiation (see figure 3.3). Using FISH it was observed that the stem cells and progeny of wounded animals appear to increase their directed dispersal toward the wound site compared to uncut counterparts. Qualitative assessment of stem cell dispersal across the two groups clearly showed that the progressive spread of stem cells was seen from 4 days post irradiation and continued to be detectable at day 10-post irradiation. These data correspond with that published by *Guedelhoefer et al., 2012*[70] and provide additional support for the proposition that extrinsic regulators of stem cell behaviour are crucial to the proper understanding of their roles *in vivo.*

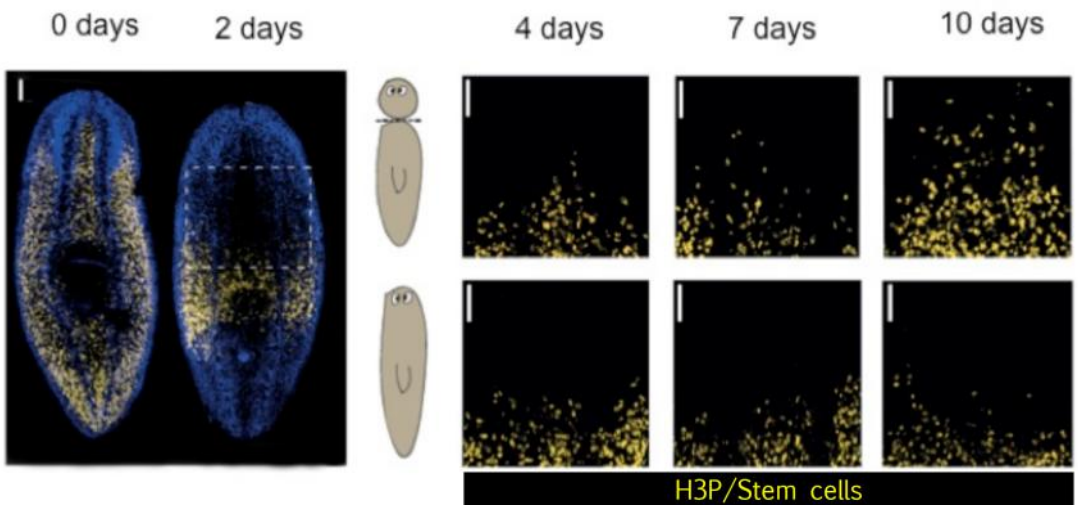

Figure 3.3. FISH post shielded irradiation showing stem cell migration post anterior amputation

At 24 hours animals were split into 2 groups; those that were wounded (anterior amputation) and another that were left intact. Wounding/amputation induced stem cell migration, which increased over time. Conversely in the absence of wounding, partial irradiation was insufficient to induce stem cell dispersal. Scale bars represent 100 **µ**m (n=5).

3.3.4 *NB21.11.E* and *AGAT-1* are down regulated at different time points after partially shielded irradiation in unwounded animals

FISH observations showed that progeny markers, *NB.21.11.E* and *AGAT-1* progressively disappear in irradiated tissues because progeny cells die, and are not replaced due to an absence of mother stem cells (see figure 3.4). However, marker expression persists in shielded regions where the progeny population continues to be replenished by resident stem cells (see figure 3.4). These data correspond with work published by Eisenhoffer *et al* 2008 [25] where lethally irradiated animals gradually lost all progeny markers at similar time points. Progeny markers appear to have different temporal responses to irradiation, with *NB.21.11.E* cells disappearing at 4 days post irradiation, and AGAT-1 cells by day 10. This is proposed to be the result of their average life span. Specifically the early progeny state is suggested to last 4 days, after which these cells then differentiate into late progeny cells types with a life span of approximately 10 days before ultimately terminally differentiating. In the case of *Eisenhoffer's* work, it is clear that the ultimate absence of progeny marker expression by day 10 is the result of total stem cell niche ablation, without which new progeny cannot be produced. However the data presented here indicates that even in the presence of a

preserved stem cell population, progeny repopulation of irradiated tissues is minimal without wounding.

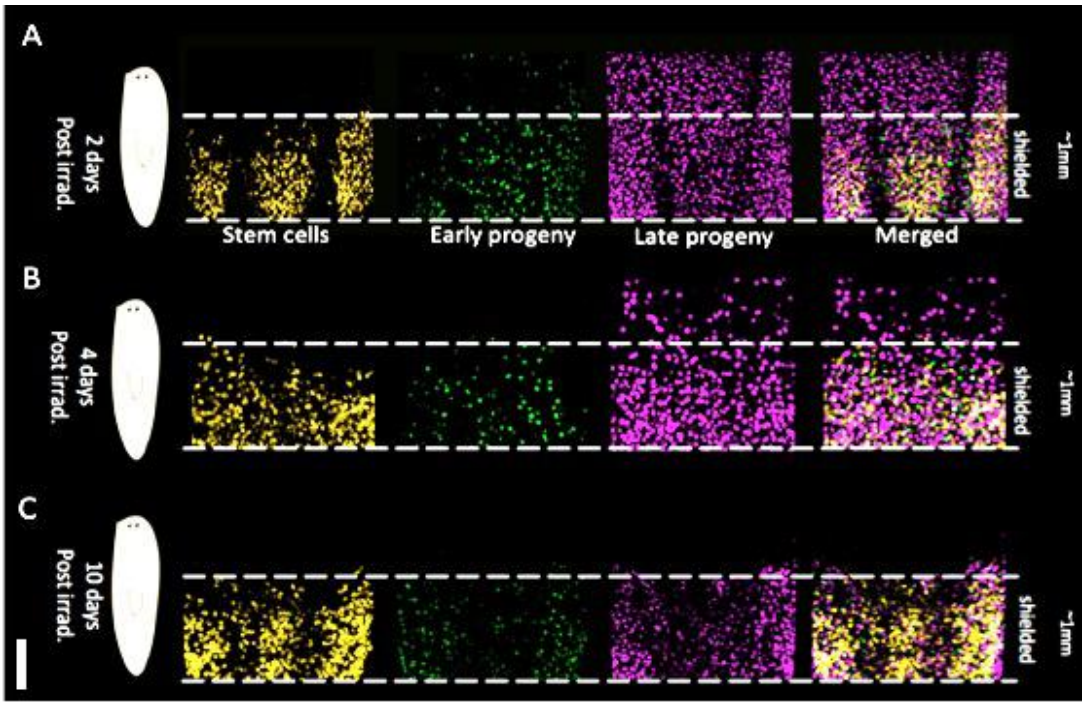

Figure 3.4 FISH showing lack of migration of stem cell progeny in the absence of wounding.

A. FISH of an unwounded partially irradiated animal showing the restriction of stem cells (yellow) to the shielded regions 2 days post irradiation. In this image early progeny (green) expression is also significantly down regulated in irradiated tissues. Additionally late progeny (magenta) expression outside of the shielded region remains comparable with wild type distribution. **B.** By 4 days post irradiation early progeny expression (green) is no` longer detectable in irradiated tissue regions. At this time point late progeny expression (magenta) also begins to decrease in the irradiated portion of the animal but remains detectable. **C.** At 10 days post irradiation late progeny (magenta) have transitioned to differentiated tissue types, and in the absence of wounding the irradiated tissues are not repopulated or rescued by stem cells and progeny. Scale bars represent 500 μm (n=5).

3.3.5 The spatial relationship between stem cells and their progeny is interrupted during amputation-initiated dispersal

Stem cell dispersal is accompanied by the production of new progeny cells, which are found to accumulate at the wound site. FISH observation of the spatial dynamics of these cell types clearly shows that the normal parenchymal distribution of stem cells and radiating peripheral compartmentalization of progeny is interrupted during dispersal (see figure 3.5). It is known that the life span of progeny cells ranges from 4 to 10 days and hence that a proportion of the progeny observed during these experiments have been synthesized *de novo* by migrating stem cells. Upon the reestablishment of homeostasis normal spatio-temporal relationships between stem cells and their progeny are restored. These results demonstrate that the cellular response in planarians to wounding is extremely dynamic. Experiments that aim to look for patterns in the changes of cell – cell spatial dynamics could provide important mechanistic detail about complex processes *in vivo*. This opportunity in planarians addresses a key limitation of *in vitro* studies where the nature and properties of both endogenous and exogenous objects must be considered in a scenario independent of the whole organism.

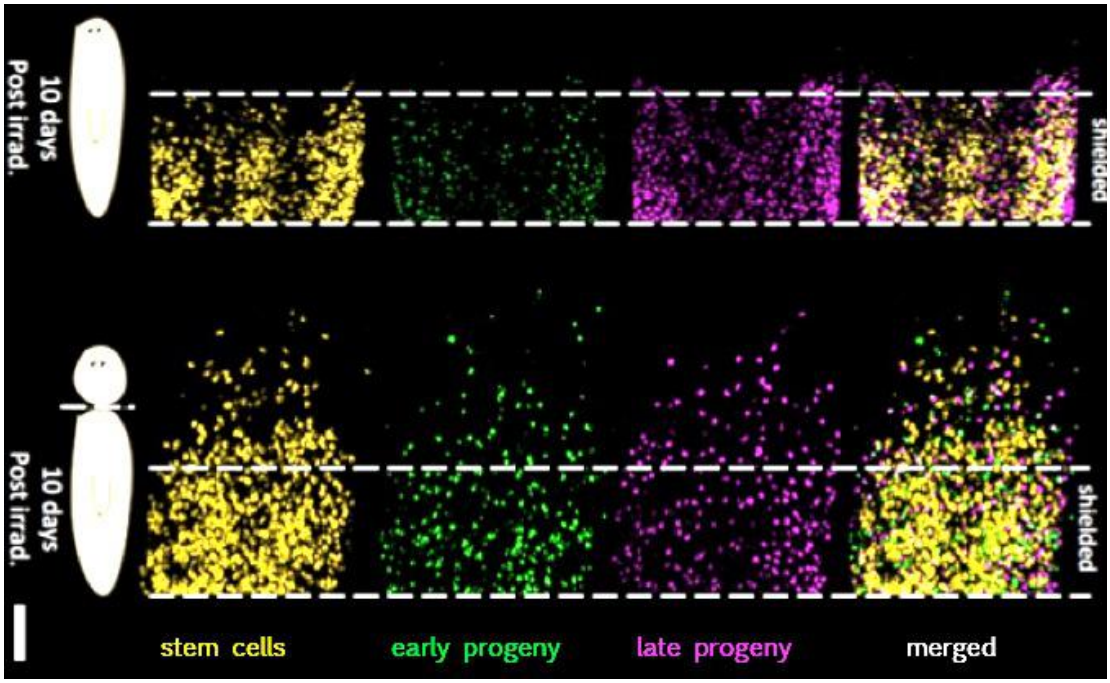

Figure 3.5. Triple FISH image comparing cell dispersal patterns in unwounded and wounded partially irradiated animals (top panel) at 10 days post irradiation.

The bottom panel shows a wounded animal; and depicts significant stem cell, early progeny and late progeny migration/dispersal, which is preferentially directed toward the wound site. Note that the normal temporal stem cell and progeny relationships are disrupted during this process. A direct comparison can be made by referring to homeostatic distributions in introductory Figure 1.4. Scale bars represent 500 μm (n=5).

3.3.6 Significant tissue decay is required to activate stem cell rescue and regeneration of anterior structures

Head regression of unwounded partially irradiated animals as seen in this and earlier work precedes the regeneration of anterior structures [70] (see figure 3.6). The delay in regeneration corresponds with an increase in tissue decay, which may produce signals analogous to those generated by wounding, which ultimately prompt regeneration to

occur at later time points then wounded counterparts. These data strongly support the hypothesis that signals generated at wound sites are responsible for the activation of stem cells [39]. Differential expression analysis to identify wound-induced transcriptional changes to genes were carried out [39]. Genes were then grouped, and based on their expression profiles were categorized. One category of particular interest is the so named *W2* group that is comprised of genes expressed shortly after wounding in differentiated tissues localized near the wound site. Future experiments designed to test the knockdown effects of *W2* genes on stem cell and progeny activation within the context of the shielded assay presented in this thesis should be carried out. These efforts could identify extrinsic stem cell regulators that are responsible for coordinating complex regenerative processes.

3.3.7 Stem cell repopulation of irradiated tissues restores homeostasis

Rescue of irradiated host tissue is achieved through stem cell repopulation of irradiated tissues. Using FISH it was observed that at 2 days post irradiation the only tissues positive for stem cell marker H2B were those within the shielded zone. By 4 days post irradiation stem cells were clearly seen to begin repopulating irradiated compartments in wounded animals (see figure 3.6). A progressive

repopulation of the irradiated tissues is observed over time points 7, 10, 15 and 35 days post irradiation. All animals observed at 35 days post irradiation from both experimental conditions (cut and uncut) showed full anterior structure regeneration, with bi-lobed brain and photoreceptors fully re-established. FISH using progeny markers shows that normal progeny distribution and production is seemingly re-established by day 35 post irradiation. All animals also retain normal regeneration capacity with a second round of anterior amputation at day 35 post irradiation (7/7 photoreceptors visible by day 6 of regeneration). The anatomical normality, in conjunction with restored regeneration ability, indicate that the stem cell repopulation of irradiated tissues results in the restoration of homeostasis in animals exposed to partial shielded irradiation by day 35 post treatment.

These data show that within the ~1mm shielded region there exists a stem cell population capable of giving rise to all required tissue types for re-establishing homeostasis. However the question as to whether this population is mixed or homogenous still remains unanswered.

Potential experiments to address cell heterogeneity could involve taking a partially repopulated region of tissue, and isolating it by amputation. If the starting number of stem cells could be confidently predicted for a given portion of tissue at a selected time point, and it

was known that this number was not less than the absolute minimum required for rescue, then a tentative proposal about the presence or absence of heterogeneity could be formulated based on the survival rates of tissue samples.

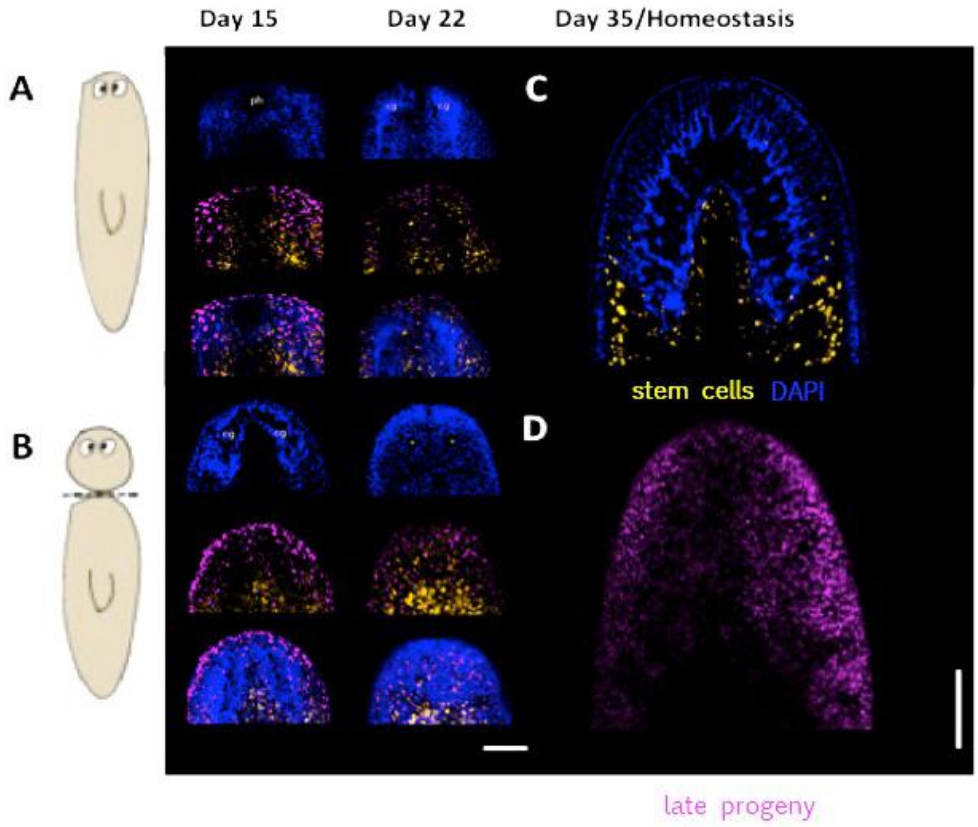

Figure 3.6. FISH showing anterior tissue regression in the absence of wounding.

A. In the absence of wounding stem cell and progeny repopulation of irradiated tissues does not occur. Instead anterior tissue regresses, and by day 15 all tissue anterior to the shielded region (placed over the pharynx *ph*) is missing. This loss of tissue integrity prompts stem cell activation, and by day 22 post irradiation animals have begun the processes of brain regeneration. **B.** Conversely in animals that were wounded anterior regeneration begins earlier, and by day 22 anterior regeneration, including the development of eyespots has been completed. **C.** & **D.** show that by day 35 all animals – wounded and unwounded have been rescued and appear to have returned to homeostasis in relation to stem cell (yellow) and progeny (magenta) gene expression. Scale bars represent 100µm (n=7).

3.3.8 During regeneration stem cell progeny actively migrate to regions beyond the stem cell niche

Although visualisation of cell distribution over time is possible using FISH, this method is static. Without the ability to observe live cells, it is not apparent whether a cell located in a region of interest did in fact migrate there, or was a division product of a nearby cell. Subsequently experiments were carried out which allowed us to explore the hypothesis that stem cell progeny, AGAT-1 expressing cells, do actively migrate. Images taken of the pharynx in a regenerating animal clearly show that stem cells are only ever located along the boundary of the pharyngeal region (see figure 3.7 and 3.8). We failed, despite multiple efforts, to successfully image stem cells in the pharyngeal region, which led us to propose that they (stem cells) do not enter this niche with any significant frequency. Conversely, the abundant presence of AGAT-1 positive cells in the pharynx can therefore most likely be attributed to active cell migration. More specifically, we hypothesise that stem cells located around the pharyngeal boundary, asymmetrically divide to produce AGAT-1 progeny cells, and that these progeny cells then migrate into the pharyngeal region.

Other images taken of the tail regions of animals post shielded irradiation (Figure 3.8) show that cells which are both H2B (stem cell marker) and AGAT-1 (progeny cell marker) positive appear to migrate, distances up to 120μm. The presence of a single cell, removed from its nearest neighbour >120μm leads us to conclude that the cell must have actively migrated to this location, at least from the distance of its closest neighbour.

Evidence of active stem cell migration in planarians lends support to this project's proposal that through investigating planarian stem cells we can learn lessons relevant to cancer metastasis.

Metastasis is an active migration progress, with cells taking on motility-related attributes. In theory, based on the conserved nature of gene function across phyla, genes which are implicated in human cancers, should also play a synonymous role in planarian stem cells. Consequently, it is conceivable that one could take poorly characterised cancer implicated genes and test their actual role *in vivo* in planarians using RNAi and shielded irradiation.

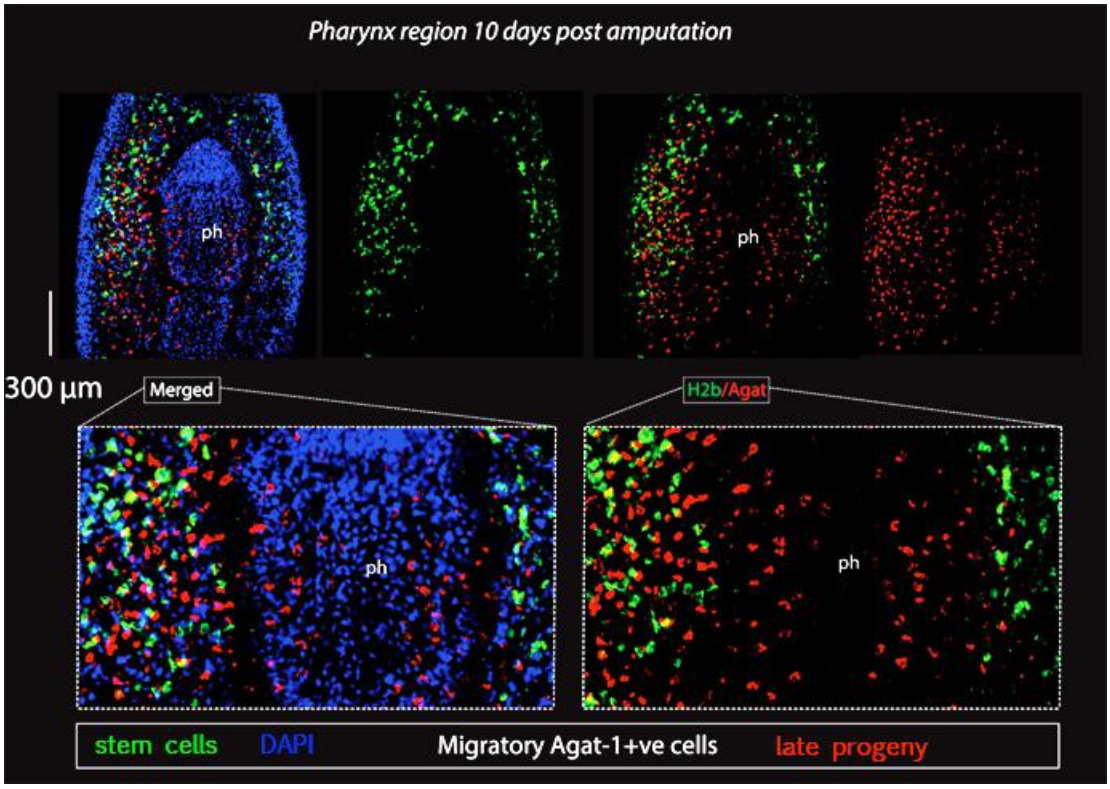

Figure 3.7. FISH image demonstrating progeny migration around the pharynx region

FISH confocal image at 20x shows the differential distribution of stem cells (H2B) in green, and late progeny (AGAT-1) in red both in and around the pharynx region. The absence of stem cells in the pharynx is in opposition to the clear presence of their progeny in this region. This observation supports the hypothesis that AGAT-1 positive cells can actively migrate, and do so into the pharynx region post differentiation. Scale bar represents 300µm (n=5).

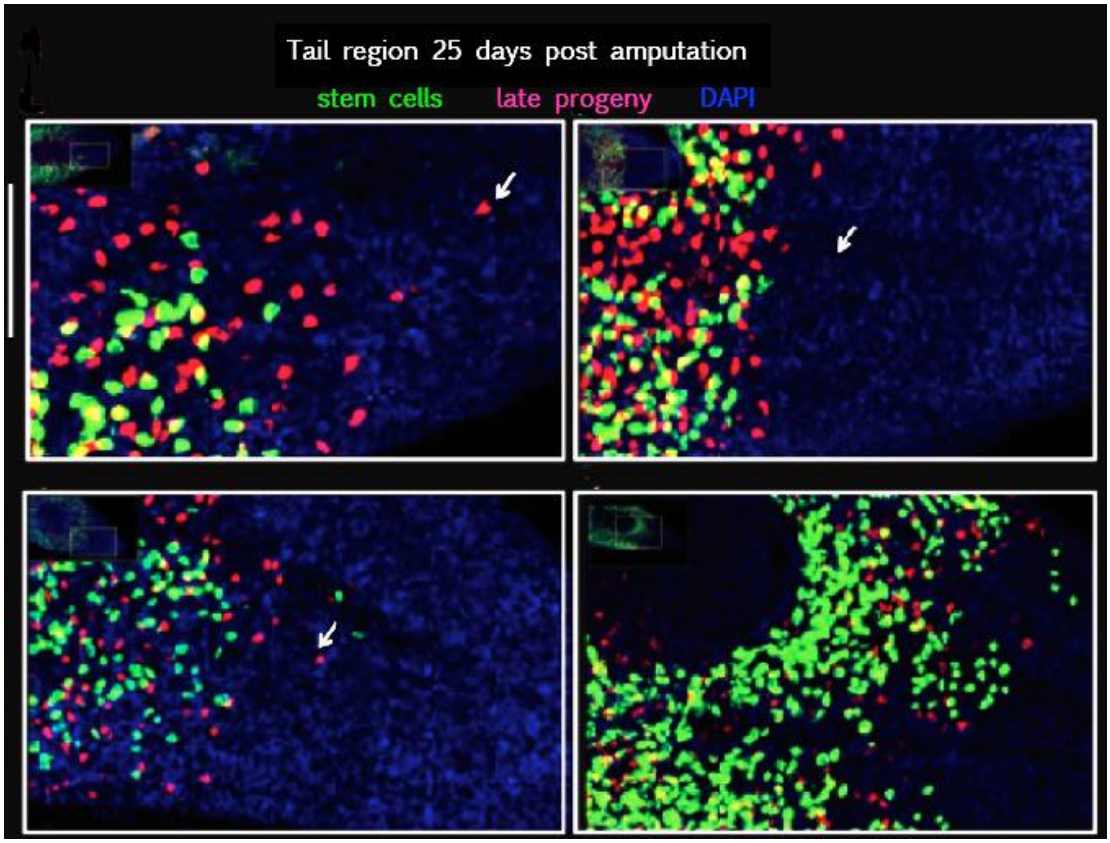

Figure 3.8. FISH image showing progeny migration toward the posterior tail tip.

FISH confocal image at 20x also shows the differential distribution of stem cells (H2B) in green, and late progeny (AGAT-1) in the posterior tail region of the animal post irradiation. This region is posterior to the shielded zone, and shows that even in the absence of posterior wounding, progeny can be detected at distances up to 120 μm from the shielded zone as indicated by white arrows. Additionally in one some animal's stem cells could also be detected in regions outside of the shielded zone (as shown in 3). These data further support the hypothesis that AGAT-1 cells are capable of active migration, and that so too are stem cells. Scale bars represent 100μm (n=5)

3.4 Conclusions

This is the first demonstration that shielded irradiation can be up-scaled to allow the simultaneous processing of multiple animals. The method of positioning animals above the shield and exposing them to a bottom source X-ray are novel and has been integral to expanding the assays processing potential. The shield will be used to help determine the genetic regulators of (stem) cell behaviours such as cell migration, which is associated with both regeneration and cancer.

4. Characterization of SMG-1 and MMP Knockdown Effects

4.1 Abstract

This is the first use of a shielded irradiation assay in planarians to observe RNAi effects. FISH protocols were successfully used to visualise stem cell (H2B) and progeny markers (CHAT, NB21.11E and AGAT-1) post-shielded irradiation. The role of a Matrix Metalloprotease (MTMMPA) was previously characterised by Isonali et al., 2013 [77]. However, the authors were unable to ascribe their regeneration defect phenotype to migration affects. These data are the first to demonstrate a migration inhibition effect of stem cells and progeny by MTMMPA in planarians. Additionally the Serine/Threonine Kinase SMG-1 was for the first time in these data shown to be required for the control of cell migration. Previous work carried out by Gonzalez-Estevez *et al.* 2012 [41] observed tumour-like mass formations when SMG-1 was knocked down by RNAi. The research presented herein expands on these findings, and demonstrates that *SMG-1 RNAi* animals exposed to shielded irradiation regenerate at an accelerated rate relative to homeostatic animals. We also demonstrate and that this process is driven by increased cell proliferation and migration leads to ectopic tumour-like growths.

4.2 Introduction

Cancer is a term used to describe a variety of diseases that share common traits. Of fundamental interest to the broader cancer research community are traits that are associated with mortality. As highly mutable diseases, aggressive cancers result in affected cells developing phenotypic traits that allow territorial expansion through the up-regulation of processes such as cell proliferation and migration [78].

Two separate kinds of effectors that have been heavily studied, and are firmly associated with cancer development are proteolytic enzymes (metalloproteinase's) and tumour suppressors. Several research projects using planarians which focus on both metalloproteinase's and tumour suppressors have been published, and a detailed description of these works is available in Chapter 1 of this thesis.

Of particular interest were papers published by Isolani *et al.* in 2013 [77] discussing the role matrix metalloproteinase's (MMP's) in regeneration, and also a second paper published by Gonzalez-Estevez *et al.* published in 2012 [41] which looked at the then recently emerged tumour suppressor SMG-1.

Isolani et al [77]found that animals without the protease MTMMPA could not regenerate, and experimental efforts by the author to isolate the

cause of this phenotype were extensive. After ruling out defects in proliferation, maintenance, apoptosis and differentiation, Isolani et al. hypothesised, based on an observation that new cells were absent from the regenerative blastema, that MTMMPA as seen in other organisms, may be required for cell migration.

In contrast, animals without SMG-1 were characterised as hyper proliferative, hyperplasic and hypertrophic. Gonzalez-Estevez[41] et al observed the ectopic accumulation of cells, which went on to form tumour-like masses. Gonzalez-Estevez et al. described SMG-1 as having a tumour-suppressor like role.

The research presented in this Chapter is based on the proposal that the shielded irradiation assay detailed in Chapter 3, if effective, should be able to expand our characterisation of genes such as MTMMPA and SMG-1.

4.2.1 Study Aims

The aims of the research presented in this Chapter were to expand our understanding of the roles of MTMMPA and SMG-1 in the planarian model. By using the bespoke shielded irradiation assay on MTMMPA and SMG-1 RNAi animals we hoped to observe cell behaviours more clearly, including migration and proliferation.

Specific questions raised by published research from Isolani et al. and Gonzalez-Estevez et al. were:

1. Is the MTMMPA RNAi regeneration phenotype the result of migration inhibition, due to proteolytic suppression?
2. If migration inhibition is an effect of MTMMPA knockdown, then which cell types are affected? Specifically, are stem cells or their progeny prohibited from migrating?
3. Is the SMG-1 phenotype associated with increased migratory capacity?
4. Can our understanding of the division dynamics of SMG-1 knockdown animals be improved?
5. In the shielded irradiation paradigm will regeneration phenotypes correspond with the published descriptions?

4.3 Results & Discussion

4.3.1 Stem cell dispersal and migration is affected by the RNAi mediated knockdown of target genes

Two genes SMG-1 and MTMMPA were selected as RNAi phenotypes to test the shield. The aim was to determine if the assay could be used to provide data of gene function relative to migration and dispersal. All genes had published traditional functional characterization studies associated with them. However in the absence of the migration-

shielding assay presented in this thesis, no statements about their roles in this context have been made previously. FISH observations were carried out at 10 days post-amputation as this was shown in wild type animals to be a time point by which migration and dispersal should be readily observable (see figure 4.1). Gonzalez *et al.* identified SMG-1 to have a tumour suppressor role in planarians. Its knockdown resulted in tumor formation and hyper proliferation. Corresponding with this research, the SMG-1 RNAi animals exhibited a striking increase in overall cell mass relative to the control (GFP RNAi) and an increased dispersal range. These data correspond with Gonzalez-Estevez et al. [41], and suggested that SMG-1 (RNAi) results in hyper proliferative cellular spreading seen in many cancers. MTMMPA, a membrane bound matrix metalloproteinase was shown to have pleiotropic roles in planarian regeneration. Lin *et al.* (2014) [77] attempted to triangulate the observed phenotype characteristics in order to establish if the gene had a migration associated role as seen in humans. However, in the absence of a migration assay they were unable to present a robust argument for MTMMPA as a migration associated gene. The data presented here clearly show that stem cells fail to disperse outside of the shielded region in MTMMPA (RNAi) animals. Subsequently we propose that MTMMPA RNAi results in a reduction of extra cellular matrix proteolytic

degradation that stifles cell-directed movement toward the wound site. MTMMPA also represents a high confidence positive control for future experiments to test potential migration genes using the assay.

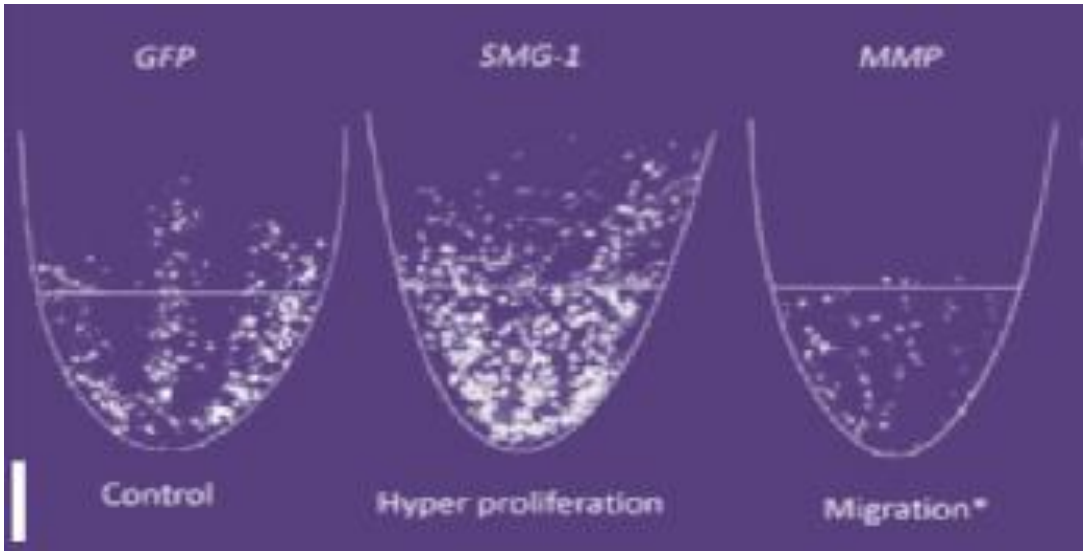

Figure 4.1. FISH confocal images showing stem cell distribution at 10 days post amputation in RNAi, partially shielded tailpieces.
From left to right: GFP (RNAi) negative control representing normal stem cell dispersal; SMG-1 (RNAi) hyper proliferation phenotype showing elevated stem cell dispersal and number. The far right image labelled MMP (MTMMPA) (RNAi) demonstrates a distinct lack of stem cell dispersal and migration. Scale bar represents 500µm (n=7).

4.3.2 The loss of SMG-1 tumor suppressor function is characterised in part by accelerated stem cell and/or progeny placement in anterior regions

In GFP animals cells have not begun to migrate, although they have started to reorganize themselves, with cells tending to push toward the centre of the animal forming an anterior facing peak (see figure 4.2). In SMG-1 animals the effect is more pronounced (see figure 4.2).

Cells have preferentially centralised, and have at this time we hypothesise have begun migrating. Clusters of cells are present from lower quadrats of the schematics in Figure 4.2, right up to the wound site. The centralization of the cells seen in both GFP and SMG-1 animals could be attributed to form a collective active migration in which leader cells respond to the distant wound signal, and in turn emit signals to follower cells, orchestrating their directed response and migration. The hypothesis would be dependent on the original wound signal emanating from the central region of the wound site, thus reaching a centrally located responder cell located in the shielded area. This cell would then mobilize and emit directional cues to the other cells in order to orchestrate collective targeted migration. Collective migration is seen in wound healing paradigms and is also observed in cancer metastasis[79]. However it is important to note that the cause of cell spread anteriorly could also be hyper proliferation. The pronounced or accelerated collective migration or proliferative spread of SMG-1 RNAi cells corresponds with the accelerated regeneration observed in brightfield imaging (see Figure 4.5). We hypothesise that SMG-1 tumour suppressor knockdown not only increases cell proliferation, but also promotes cell migration by pathways as yet undetermined.

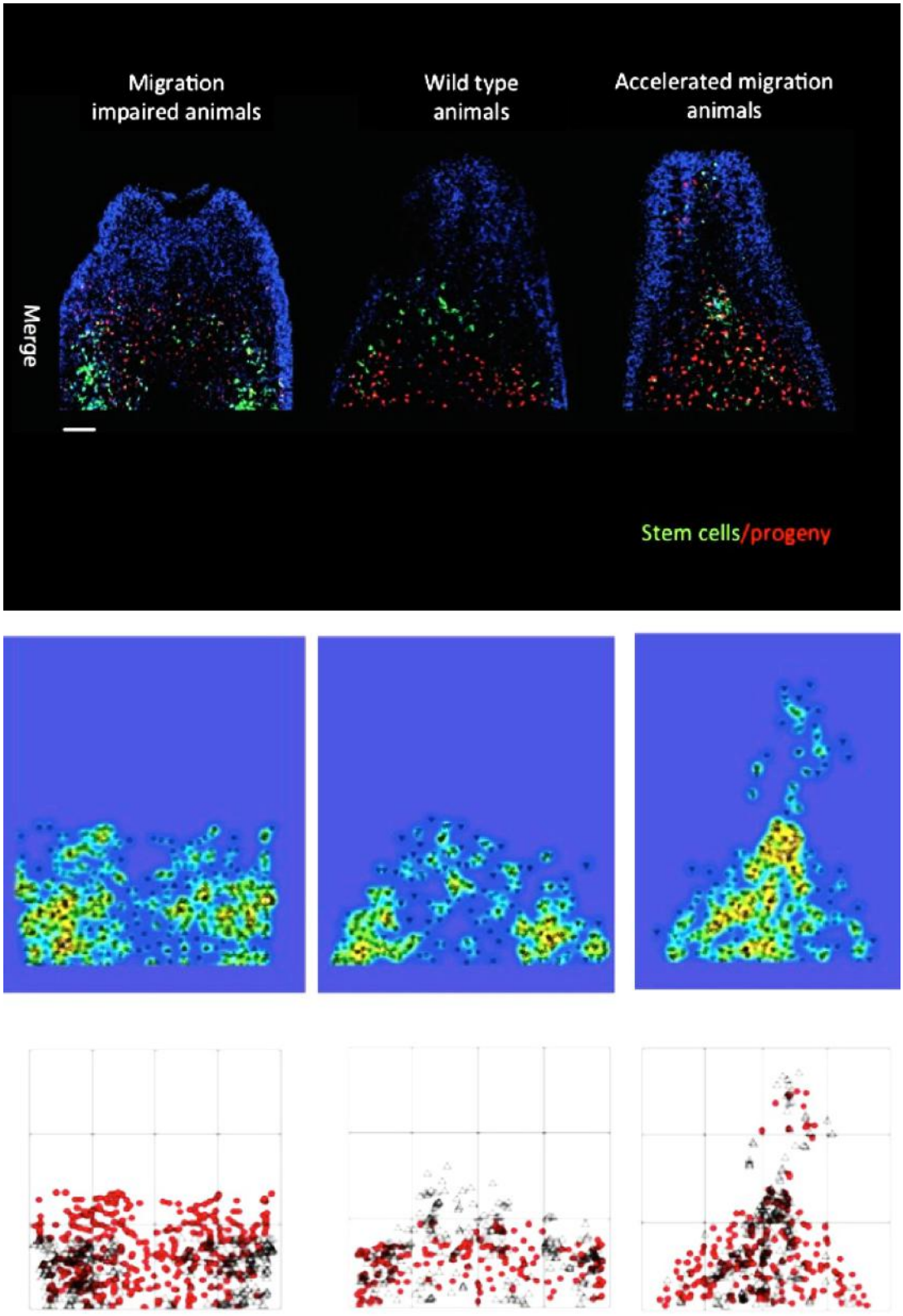

Figure 4.2. 20X confocal image showing a double fluorescent insitu of stem cell, H2B (green) and late progeny, AGAT-1 (red) cells in 10 days post irradiation/amputation animals.

Far left (top, middle and bottom) shows a migration impaired MMP RNAi animal with no migration of either cell type. Consequently, no anterior

regeneration is visible. The centre row of images (top, middle and bottom) is a GFP, wild type animal that shows some cell movement categorised by the visible breakdown of the horizontal anterior shield boundary region. Far right (top, middle and bottom) is an SMG-1 RNAi animal which exhibits considerable cell migration at this time point. Both stem and progeny cells are visible at the anterior tip of the amputated animal. There is also a visible clustering of stem cells at the anterior edge of the shielded zone. Scale bars represent 100μm (n=5). A 2D quantitative conversion of 3D confocal image data using the R statistical package "spatstat". The top row of images shows a density map with yellow representing high-density regions. The bottom row is a quadrat representation of the same cells/samples. MMP-1 knockdown animal clearly show the retention of the horizontal shield boundary and an absence of central midline accumulation. GFP wild type animals show what appears to be an intermediary state, although no cells are present in the most anterior quadrats, an accumulation of cells in the central midline, and hence a breakdown in lateral preference is visible. In SMG-1 animals, the cell distribution in both the quadrat and heat map views show an accumulation of cells in the central midline of the animal, and a migration of cells into the most anterior quadrats/regions.

4.3.3 The regeneration of neuronal structures is accelerated in SMG-1 loss of function animals

By 16 days post-amputation (**animals were earlier cut just below the eyes to maximise the migration zone tissue size**) the difference between GFP, SMG-1 and MMP RNAi animals is marked (see figure 4.3 and 4.4). In the GFP animals, cells have spread to the anterior and a significant number of cycling cells have now repopulated the anterior region, giving rise to progeny with lineage-restricted fates. The SMG-1 RNAi animals have already reformed neuronal structures. The bi-lobed brain (Figure 4.3) and ventral nerve cords are clearly discernable, and both stem cells and their progeny have begun to reorganise themselves into their respective spatial

niches. Conversely the MMP RNAi animals have failed to maintain their cycling cell populations, and the few cells still positive for stem cell markers are located posterior to the wound site in the shielded region. Consequently it is proposed that the MMP RNAi animals are unable to rescue or adopt alternative methods by which to migrate and repopulate the irradiated tissues. By also labelling the neuronal progeny cells (Chat) and a separate early subset of stem cell progeny (NB21.11E) (Figure 4.4) we were able to further investigate the neuronal regeneration differences. In these images GFP animals have begun brain regeneration, the beginnings of the bi-lobed brain structure can be seen. However the SMG-1 animals have clearly formed their bi-lobed brain and have an abundance of neuronal progeny cells, as well as early progeny cells. Once again the MMP RNAi have failed to produce progeny that are able to migrate. The apparent presence of bi-lobed structures in the anterior are categorized as 'old tissue', which was not fully excised by the amputation process. This is proposed based on two observations: 1) that no cells have observably migrated to the region in order to mediate regeneration of the brain and 2) the remnant lobes are fully differentiated, with cells respecting homeostatic niches (regions of black indicate spaces between the neuronal cells). In the GFP animal

no such niche is visible, and instead the lobes are ubiquitously filled with CHAT positive cells (purple), suggesting they are still regenerating the region, and have not yet settled into their homeostatic spatial niches.

4.3.4 The absence of MMP-1 protease function results in cell migration failure, and cell death at later time points

At 10 days post-irradiation FISH imaging of stem cells and progeny clearly show that MMP RNAi animals have no migration occurring (Figure 4.2). Moreover, there appears to be a regression of the stem cell population from the most anterior portion of shield. The result is a region that is dominated by progeny cells. The MMP RNAi cells do not appear to be moving laterally either. They have maintained the straight horizontal shield boundary (Figure 4.2) and we hypothesize that cell movement in all directions is inhibited due to the absence of proteolytic activity required to break down and remodel ECM components when cells become mobile. Ultimately the lack of migration, correlating with a lack of regeneration leads to animal death.

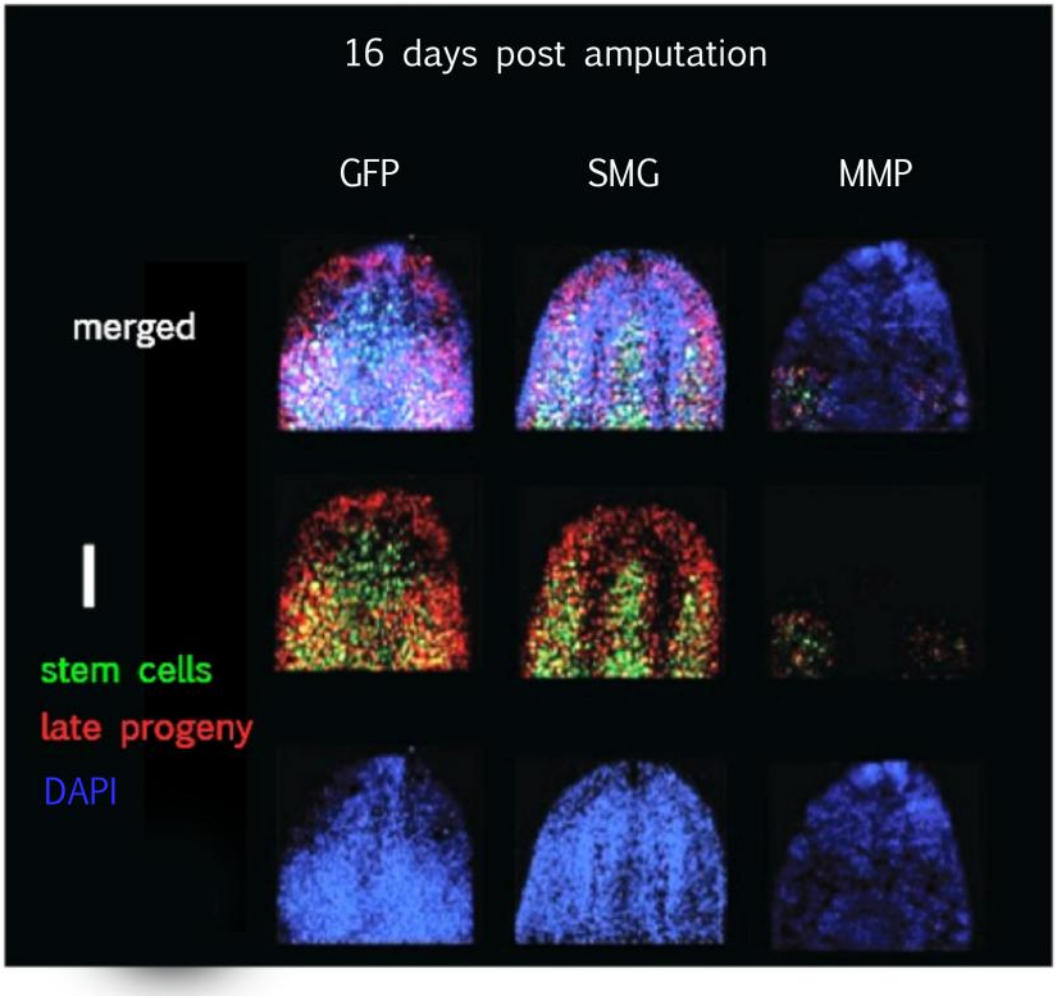

Figure 4.3. 10x confocal image showing a double fluorescent *in situ* of stem cells, H2B (green) and late progeny, AGAT-1 (red). At 16 days post amputation/14 days post irradiation in GFP animals stem and progeny cells have repopulated the anterior irradiation zone, and anterior regeneration has begun. At this time point the stem cell and progeny are not ubiquitously distributed, not yet returned to their distinct spatial niches (b) SMG-1 animals also have repopulated in their anterior however the regeneration process in comparatively advanced. The bi-lobed brain and ventral nerve cords are organised, and stem cells and progeny cells have settled into their niches (c) MMP-1 animals fail to regenerate their anterior due to a failure of stem cells and their progeny to repopulate the anterior regions. At this time point the numbers of stem cells and their progeny are also reduced. (n=5) Scale bar represents 100µm.

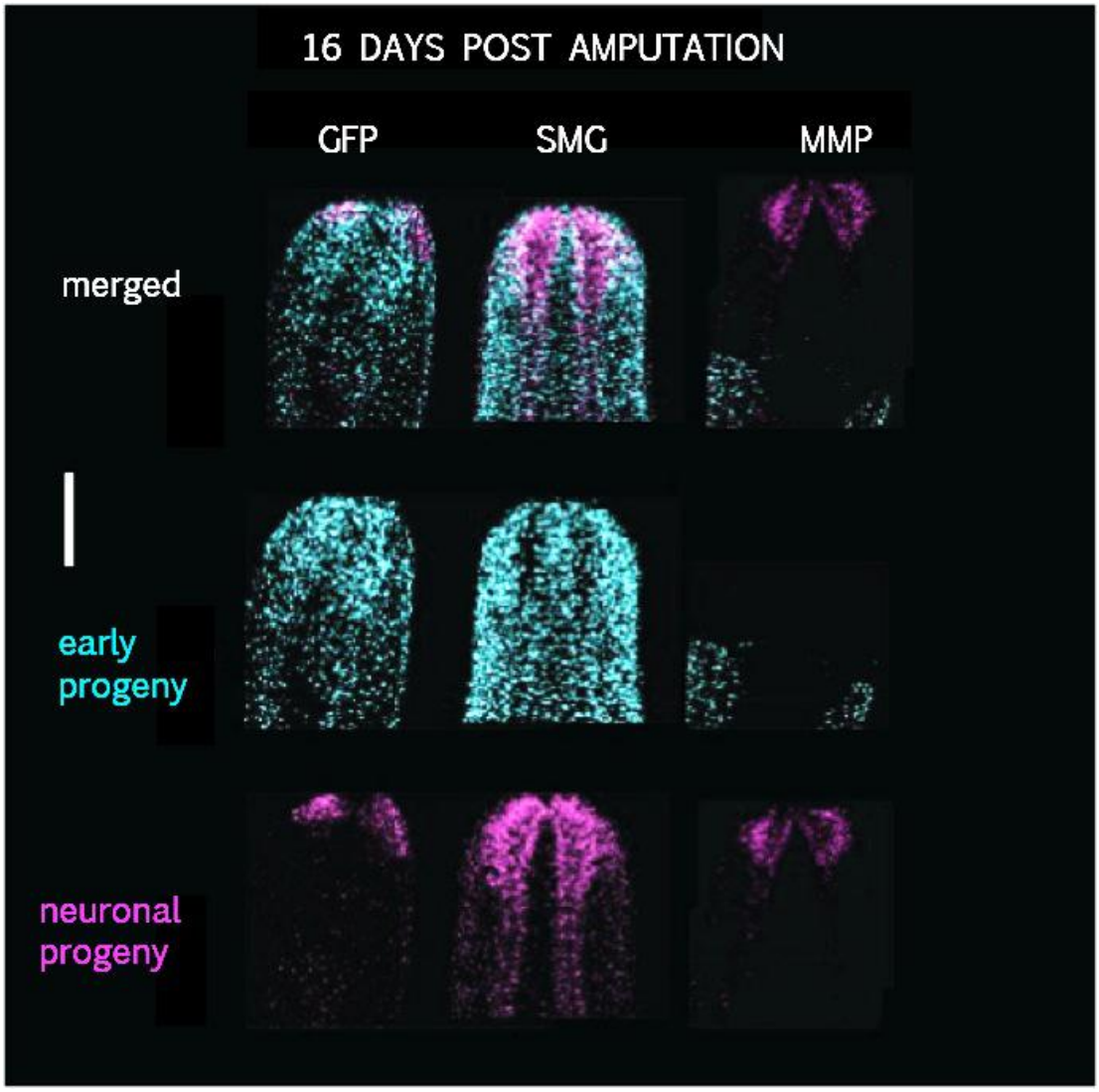

Figure 4.4. 10x confocal images showing a double fluorescent *in situ* of early progeny, NB21.11E (turquoise) and neuronal progeny cells (CHAT).

At 16 days post amputation/14 days post irradiation in GFP animals both cell types are visible in the anterior region, in SMG-1 animals the near completion of neuronal regeneration is seen at this time point, with progeny and neuronal cells organized into distinct structures as seen in homeostasis. The early progeny cells in MMP-1 knockdown animals have failed to migrate, and their overall number is reduced compared to GFP and SMG-1 animals. CHAT positive cells are also reduced, with residual expression in the anterior attributed to differentiated cells that were not removed by the amputation process. Error bars represent 500µm (n=5).

4.3.5 The absence of SMG-1 results in visible endothelial disruption due to the ectopic formation of tumour-like masses

In our research we determined that SMG-1 (tumour suppressor) RNAi, when combined with our shielded irradiation assay, in fact accelerated regeneration. At 22 days post-amputation the SMG-1 animals had completed regeneration, and continued to produce tissue ectopically (see figure 4.5). The SMG-1 knockdown phenotype reported by Gonzalez-Estevez et al. supports our observation of endothelial disruption and tumour formation. Our observations lead us to hypothesise that the increased proliferation caused by SMG-1 knockdown (as reported by Gonzalez-Estevez et al. 2012) initially had a beneficial effect on post-shielded irradiation regeneration. Specifically we proposed that the increased cell number mediated an advanced rate of repopulation of the irradiated regions, which in turn allowed regeneration of anterior structure to begin sooner. However, in the absence of a proliferation stop cue, the SMG-1 RNAi continued to produce tissue, ultimately exhibiting visible tumour-like disruption.

4.3.6 SMG-1 RNAi animals exhibit accelerated regeneration that progresses to the pathological and ectopic accumulation of cells synonymous with tumour formation

The accelerated regeneration seen in SMG-1 RNAi animals progressed into the ectopic accumulation of cells causing structural disruption

(see figure 4.5). At 22 days post-irradiation the GFP wild type animals had regenerated eyespots, and the stem cells and AGAT-1 progeny had settled into their homeostatic niches (characterised by being absent from brain structure areas shown in the Figure 4.5 as black regions). Conversely cells in SMG-1 animals have continued to proliferate. The result is that cells are resident in the brain region ectopically, and the overgrowths begin to disrupt discrete structures including the optic cup. We hypothesise that the knockdown of SMG-1 results in an increased rate of proliferation and migration that at early stages mediates accelerated regeneration, but without the tumour suppressors' function, cells continue to proliferate and become pathogenic. This observation supports the known role of tumour suppressers across phyla, often such as P53 being implicated in cancer and tumour formation.

4.4 Conclusions

This is the first use of a shielded irradiation assay in planarians to observe RNAi effects. The use of FISH to visualise cell behaviours post shielded irradiation has proved effective in identifying genes which inhibit and accelerate cell migration and regeneration. In particular these experiments have expanded our understanding of the biological roles of SMG-1 and MMP in planarians. Previous research into MMP

demonstrated that it did in fact affect regeneration. However without the shielded irradiation assay developed herein, researchers previously have been unable to attribute the MMP phenotype to migration. In this research we are able to do so, and therefore we propose that MMP in planarians acts in a similar biological fashion to that seen in other (vertebrate) models. In these instances the secretion of MMP's are necessary for the proteolytic degradation of the extra cellular matrix (ECM), which in turn results in pathway clearance for migrating cells. Based on this hypothesis of MMP function, the observed 'no migration' phenotype can be attributed to a failure of cell with migration potential to break down obstructive ECM tissues. Moreover we make the proposal that SMG-1 RNAi results in accelerated regeneration. The nature of this effect not definitively determined. Instead we observe what appears to be accelerated migration, however the visible placement of cells in regions anterior to their GFP counterparts could in fact be the result of elevated cells proliferation, an effect of SMG-1 knockdown recorded by previous researchers. Despite further testing being required to determine the exact cause of accelerated regeneration in SMG-1 knockdown animals, the fact remains that an acceleration does occur. Consequently these data are a crucial first step in demonstrating planarians as a model organism for cancer

research. This work provides key controls (SMG-1 and MMP), which will be essential in expanding the assays' use to investigate novel gene regulators in cancer-implicated processes where researchers will have the power to analyse candidate cancer associated genes to see if they accelerate or reduce cell migration relative to controls MMP and SMG-1.

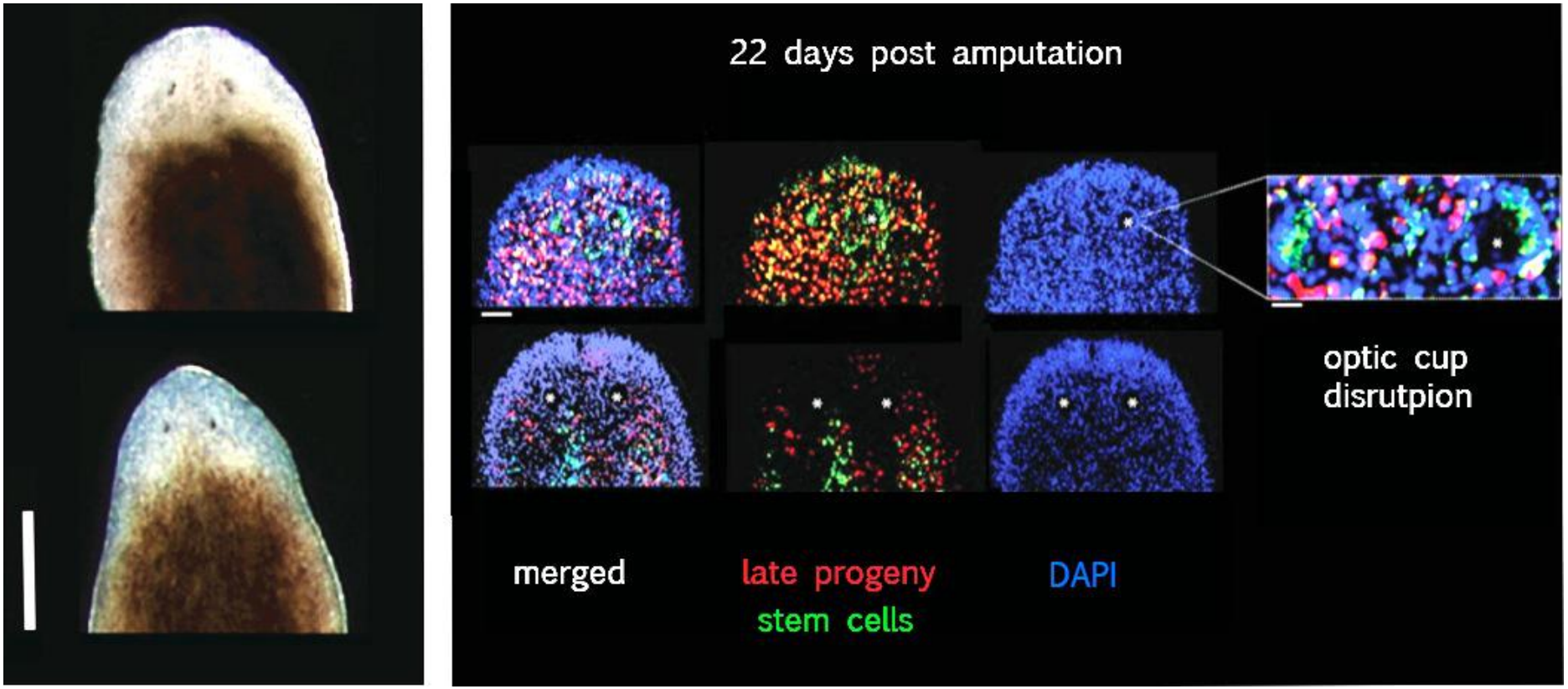

Figure 4.5: overleaf

Figure 4.5. Composite image showing SMG-1 associated ectopic endothelial disruption.
Top left live brightfield image showing the SMG-1 (RNAi) animal exhibiting ectopic endothelial disruption at time point. Error bar represents 500**µ**m (n=4). Bottom brightfield image of wild type GFP animal with eyespots formed and smooth, undisrupted endothelial. Double FISH showing the ectopic presence of stem cells (H2B, green) and late progeny (AGAT-1, red) in anterior regions of SMG-1 animals, relative to GFP animals at 22 days post amputation. In the presented example, the ectopic presence of these cell types is responsible for tissue disruption affecting eye regeneration. Scale bar represents100µm(n=5.

5. Characterization of SNAIL and MBD Knockdown Effects

5.1 Abstract

This work demonstrates a) a correlation between asymmetric cell division and b) a role of SNAIL zinc finger protein in planarian regeneration/migration is presented herein. Methyl-CpG-binding domain protein MBD 2/3 was demonstrated by Jaber *et al*[68]to affect stem cell production of late progeny (AGAT-1) cells. These data demonstrate that MBD 2/3 RNAi animals when exposed to shielded irradiation fail to regenerate. Using FISH protocols for stem cell and progeny markers allowed visualisation of the underlying cell behaviours. In the shielded irradiation paradigm MBD 2/3 RNAi animals also failed to maintain a progeny population as published previously. However, for the first time we report that MBD 2/3 knockdown effect include an absence of cell migration. SNAIL RNAi was carried out on animals under normal regeneration conditions, and as predicted based on unpublished work carried out by Dr. Jochen Rink, no phenotypes were visible, and animals regenerated normally. Using the shielded irradiation paradigm SNAIL RNAi animals failed to regenerate. FISH investigations were used to visualise the underlying cell behaviour, and SNAIL RNAi animals were able to maintain their stem cell and progeny populations, however these cells were unable to migrate. This presents the first example of an assay able to detect phenotypes undetectable

by traditional techniques. This work demonstrates that the developed shielded irradiation assay can be used to provide novel insight into gene function for future studies.

5.2 Introduction

The experimental investigation of molecular regulators involved in cancer progression form the foundation of this thesis. In Chapter 4 we focused on the cancer cell processes of ectopic migration (MTMMPA) and hyper proliferation (SMG-1). In Chapter 5 we expand our investigations to include the cancer implicated processes of 1) Epithelial to Mesenchymal Transition (EMT) and 2) Proper progeny production which could be related to asymmetric cell division or differentiation.

1) EMT is a key process during critical phases of embryonic development and results in a cell's transformation from an epithelial phenotype to a mesenchymal one [80-83]. These newly formed mesenchymal cells acquire a morphology which allows them to migrate within the extracellular matrix environment (ECM) and settle in regions where they are involved in organ development [84]. However, in cancer there is good evidence that EMT processes occur as part of a dedifferentiation program that facilitates the dissemination of epithelial originating carcinoma cells from primary tumour sites, where they are then involved in secondary tumour establishment [85-89]. Specifically, research has shown that the activation of signal transduction pathways associated with a variety of receptor tyrosine kinases and

transforming growth factor (TGF'S) receptors, results in the transcriptional repression of the E-Cadherin gene [85]. E-Cadherin protein clusters when active are important stabilisers of epithelial cells through anchoring them to one another using actin microfilament linking. Consequently the repression of E-Cadherin severs these anchoring connections, leaving cells free to migrate. The Snail family of zinc finger transcription factors are best known for their role as direct repressors of E-Cadherin transcription during tumour progression. Subsequently a Snail family member was chosen for experimental investigation in this chapter.

2) Proper cell division and the differentiation of progeny is a complicated yet interesting concept. Tumours are formed, maintained and expanded as a result of constant cancer cell divisions [74]. Asymmetric division seen in healthy cells results in the production of functional daughter cells that divide and differentiate in order to contribute to tissue renewal and organ formation [74, 90]. However in cancer, we see the asymmetric division and or differentiation are adversely affected, resulting in the production of defective daughter cells that are unable to give rise to healthy tissue. Instead these mutated cells form key propagating components of the tumour mass [74, 90]. In some cancers progeny transiently amplify, giving rise through

symmetric division to many more of themselves. However, a growing mutational load is amplified with each cell division, making true symmetric division and differentiation by transiently amplifying daughter cells improbable. This mutable phenotypic paradigm represents the core treatment barrier in all cancers. The ability to target a cancer cell, and ablate it, along with all its partners is dependant on an ability to identify them using common markers. Phenotypic variation due to deranged cell division makes conserved marker identification difficult. The gene MBD 2/3 is one identified in planarians by Jaber et al., 2013[68] to encode for a Methyl-CpG Binding Domain (MBD) protein. Its knockdown resulted in a regeneration defect, which when investigated further by Jaber *et al.* was found to be associated with a breakdown in progeny production, which could be the result of an affect on stem cell division, or progeny differentiation. MBD RNAi animals' stem cells were able to divide symmetrically, to maintain their population. They were also able to give rise to early progeny cells (NB21.11E positive). However, late progeny (AGAT-1 positive) cells were depleted in MBD 2/3 knockdown, leading the author to conclude that the gene was required for proper differentiation of AGAT-1 progeny cells. Consequently it was decided

that MBD 2/3 would make an interesting subject for our investigations in this chapter.

5.2.1 Study Aims

The broad aim was to expand our use of the bespoke shielded irradiation assay to investigate and partially characterise a gene previously uncharacterised in planarians (SNAIL). We were aware that unpublished works had been carried out that attempted to knockdown SNAIL, but no observable phenotypes had been identified. We also wanted to see what effects of the MBD 2/3 knockdown might have on cell migration.

Specific questions raised as a result of both the Jaber-Hijazi et al. 2013[68] publication, and a review of the wider literature were:

1. Could the shielded irradiation paradigm be used to uncover otherwise undetectable phenotypes?
2. Was SNAIL required for stem cell and/or progeny migration in planarians?
3. Did stem cells and/or their progeny migrate in MBD 2/3 knockdown animals?
4. In which case could stem cells migrate in the absence of Agat-1 progeny cells?

5.3 Results & Discussion

5.3.1 The Identification of 3 planarian SNAIL superfamily homologs using bioinformatics analysis

Searching available transcriptome databases identified three planarian homologs of the Snail family of zinc finger transcription factors (see figure 5.1 and 5.2). When aligned with 34 SNAIL family genes from different species the identity of the planarian genes were confirmed as *SNAIL*, *SNAIL-like* and *scratch* homologs. The results presented here correspond with predictions based on a metazoan-wide phylogeny of the family published by Nieto *et al.,* 2005 [80] where it is proposed additional members of Snail family such as *Worniu* and *Slug* arose only in Ecdysozoa and Chordata lineages respectively. This gene family is of particular interest because of its known role in cancer biology [91]. Specifically Snail transcription factors act as primary inducers of the Epithelial-mesenchymal transition (EMT)[91]. EMT is a complex process that is involved in the loss of E-cadherin and the truncation of glycoprotein MUC1 [84]. Both E-cadherin and MUC1 aberrance are associated with cancer invasiveness and metastasis [92, 93]. Subsequently SNAIL expression has been used to mark invasive cells in several cancers [92]. In invasive breast cancer, SNAIL expression is detectable but is not in healthy breast tissues [94]. It would therefore

be potentially interesting to compare SNAIL expression levels between wild type and SMG-1 (RNAi) animals.

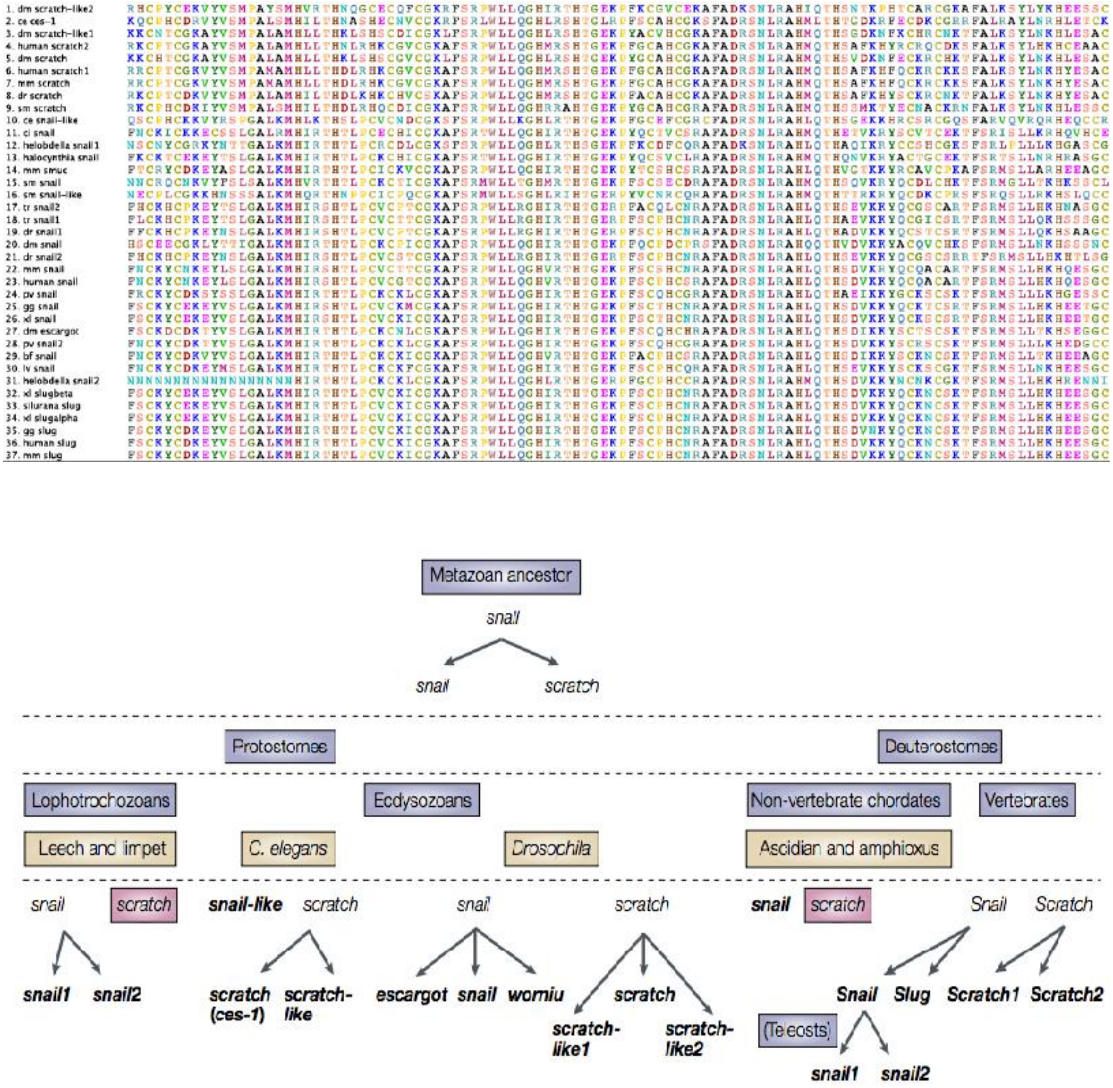

Figure 5.1. An alignment of three putative planarian SNAIL family homologs

A. An alignment of three putative planarian SNAIL family homologs (sm) with a selection of SNAIL family members from the Lophotrochozoa, Ecdysozoa and the Deuterostome clades taken from Nieto 2002[80]. *Schmidtea mediterranea* sequences are numbers 9, 15 and 16 in the alignment list **B.** The proposed evolution of the SNAIL gene superfamily begins with the duplication of a founding SNAIL gene in the common ancestor, giving rise to two genes, SNAIL and SCRATCH. Independent duplication events in Protostomes and Deuterostomes gave rise to a different number of family

members in each group; this figure is unchanged and taken from Nieto , 2002[80].

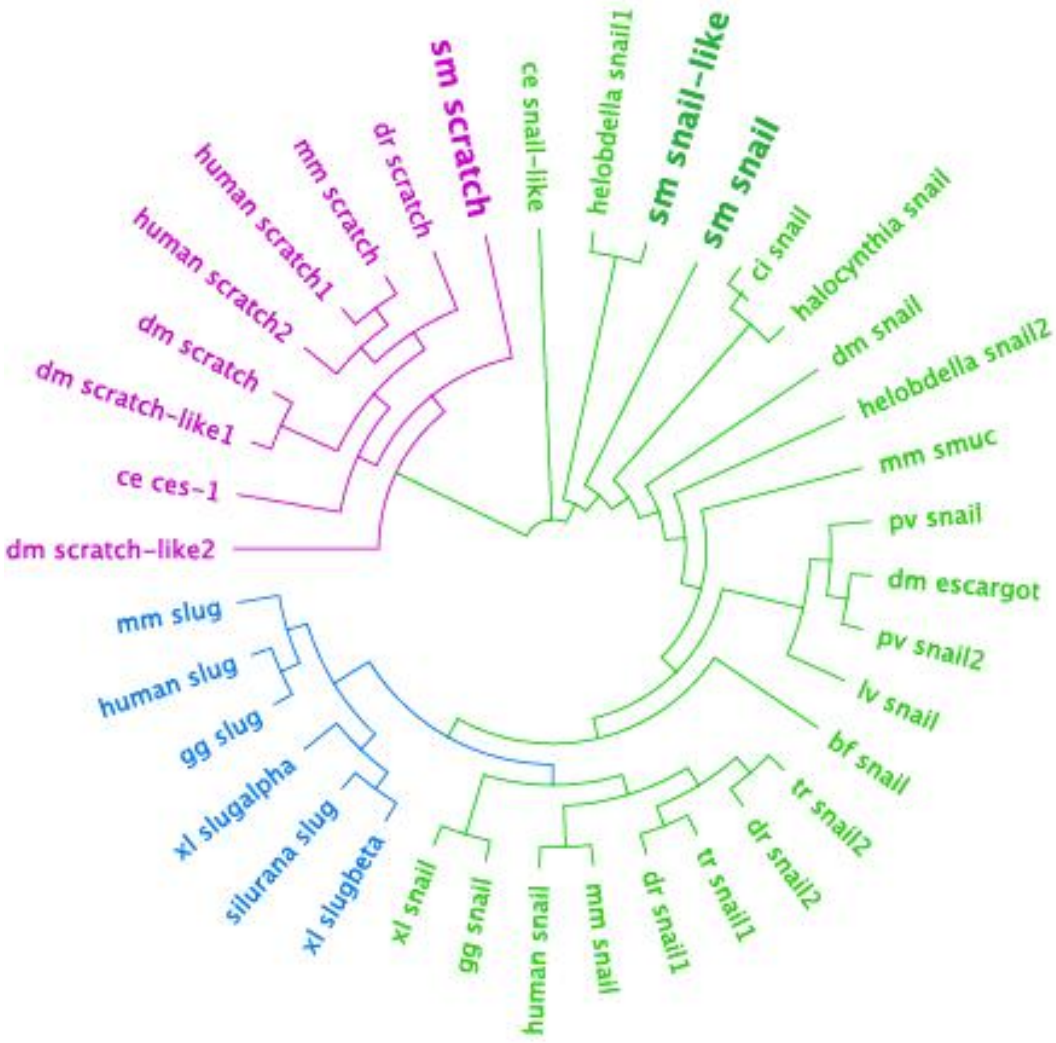

Figure 5.2. Un-rooted radial tree of the SNAIL superfamily using zinc finger alignment

Un-rooted radial tree of the SNAIL superfamily using zinc finger alignment from Figure 8. **A.** Magenta highlights the Scratch family members while Slug and SNAIL members are grouped in blue and green respectively. The species shown represent members of the lophotrochozoans: pv, *Patella vulgata* (limpet) and sm, *Schmidtea mediterranea;* ecdysozoans*:* ce, *Caenorhabditis elegans* (nematode); dm, *Drosophila melanogaster* (fruitfly); and deuterostomes*:* bf, *Brachiostoma floridae* (amphioxus); ci, *Ciona instestinalis* (ascidian) and hr, *Holocynthis roretzi (ascidian);* dr, *Danio rerio* (zebrafish); gg, *Gallus gallus* (chicken), hs, *Homo sapiens* (human); lv, *Lytechinus variegatus* (green sea urchin); mm, *Mus musculus* (mouse); tr, *Takifugu rubripes* (pufferfish); and xl, *Xenopus laevis* (African clawed frog). This tree is a modified version from the tree published by Nieto 2002[80].

5.3.2 A shielded irradiation technique can uncover otherwise undetectable phenotypes

The bespoke shielded irradiation assay developed by this project produces significant regions void of proliferating cells. We hypothesised that this blank canvas paradigm would induce cell migration, a proposition supported by work carried out by Guedelhoefer *et al.* (2013). We also surmised that in the normal planarian regeneration context, the ubiquitous distribution of stem cells meant that certain cell behaviours of interest to us might not be highly expressed. Specifically, if stem cells are usually situated near and around the wound site, then the loss of active migration ability through SNAIL RNAi may not produce a visible phenotype. Conversely, in the shielded irradiation paradigm, stem cells are no longer ubiquitously distributed. In fact stem cells are instead clustered in regions distant from the area (anterior) requiring regeneration. We hypothesised that this restricted population effect of shielded irradiation would produce a migration assay. Specifically, cells would need to migrate from the shielded zone up to the wound site in order to respond to wound signals and to begin the regeneration process of repair. Consequently we hypothesised that SNAIL RNAi may produce an observable phenotype in this paradigm. Based on the

significant body of literature presenting increased SNAIL expression as being associated with increased cell migration, we predicted that SNAIL RNAi would prevent cell migration in planarians. Brightfield images taken of SNAIL RNAi animals 23 days post shielded irradiation show no regeneration when compared to wild type (GFP RNAi) animals at the same time points (see figure 5.3 and 5.4). A positive control, MBD 2/3 RNAi animal, shown by Jaber-Hijazi et al. 2013[68] not to regenerate in traditional regeneration experiments, also failed to regenerate post shielded irradiation. Our subsequent prediction was that in the absence of SNAIL function, planarian stem cells and or their progeny were unable to repopulate anterior regions as required to ultimately regenerate them.

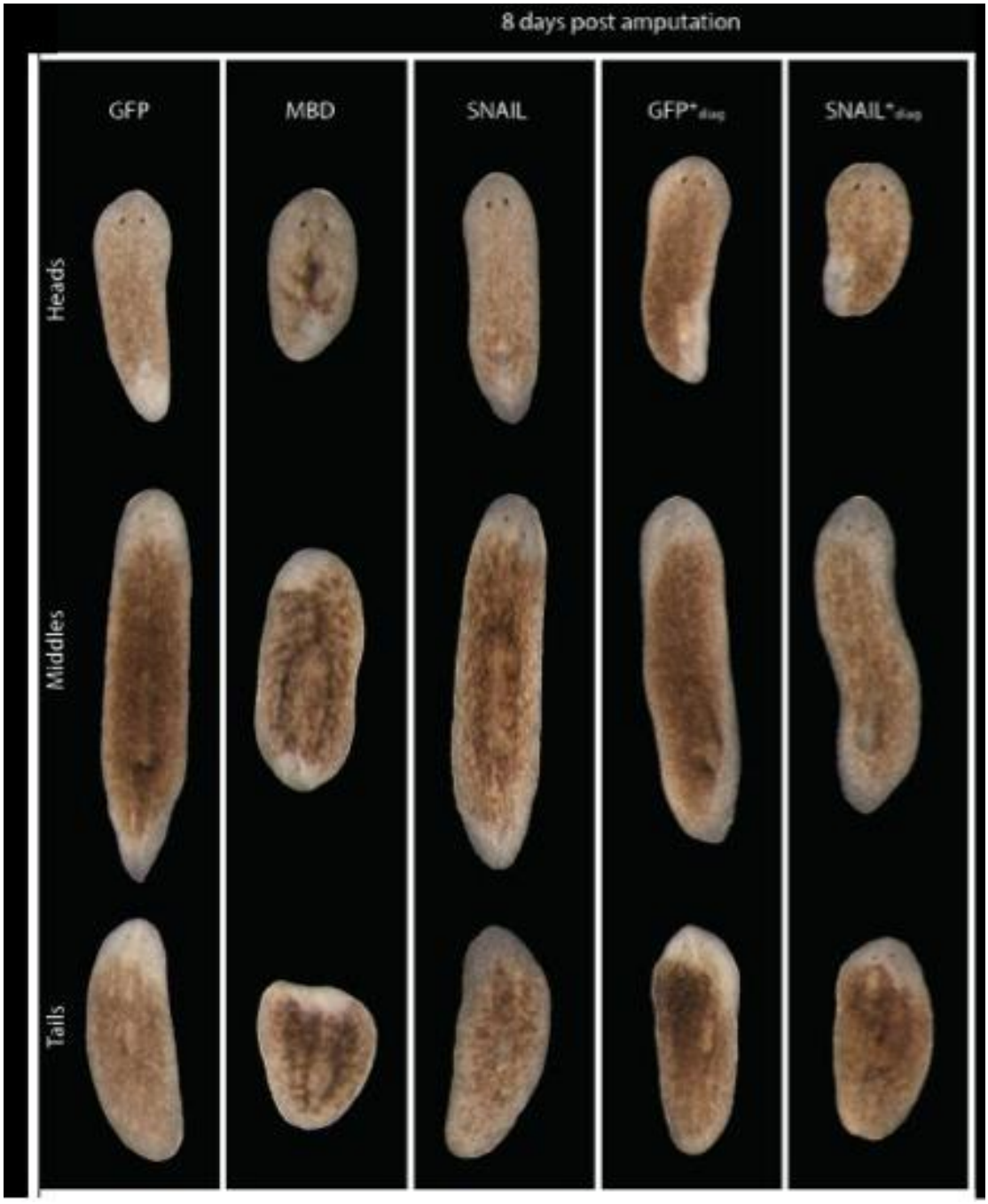

Figure 5.3. Brightfield images showing SNAIL, MBD and GFP at 8 days regeneration

Brighfield images show regeneration 8 days after pre and post pharyngeal amputation to produce head, middle and tail pieces. All animals were subjected to 2 weeks of DsRNA injections. Each column of images represents a different loss of function experiment. From left to right the columns show GFP (negative control), MBD and SNAIL RNAi animals. All GFP animal pieces have regenerated eyespots, MBD animals have failed to regenerate anterior structures and also have not produced a new pharynx in the headpiece.

There is also no notable remodelling on existing structures to accommodate rescaling. SNAIL animals also appear to regenerate normally. The subsequent two columns show brightfield images of GFP and SNAIL after diagonal pre and post pharyngeal amputations to see. The aim of diagonal cuts was to observe if a SNAIL phenotype could be induced. However both GFP and SNAIL diagonally amputated animals appear to regenerate normally. Scale bar represents 500 **µ**m (n=8).

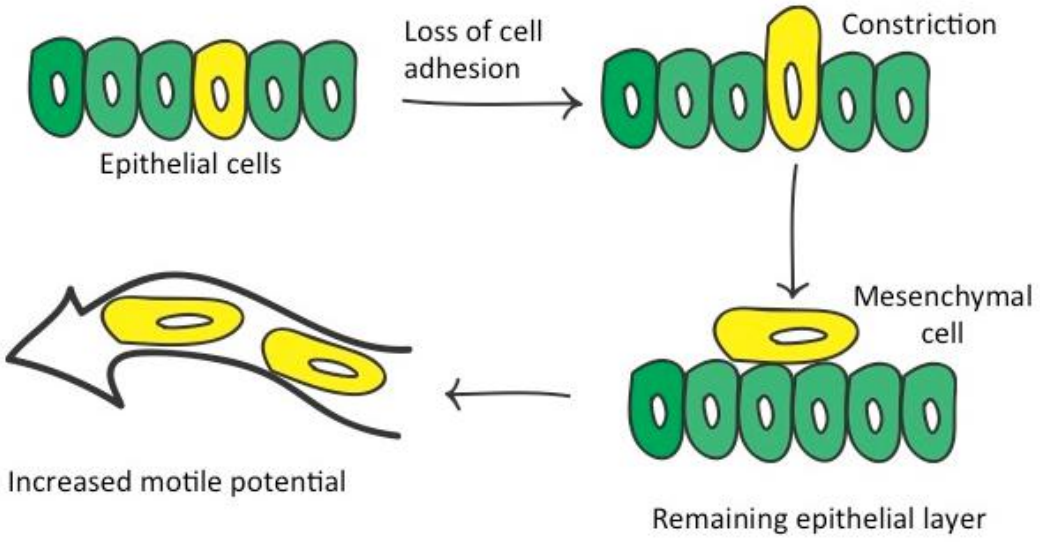

Figure 5.4. Brightfield images showing SNAIL, MBD and GFP at 23 days shielded irradiation with simplified schematic of EMT

Brightfield images show regeneration 23 days post shielded irradiation for RNAi animals (GFP, MBD and SNAIL). All animals were subjected to 2 weeks of DsRNA injections, followed by 30 Gy irradiation using 1mm shield as previously described, followed by anterior amputation at 48 hours post irradiation. GFP animals (9/10) have by 23 days regenerated anterior

structures, however as expected, tail regression and posterior tissue darkening is visible. This posterior regression will resolve in all animals by 35 days post irradiation as reported by Guedelhoeffer *et al.* (2013). SNAIL animals, which did not prove phenotypic in a normal regeneration paradigm, fail to regenerate after exposure to shielded irradiation. The above diagram represents the primary known function of SNAIL in other organisms. SNAIL promotes the decreased expression of Cadherin's, which are responsible for the adhesion of cells to basements membranes. The absence of Cadherin's, due to SNAIL activity increases cell motility in many cancers. Error bars represent 100 μm (n=8).

5.3.3 Proper cell division dynamics and active migration are essential for anterior regeneration

At 10 days post-irradiation the stem cell and progeny niche of wounded control wild type animals (GFP) have not yet migrated significantly (Figure 5.5). The majority of cells are found within the shielded region. From earlier research carried out in this project it is known that an element of cell spread can be observed when compared to an unwounded animal. However wild type animals maintain a dense population of stem cells and progeny in the shielded region throughout the post-irradiation regeneration process. This cell reserve is hypothesised to be responsible for migrating to the wound site to directly initiate regeneration, and for proliferating to produce progeny of various lineages that will themselves contribute to tissue production. In the MBD 2/3 RNAi animals at day 10, the levels of stem cells and of their progeny are noticeably reduced (Figure 5.5). Specifically, stem cells appear to be present, albeit in reduced numbers relative to the wild type, however, progeny AGAT-1 positive

cells are drastically reduced to almost undetectable numbers. This observation supports the published work by Jaber et al. (2013)[68] who concluded that MBD 2/3 was required for proper asymmetric cell division, while was less important for symmetric, self-renewal divisions. At this time point there is also no migration visible in MBD 2/3 animals. The SNAIL RNAi animals appear at this time point to represent a mean phenotype. The overall number of stem cells and progeny are reduced relative to the wild type animals, but are elevated when compared to MBD 2/3 RNAi. At this early time point we hypothesise that the 'failure to regenerate' as observed by Brightfield for both MBD 2/3 and SNAIL RNAi may be to some level associated with reduced cell numbers. At 18 days post-irradiation (Figure 5.6) wild type GFP animals have entered anterior regeneration. Their stem cell and progeny cell populations now span from the shielded region and include the most anterior portions of the animals. A significant amount of tissue repopulation has occurred, with cells now ubiquitously distributed across the anterior region. At this time point stem cell and progeny are not restricted to their homeostatic niches.

Conversely the MBD 2/3 animals still do not show any significant cell migration. Their numbers of stem cells are still high, but progeny

production and maintenance remains extremely low. It is possible therefore that MBD 2/3 has an unknown role in stem cell migration, and that its RNAi prohibits stem cell movement.

Alternatively, we propose, that progeny cells are integral in facilitating cell migration, and that they play a permissive role in enabling stem cells to mobilise. Specifically we hypothesise that progeny cells receive and integrate signals from both the wound site and other differentiated tissues, which they then relay to stem cells, mediating their guided mobilisation.

In the case of SNAIL RNAi at day 18 post-irradiation we see a different phenomena. Both stem cells and progeny are present, their numbers are reduced compared to wild type, however there is a significant population of H2B (stem cell) and AGAT-1 (progeny) cells still maintained.

Consequently we propose that the absence of SNAIL function does not directly affect stem cells ability to self renew or to asymmetrically divide, but does affect migration. In SNAIL RNAi no migration is observable at this time point. A lack of migration would support the hypothesis that SNAIL function is required for active migration, possibly through its role in Cadherin down-expression seen in other

species. Consequently we propose that SNAIL is required for stem cell and progeny migration in planarian regeneration, and that the failure to regenerate observed in Brightfield images is at least somewhat attributable to a failure in cell migration.

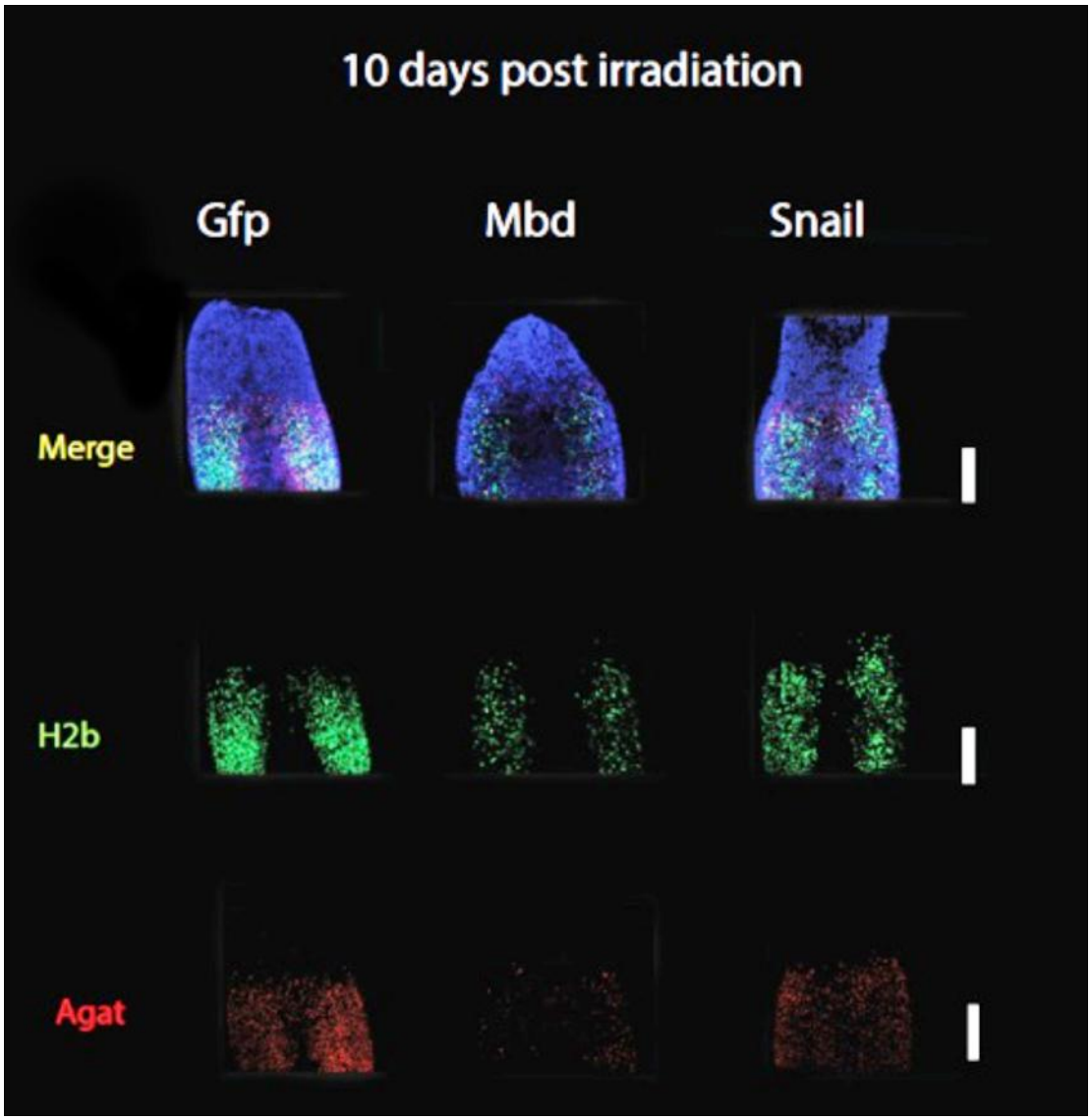

Figure 5.5: overleaf

Figure 5.5. Confocal FISH images at 10x showing the distribution of stem cells and late progeny at 10 days post shielded irradiation
Confocal FISH images at 10x showing the distribution of stem cells (H2B) in green and late progeny (AGAT-1) at 10 days post-shielded irradiation. GFP

animals have the expected distribution of stem cells and progeny. No significant migration has at this time occurred, but stem cell and progeny numbers are being maintained, and at closer magnifications some cell spread anteriorly has begun. The MBD animals have an observable reduction of progeny, as expected, and reported by Jaber *et al.* (2013). The SNAIL RNAi animals appear similar to GFP animals at this time. Both stem cells and progeny are being maintained, and no significant migration is observable at this magnification. Error bars represent 500 µm. (n=5)

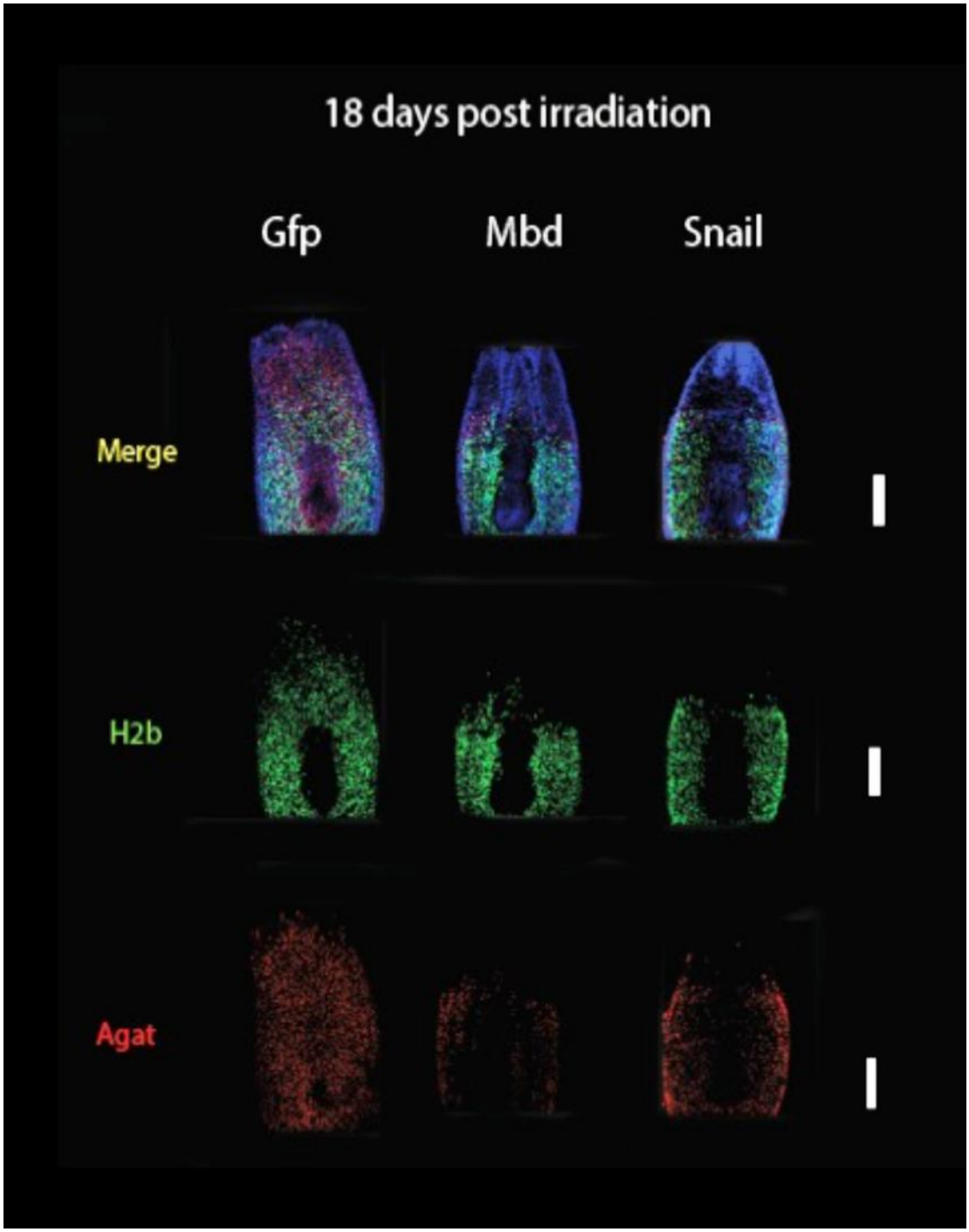

Figure 5.6: see overleaf

Figure 5.6. Confocal FISH images at 10x showing the distribution of stem cells and late progeny at 18 days post shielded irradiation
Confocal FISH images at 10x showing the distribution of stem cells (H2B) in green and late progeny (AGAT-1) at 18 days post shielded irradiation. GFP stem cells and progeny occupy the most anterior regions of the animal. In gfp animals the progeny appear to dominate in number at the most anterior tip. MBD animals continue to maintain stem cell numbers, however no significant migration occurs, and progeny depletion is still evident. SNAIL animals interestingly also show little migration. Unlike MBD animals, the failure to migrate phenotype is not associated with a reduction in progeny numbers.. Scale bars represent 500μm.

5.4 Conclusion

This is the first effort in the planarian model to investigate the relationship between cell division, differentiation and cell migration. These data are the first to demonstrate that a loss of late progeny as seen in MBD 2/3 correlates with a lack of cell migration. Moreover, this is the first instance in the planarian model where RNAi of the well-known zinc finger protein associated with EMT in cancer SNAIL has given rise to a phenotype. Importantly, this demonstrates that SNAIL function is required for cell migration as reported in other phyla, and that the shielded irradiation assay can be used to detect phenotypes that are unobservable in other approaches. It is likely that the lack of observable phenotype seen in previous SNAIL RNAi in planarians may be due to the ubiquitous distribution of stem cell sin healthy animals. The planarian is itself one large fairly un-compartmentalised entity consisting of stem cells which occupy 80%

of its body mass. Consequently is it possible that as a result the animal is able to regenerate even without SNAIL mediated migration.

6. Novel Regulators of Regeneration

6.1 Abstract

The first use of the Oncomine web-based microarray database to identify 289 planarian orthologs for cancer-implicated genes. Planarian orthologs were selected based on a filtering process to exclude non-coding RNA's, pseudogenes, fusion genes, core eukaryotic genes and genes which were already highly investigated (determined based on publication number). Ten genes were taken forward for experimental investigations including controls (GFP and SMG-1), a common tumour suppressor of interest (P53) and 7 Oncomine genes (FAM21A, KIF20A, AHNAK, WDR12, TRIP13, UAP1 and BYSL). Animals were injected with DsRNA on a standard 2-week regime and then separated into condition groups. A homeostatic sample group were put aside immediately after injections and left. These animals were live imaged ~1 week later and UAP1 RNAi (numerical ID 81) animals were exhibiting head regression. Head regression is associated in planarians with stem cell dysfunction [2]. No phenotypes were observable in a traditional regeneration phenotype, however with RNAi, three of the remaining Oncomine genes (WDR12, TRIP13 and BYSL) with numerical IDs 15, 81 and 87 respectively, produced animals with regeneration defects. This research forms a foundation for future research into

these previously uncharacterised genes in planarians using FISH to observe cell behaviour. This work also critically demonstrates the success of a non-candidate gene approach using RNA-seq data.

6.2 Introduction

Genes of interest in this thesis have thus far been selected using a traditional candidate gene approach. However, choosing specific candidate genes based on *a priori* hypotheses about their role in disease is somewhat subjective, and essentially precludes the identification of novel genes and pathways which have putatively important roles in disease. Consequently, in this chapter, we mined existing web-based microarray data to examine differential gene expression between cancer and control tissues in order help pinpoint potential genes of interest for experimental investigation.

We elected to use the web-based data-mining platform Oncomine (www.oncomine.org) [95, 96] which contains over 48 million gene expression measurements from 500 microarray experiments. Differential expression analyses results comparing most major types of cancer with respective normal tissues are available from the Oncomine platform for exploration by interested researchers [95, 96].

In addition to exploring a non-subjective gene selection process, the experiments designed in this chapter also aimed to test the viability of 'upscaling' the shielded irradiation assay to allow the simultaneous investigation of multiple genes experimentally.

Consequently, a pilot group of 10 genes including controls were selected for testing.

6.2.1 Study Aims

The aim of the research carried out in this chapter was to test the use of microarray differential analyses to select genes for experimental investigations. The hypotheses being that a) a less subjective approach than candidate gene selection would be desirable and b) may encourage the identification of novel putative regulators of disease.

It also is the aim of this body of work to test the upscale potential of the shielded irradiation assay, to determine if it is plausible for a single or pair of researchers to launch a large-scale screen using differential expression data.

Specific questions posed in this research were:

1. Is it practically possible to experimentally investigate 10 genes simultaneously taking into consideration the injection, cutting and observation regimes required?
2. Can Oncomine data be filtered to successfully generate a list of candidate genes?

3. Would any of the generated candidates give rise to observable phenotypes?

6.3 Results & Discussion

6.3.1 Identification of 289 planarian orthologs to putative cancer related genes

From an initial dataset of 600 human (h) differentially expressed genes selected from the Oncomine database, 289 were determined to have high confidence putative orthologs in *Schmidtea mediterranea* (see figure 6.1). The original 600 (h) gene dataset was selected from across six cancers (lung, breast, colorectal, prostate, stomach and liver). A decision to restrict/target the types of cancer addressed in this study was made in order to produce a manageably sized dataset from our initial Oncomine extraction. The six cancers were selected based on the premise that when considered in combination, they represent approximately 70% of cancer incidences worldwide. Dr. Nobuyoshi Kosaka manually checked the 600 genes using NCBI blast. Any genes that were categorised as non-coding RNAs, pseudo genes and fusion genes were excluded. Genes categorised as hypothetical proteins were retained in the dataset for their potential as novel cancer implicated genes. The 600 (h) genes encoded for 2119 unique protein sequences (all duplicated sequences were removed, and all splice variants were retained). The 2119 protein sequences were batch

blasted against the *Schmidtea mediterranea* (smed) transcriptome database (Aboobaker-Oxford version) by Dr. Sujai Kumar using tblastn and an E-value of <1e-5. All hits to the smed transcriptome were in turn batch blasted against the complete human refseq protein database using blastx and <1e-5. The results were filtered, and instances where the original Oncomine human query featured in the top 10 blast results were classed as 'hits' and categorised as putative orthologs. This resulted in 289 putative orthologs, of which 20 were dismissed as core eukaryotic genes after blasting against the core eukaryotic gene mapping approach (CEGMA) database. All genes were allocated numerical IDs for convenience. It was decided to select 10 genes for an initial upscale attempt of the RNAi/shielded irradiation approach developed and discussed in Chapters 3, 4 and 5. Of these 10 genes 2 were controls (SMG-1, GFP), 1 was a well known tumour suppressor of interest (P53) and 7 were selected from the final Oncomine ortholog dataset (with the following numerical IDs 4, 7, 14, 15, 81, 83 and 87).

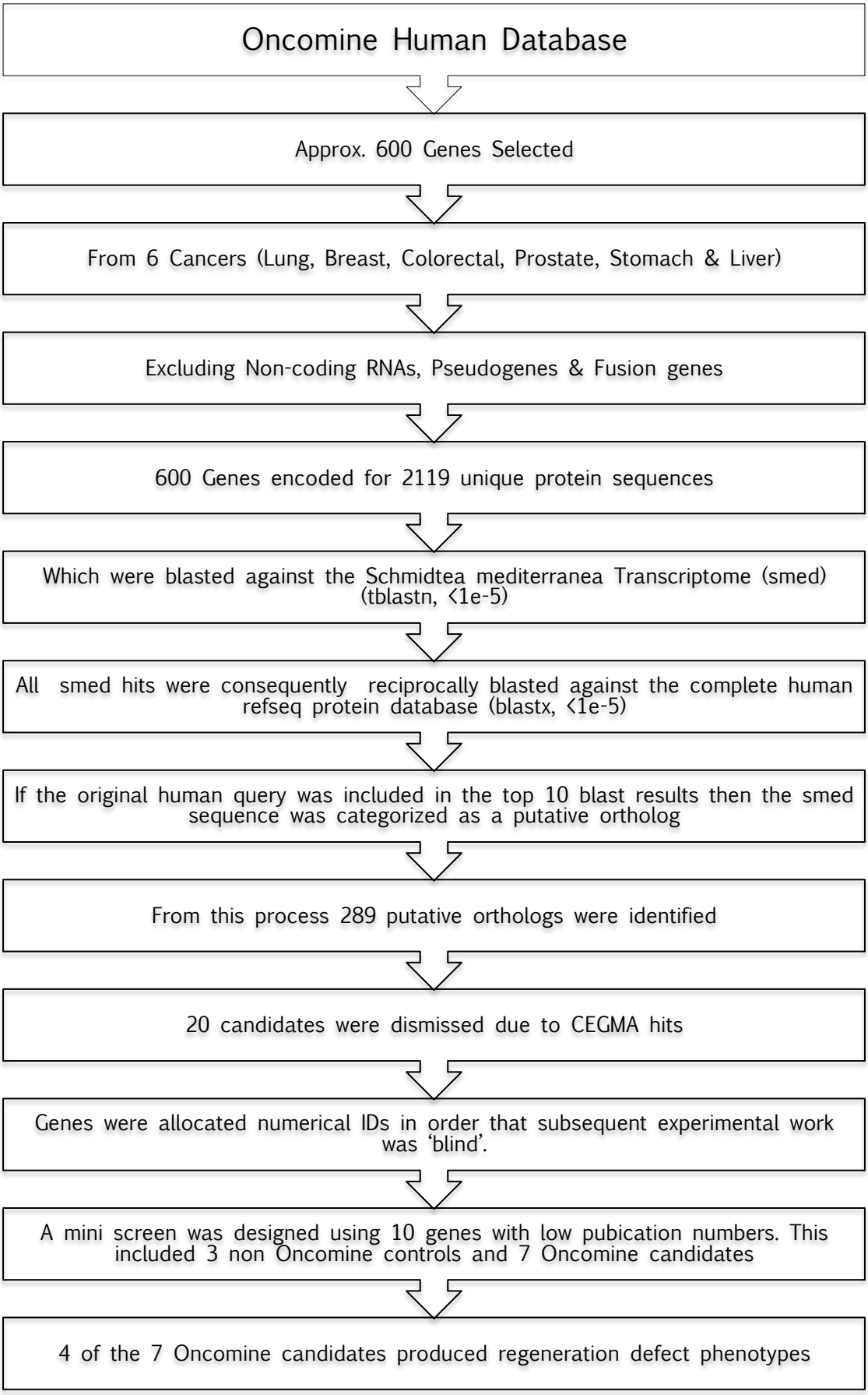

Figure 6.1: overleaf

Figure 6.1. Flow diagram showing Oncomine selection criteria
Flow diagram showing Oncomine selection criteria where ~ 600 human gene sequences were selected from across 6 cancers (lung, breast, colorectal, prostate, stomach and liver). Non-coding RNAs, pseudo genes and fusion genes were excluded through manual blast searches. The 600 genes were found to encode for 2119 unique protein sequences that were then cross-referenced against the CEGMA database. Those proteins determined as Core Eukaryotic were discarded. Remaining sequences were blasted against the *Schmidtea mediteranea* (smed) transcriptome. All smed hits were consequently reciprocally blasted against the complete human refseq protein database, and those with the original human query in the top 10 blast results were deemed putative orthologs. From this process 289 orthologs were identified. A sample of 7 Oncomine genes from the 289 were selected to take forward for experimental testing, selected by their low publication numbers as determined from PubMed. Three genes were controls used in earlier chapters.

6.3.2 A significant number of genes were differentially expressed in all 6 selected cancers

Of the ~ 269 genes with planarian orthologs 23% were shown to be differentially expressed across all 6 cancers types (see figure 6.2). 2% were expressed in both colorectal and gastric cancers. We found the remaining genes were only differentially expressed in individual cancers 18% (prostate), 15% colorectal, 12% liver, 11% breast, 10% lung and 9% gastric. Investigating further the underlying cause of this distribution is not within the remit of this study. However one of many hypotheses could be that key driver mutations give rise to cancer by affecting one or more genes from a core pool of genes defined as capable of propagating a carcinogenic cascade when affected by said

mutations. These core cancer-propagating genes could be conserved across tissues types.

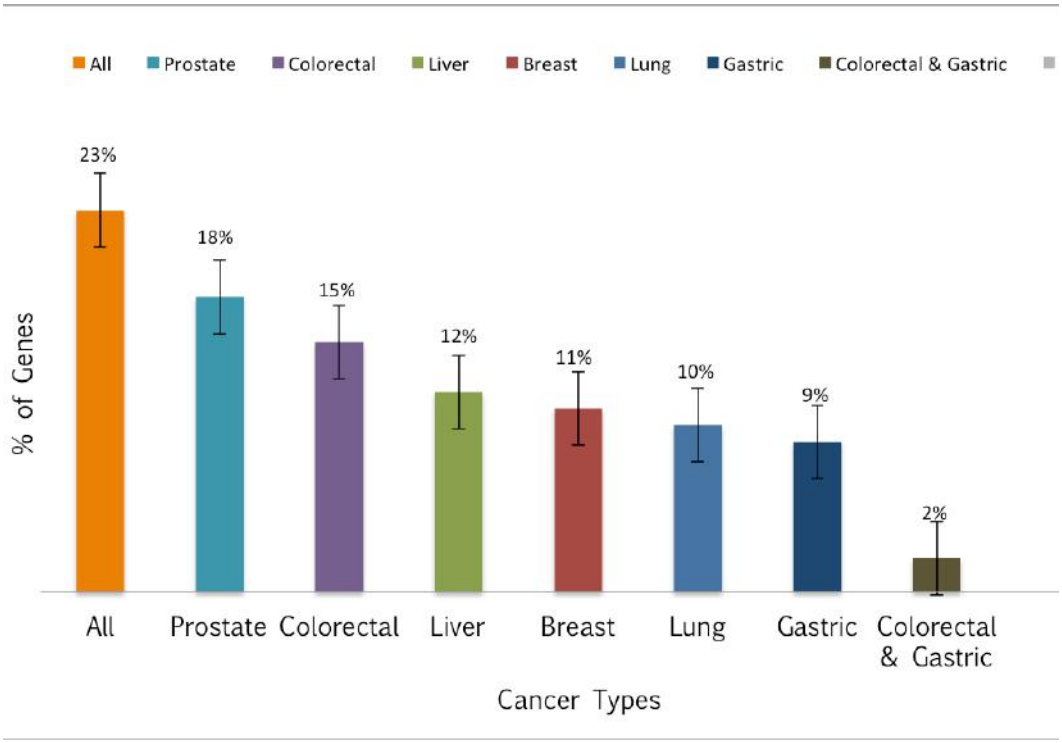

Figure 6.2. Bar chart showing the percentage of genes distributed across the selected cancer types

Of the 289 genes that were deemed to have 'hits' based on the flow diagram of Figure 6.1 23% of genes in the dataset were found across all cancers, 18% were prostate specific, 15% colorectal specific, 12% liver specific, 11% breast specific, 10% lung specific and 9% gastric specific. 2% of genes were expressed in both colorectal and gastric cancers. Error bars represent standard error of the mean (SEM).

6.3.3 The 289 orthologs data set was comprised of genes which were known to be over and under expressed in cancer microarray studies

Within each set of genes grouped based on cancer type, there is a mix of genes which are over and under expressed relative to normal tissue (see figure 6.3). In the all cancer group 54% are over expressed

(o) and 46% are under expressed (u). In prostate cancer the split is 47%(o):53%(u), colorectal 45%(o):55%(u), liver 56%(o):44%(u), breast 62%(o):38%(u), lung 55%(o):45%(u), gastric 64%(o):36%(u). Only those genes found in both colorectal and gastric cancers are 100% over expressed. A generally similar proportion of over and under expressed genes is seen across several of the groups (all, prostate, colorectal, liver, breast, lung, gastric). This in the broadest sense is likely attributable to the complex and vast array of gene network pathways involved in cancers, where both activation and repression of gene function is commonly observed.

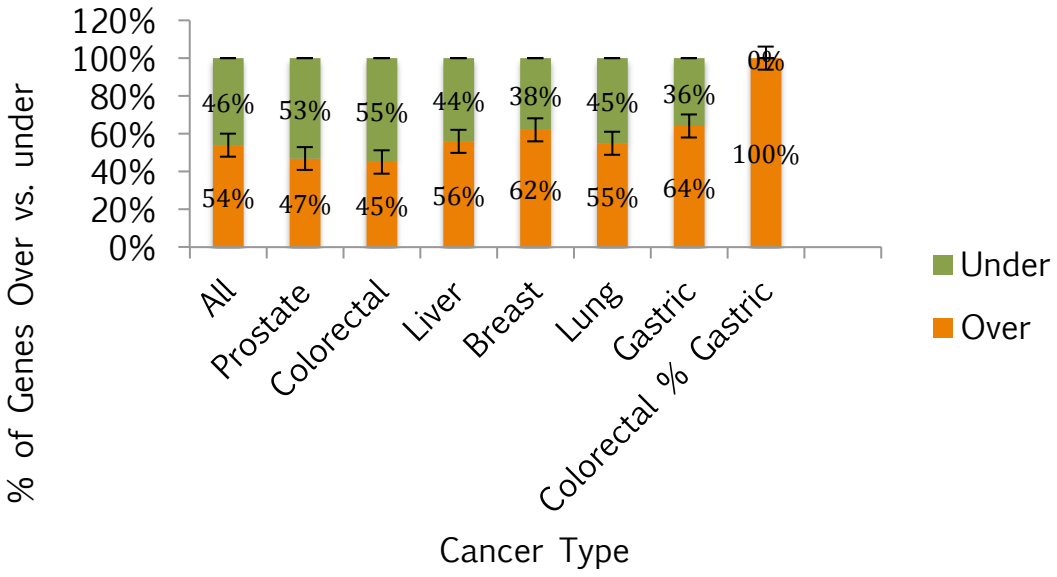

Figure 6.4. overleaf

Figure 6.4. Stacked bar chart showing the percentage of over versus under expressed genes in the total dataset, grouped based on cancer type

There is no significant difference (error bars represent standard error) in the proportion of over/under expressed genes in the groups all, prostate, colorectal, liver, breast, lung and gastric. However in genes found in both colorectal & gastric are only over expressed genes in this group.

6.3.4 10 genes were selected for experimental purposes based on their (low) publication numbers

Genes from the Oncomine dataset that we selected to be taken forward for RNAi shielded irradiation experiments were chosen based on the number of publications found for them in PUBMED (see figure 6.4 and table 6.1). The manual search of the PUBMED database for each gene by Dr. Nobuyoshi Kosaka allowed genes to be ranked based on their total publication number and on their cancer related publication number. Based on this process, genes were selected with relatively low publication numbers due to their potential for providing novel insights into cancer progression.

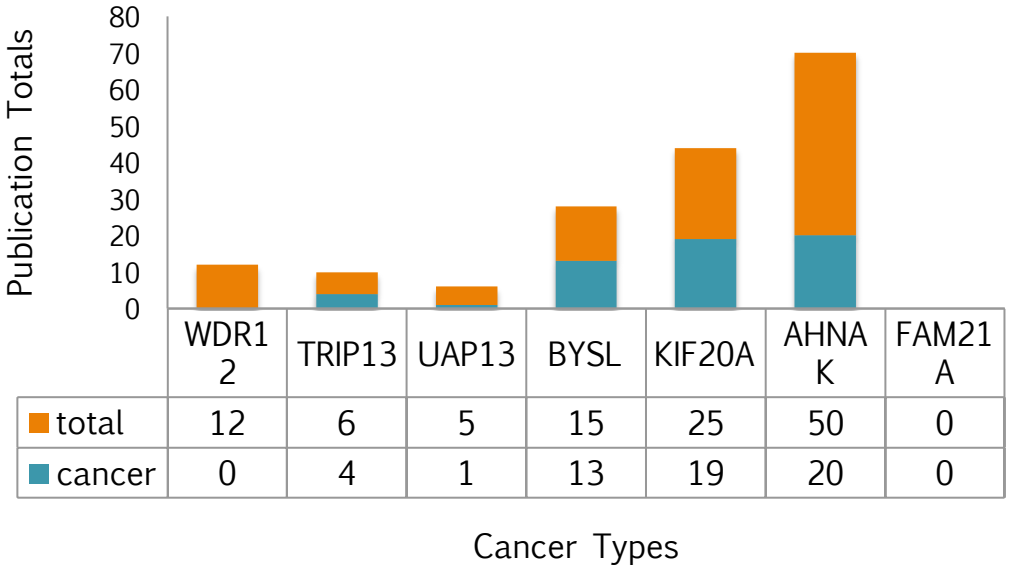

Figure 6.5. Stacked bar chart showing the number of publications for each gene (x7) selected for experimental investigation

Cancer related publications are indicated in blue and total publications (including cancer related) are show in in orange. All genes were selected in part due to their low publication number in line with the study aims of investigating novel regulators of disease processes.

Table 6.1. Table showing the 10 gene names, numerical IDs and identifiers of those genes selected for experimental investigation

Gene Name	Numerical ID	Identifier	Role
P53	N/A	gi|224485760	Experimental
SMG-1	N/A	gi|385139922	positive control
GFP	N/A	N/A	negative control
FAM21A	4	OX_Smed_1.0.01068	Experimental
KIF20A	7	OX_Smed_1.0.02695	Experimental
AHNAK	14	OX_Smed_1.0.03895	Experimental
WDR12	15	OX_Smed_1.0.03948	Experimental
TRIP13	81	OX_Smed_1.0.20272	Experimental
UAP1	83	OX_Smed_1.0.20407	Experimental
BYSL	87	OX_Smed_1.0.20673	Experimental

6.3.5 An injection, irradiation, cutting and observation regime was designed and implemented

A key study aim of the research carried out in this chapter was to determine the feasibility of upscaling the shielded irradiation RNAi experimental processes to facilitate the simultaneous investigation of multiple genes. The shielded irradiation assay itself had already achieved an upscale (as shown in chapters 3, 4 and 5) compared to the work published by Guedelhoefer *et al.* [70, 75]. However, in order to apply the assay to genome wide RNA-Seq datasets it is necessary to be able to process between 10 and 50 genes per round of

experiments. The potential bottlenecks and barriers to upscaling begin with the injection of DsRNA, the production of which on large scales is not a limiting factor for trained molecular biologists. However, injecting the animals is time consuming, and the consistency of DsRNA distribution into the gut is key. A standard 2-week injection regime was selected for the 10-gene experiment (see figure 6.5). After the final day of injections, animals were separated into samples based on their consequent experimental condition. Homeostatic samples were animals to which no further processes/manipulation was applied. Instead these animals were observed and imaged at 8 days after their last injection. Regeneration samples were amputated in 2 locations, anterior and posterior to the pharynx in accordance with standard planarian regeneration techniques. These animals were also observed, and imaged 8 days after their amputation. Finally the shielded irradiation sample set was exposed to 30 Gy of X-ray using the lead shielded described in Chapters 2 and 3. 24 hours after irradiation these animals were amputated just behind the eyes. An extreme anterior cut was decided upon so as to expand the migration field size. Behind the eyes specifically was selected because this cut would remove the eyes, allowing researchers to easily score regeneration

(defects) in part through the presence or absence of eye formation relative to controls.

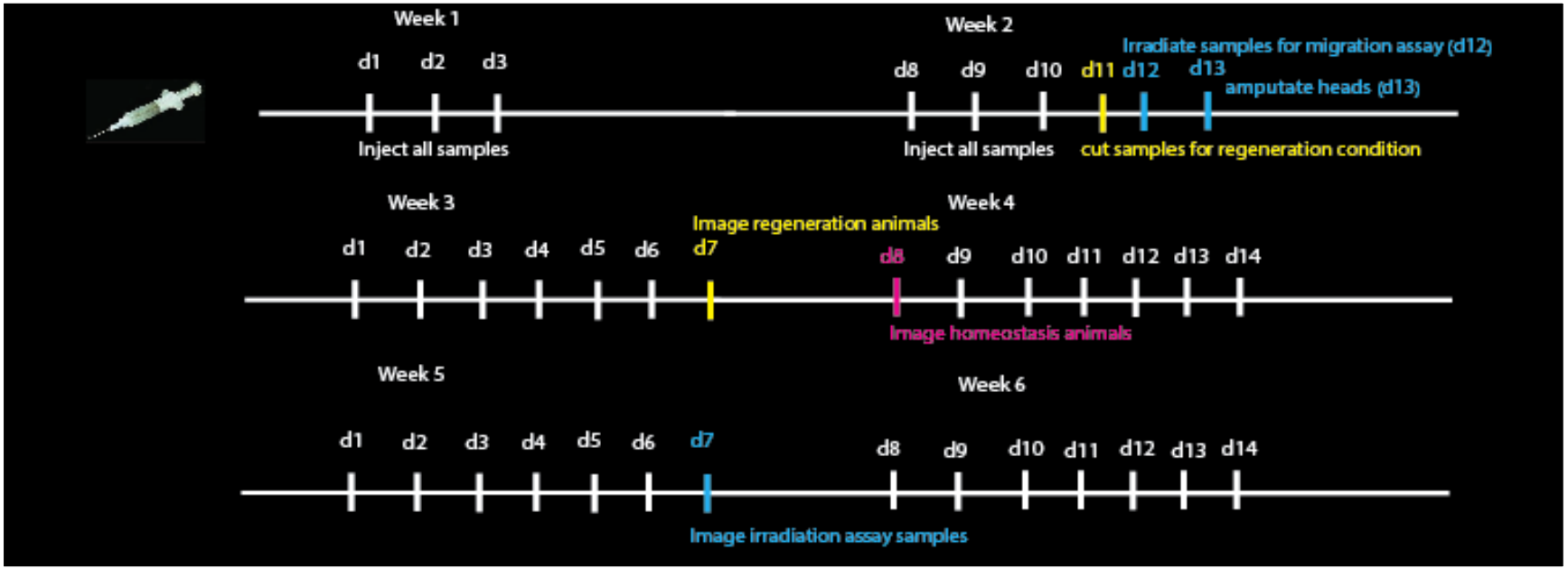

Figure 6.5. A diagrammatic representation of the experimental design for injection, cutting, irradiation and observations.

On days 1, 2, 3 and days 8, 9 and 10 animals were injected with DsRNA. On day 11, samples that were set aside to observe any possible RNAi effects on homeostasis, and others, in order to test for regeneration phenotypes, were amputated anteriorly. On day 12 of the experiment, remaining samples were irradiated using the shielded assay, and on day 13 a sub-selection of these samples underwent anterior amputation. All animals were observed and imaged over the proceeding weeks.

6.3.6 Knock down of Smed gene 83 (UAP1) produced a phenotype in homeostatic animals

Animals set aside for homeostatic observation were live imaged (Brightfield) at 9 days post injection (see figure 6.6). In this paradigm we saw that all animals for genes GFP, 4, 7, 14, 15, 81, 87, P53 and SMG-1 appeared normal. However animals from gene 83 from the Oncomine dataset exhibited severe head regression which in planarians is associated with impaired neoblast activity [2, 97]. Gene 83 labelled as the ortholog of UDP-N-acetylglucosamine pyrophosphorylase 1 (UAP1) which encodes a relatively understudied enzyme, which at the time of writing this had only 5 publications pertaining to it. One of the publications by Itkonen *et al.* [98] was cancer related. Itkonen *et al.* found that UAP1 (a prostate cancer specific gene) was involved in the N-linked glycosylation activity of the hexosamine biosynthetic pathway (HBP). The N-linked glycosylation of receptor proteins bound for cell membranes is known to facilitate their ultimate localisation. Proper glycosylation profiles of proteins serves to stabilise their presence within the cell membrane surface [99]. Consequently proteins such as the prostate cancer implicated androgen receptor (AR) when properly glycosylated are able propagate growth-promoting signals to cancer cells. UAP1 was found to protect the N-linked glycosylation process in cells from targeted inhibitors.

Although this single report is not adequate to explain the phenotype presented in planarians, it is possible that the absence of UAP1 as a result of DsRNA injection may have resulted in a reduction of intracellular glycosylation of proteins destined for the cell membrane. The outcome of which could be a breakdown in cell signalling pathways, and a cessation of cell growth and proliferation. In order to explore this hypothesis it would be necessary to carry out further experiments which allow us to observe the cell dynamics of UAP1 RNAi animals.

Figure 6.6. Brightfield observations of Oncomine RNAi animals from homeostasis subset.
These animals were injected for 2 weeks with the appropriate DsRNA, and were live imaged 9 days later. One gene from the Oncomine dataset at this time point shows a homeostatic phenotype, characterized by head regression. This gene was given the numerical identifier 83 to obscure the true gene names from the researchers. Later investigation identified the gene as UAP1 (UDP-N-acteylglucosamine pyrophosphorylase 1). UAP1 RNAi animals were removed from the subsequent planned regeneration and irradiation experiments. Scale bar represents 1mm (n=10).

6.3.7 Knockdown of smed genes 15 (WDR12) 81 (TRIP13) and 87 (BYSL) gives rise to observable phenotypes only after shielded irradiation

All animals from the traditional regeneration sample groups were found to be healthy, and regenerated when live imaged 8 days post-amputation, as seen in Figure 6.7. However animals exposed to irradiation when observed ~20 days post-irradiation were found to display regeneration defect phenotypes. From the GFP animals 90% had regenerated eyespots, and the same was observed for genes 4 (FAM21A) and 14 (AHNAK). 100% of samples from SMG-1 and gene 7 (KIF20A) RNAi had regenerated eyespots. Conversely genes 15 (WDR12), 81 (TRIP13), 87 (BYSL) and P53 had regeneration defects. All animals for genes 15, 81 and 87 had a 100% failure to regenerate rate. In all cases eyespots were absent, tail regression was visible, necrotic darkening of the epithelial skin layer was visible as was darkening of the tri-branching gut. Interestingly P53 animals displayed a delay in forming eyespots. All animals however did recover within 7 days (28 days post-irradiation).

The cause of the defects observed due to the three genes WDR12, TRIP13 AND BYSL cannot be determined from these experiments, and further experiments looking at the cell dynamics using FISH and immunohistochemistry are required. The three genes are relatively

understudied, and were selected in part for this reason (see figure 6.8). A brief literature search does proffer limited descriptions of what is known about each gene currently. As the aim of this research was to move away from a candidate gene selection approach, a brief summary is offered below:

1. WDR12 is a known member of the PeBoW nucleolar complex involved in ribosomal biogenesis[100]. An absence of WDR12 activity within the complex has been shown to result in the inhibition of rRNA maturation, and an accumulation of P53 in cells, which in turn triggers cell cycle arrest [100].
2. TRIP13 is a thyroid hormone receptor interactor. The AAA-ATPase TRIP13 overexpression is associated with malignancy in squamous cell carcinoma of the head and neck (SCCHN). Investigations carried out by Banerjee *et al.* [101] showed that TRIP13 overexpression lead to aggressive, treatment-resistant tumours with an advanced ability to repair DNA damage [101].
3. BYSL, the Bystin-like protein has been previously characterised to encode an accessory protein for cell adhesions in embryo implantation. However, Hanzhi *et al.* [102] found increased BYSL expression to be associated with hepatocellular carcinoma (HCC) cell proliferation and growth. *In vitro,* inhibition of BYSL by

hairpin RNA was shown to decrease cell proliferation, induce apoptosis and arrest the cell cycle in the G2 phase. *In vivo* experiments showed that HCC cells treated with BYSL siRNA failed to form tumours[102].

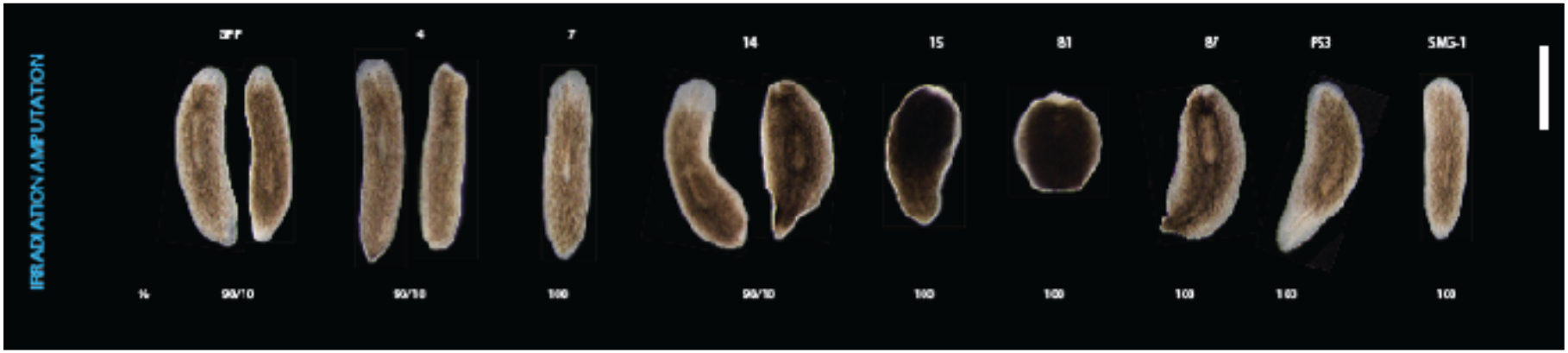

Figure 6.7 Brightfield observations of Oncomine RNAi animals from shielded irradiation subset.
24 hours post injection these animals were exposed to 30 Gys of irradiation to regions of their tissue not covered by the 1mm shield. 24 hours post irradiation these animals were amputated anterior to the pharynx and left to regenerate. 21 days post amputation the animals were imaged. In this paradigm 3 genes were shown to cause regeneration defects, characterized by a lack of regeneration. Genes 15, 81 and 87 were identified as encoding for WDR12 (Ribosome biogenesis protein), TRIP13 (thyroid hormone receptor interactor) and BYSL (Bystin like protein) respectively. Scale bar represents 2mm.

6.3.8 Smed genes UAP1, WDR12, TRIP13 and BYSL cluster according to their ascribed gene families in neighbour-joining trees

The sequence homology of the 4 genes that gave rise to phenotypes (UAP1, WDR12, TRIP13 and BYSL) was consequently manually tested by producing neighbour-joining trees (see figure 6.9 and table 6.2). In each case a variety of vertebrate and invertebrate sequences were taken and their nucleotide coding sequences were aligned. All 4 genes (UAP1, WDR12, TRIP13 and BYSL) clustered with other members of their gene family subtype. This analysis was carried out as a manual verification of bioinformatics approach in order to validate that the assigned gene names were indeed correct for future researchers. A list of the sequences used, along with their identifiers is also shown in Table 6.2.

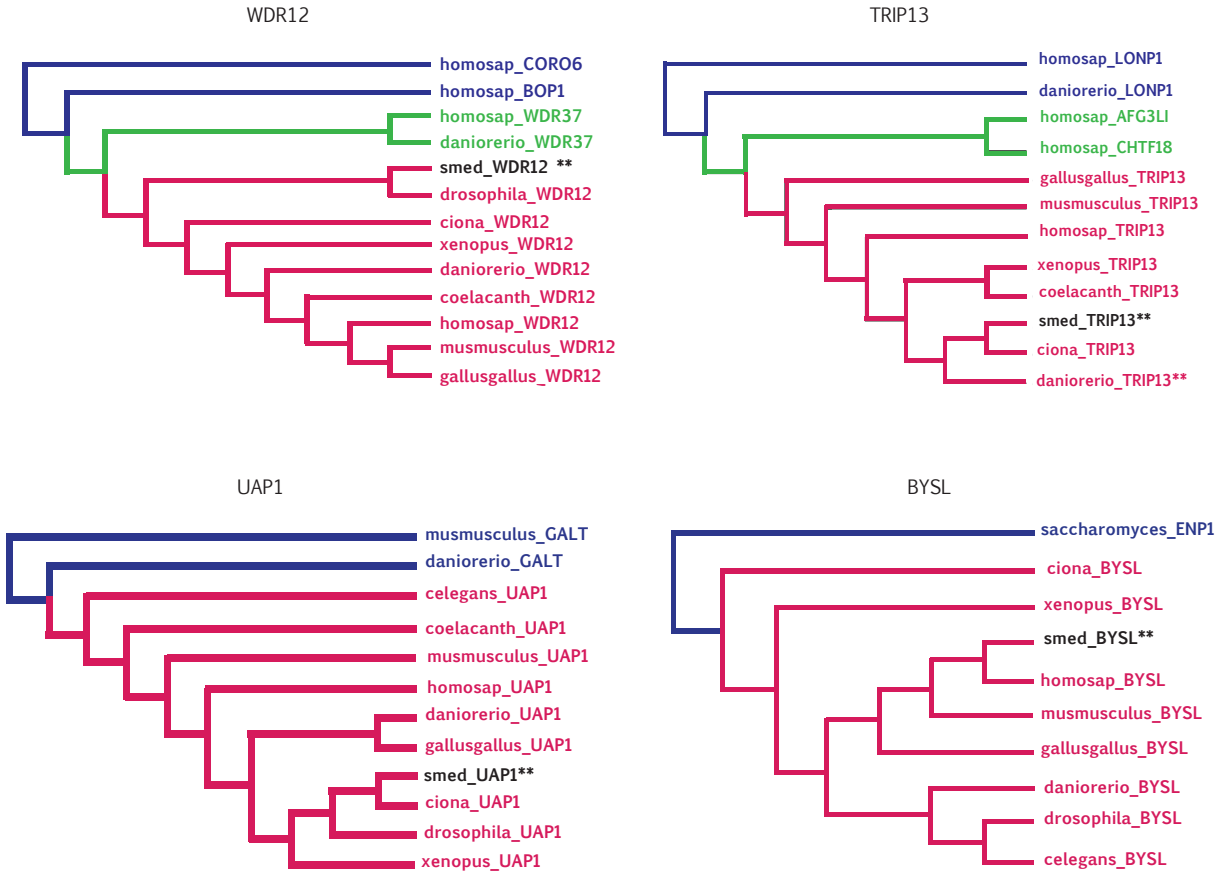

Figure 6.8. Phylogenetic trees for each of the 4 phenotype producing Oncomine associated smed transcripts (WDR12, TRIP13, UAP1 and BYSL). The nucleotide coding sequences (CDS) from a variety of vertebrate and invertebrate species were aligned. Trees were inferred using the neighbour-joining and Jukes-Cantor methods. In all cases the smed transcripts clustered members of their predicted families. The purple branches represent the tree root genes. Green branches indicate distantly related superfamily members. Magenta branches contain a representative selection of the proposed gene families (UAP1, BYSL, TRIP13 and WDR12). The list of identifiers for all sequences used for tree generation are available in Table 6.1 overleaf.

Table 6.2. Table listing the species, name and identifiers for all genes used in tree generation for WDR12, UAP1, TRIP13 and BYSL.

Name	Description
smed_BYSL	OX_Smed_1.0.20673
ciona_BYSL	ENSCING00000001646
Saccharomyces_ENP1	ENSCSAVG00000008659
zebrafish_BYSL	ENSDARG00000001057
drosophila_BYSL	FBgn0010292
c_elegans_BYSL	gi|5933138
human_BYSL	gi|51173723
xenopus_BYSL	gi|147901106
mouse_BYSL	gi|164698439
gallus_BYSL	gi|513225337
human_AFG3L1	gi|2956663
smed_TRIP13	OX_Smed_1.0.20272
ciona_trip13	ENSCINT00000036608
danio_trip13	gi|41053679
musmusc_trip13	gi|142350962
xenopus_trip13	gi|148229430
human_CHTF18	gi|157951660
human_trip13	gi|261337160
human_LONP1	gi|451327635
coelacanth_trip13	gi|557018976
danio_LONP1	gi|688607465
gallus_trip13	gi|758371904
c_elegans_UAP1predicted	c36a4.4
danio_GALT	gi|41055587
mouse_GALT	gi|700274116
smed_UAP1	OX_Smed_1.0.20407
drosophila_UAP1	ENA|JAC44202
ciona_UAP1	ENSCING00000009444
homosap_GALT	gi|12000350
zebrafish_UAP1	gi|47086790
xenopus_UAP1	gi|148236064
homosap_UAP1	gi|156627574
gallus_UAP1	gi|513196790
coelacanth_UAP1	gi|556973783
musmusc_UAP1	gi|758170407

smed_WDRlike	OX_Smed_1.0.03948
drosophila_WDR12	ENA|AY118871
danio_WDR12	gi|41054668
xenopus_WDR12	gi|60550932
homosap_WDR37	gi|71164896
homosap_WDR12	gi|217330643
human_CORO6	gi|255982619
danio_WDR37	gi|269914164
mus_WDR12	gi|312261270
Saccharomyces_WDR	gi|398366022
gallus_WDR12	gi|513194049
coelacanth_WDR12	gi|556986926
human_bop1	gi|733606096
ciona_WDR12	XM_002132024

6.4 Conclusions

The first use of the Oncomine web based microarray database to identify planarian orthologs for poorly annotated/understudied/novel cancer implicated genes. Consequent experiments are the first to use found orthologs for experimental investigation. This research identified 4 new phenotypic genes in planarians, all of which are previously unreported in planarians (WDR12, UAP1, TRIP13 and BYSL). UAP1 RNAi phenotype was observable in a post-injection homeostasis paradigm, however the regeneration defects associated with WDR12, TRIP13 and BYSL were only observed post-shielded irradiation. This work forms the foundation for consequent FISH experiments to characterise the underlying causes of the phenotypes. Ultimately the research presented

in this chapter demonstrates the potential for the planarian model, using the shielded irradiation assay, to be used for large scale screening of cancer implicated genes identified from RNA-seq datasets. This of particular interest to the cancer research community who are actively harvesting RNA-seq data in databases such as Oncomine. The purpose of which is to allow bio informaticians to analyse these data in order to identify novel candidate cancer implicated genes. The traditional paradigm of confirming the biological role of heavily studied genes (such as MMP and SNAIL) across phyla is of limited medical use. Instead by using the approach presented within this chapter it will be possible for researchers to investigate the functions of un studied genes with interesting expression profiles in cancer. The fundamental aim of which would be find new therapeutic targets for cancer therapies.

7. Concluding Remarks

7.1 Key Findings

In summary this body of work demonstrates that shielded irradiation can be up scaled to allow the simultaneous processing of multiple animals, and that this assay is useful for exploring the genetic regulators of cell (stem) cell behaviours associated with regeneration and cancer.

The work presented herein shows that a shielded irradiation assay can be used in planarians to observe RNAi effects, aiding in the identification of genes, which inhibit and accelerate cell migration and regeneration. These data are a crucial first step in demonstrating planarians as a model organism for cancer research.

This work provides key controls (SMG-1 and MMP), which will be essential in expanding the assays' use in future experiments that investigate novel gene regulators cancer implicated processes.

This research also found that the phenotypes which are otherwise undetectable (SNAIL, WDR12, TRIP13 and BYSL) can be seen using shielded irradiation, and that the identification of orthologs which in turn give rise to RNAi phenotypes is possible using the Oncomine web based microarray database.

Finally, the data presented herein demonstrates that the planarian model represents a potentially useful model organism for the cancer

research community and their scope for large-scale screening of RNA-Seq dataset.

7.2 Project Limitations

The planarian as a model organism is still in the early stages of development when compared to other model organisms. The obvious limitation to the system and consequently to all research associated with it, is the absence of transgenesis.

The establishment of transgenesis is a particularly important technique for studying regeneration, as it would allow for long-term cell fate tracing, as well as gene expression analysis, two important aspects of understanding regeneration of a mechanistic level. For example the availability of GFP transgenic animals is a valuable reagent for cell tracking experiments as it provides an indelible marking system with high spatial resolution that is visible in live animals.

GFP transgenic animals could also be used for transplantation experiments to observe cell behaviours from one environment (RNAi for example) to another.

Ultimately to expand the planarian as a model organism a systematic generation of transgenic animals is required so that better mechanistic details can be explored experimentally.

7.3 Future Directions

The work presented in this thesis was designed to form the foundation and platform from which larger experiments could be performed. Of particular interest is the continued investigation of non-candidate gene approaches to gene selection. This research demonstrates that a large RNA-Seq dataset can be filtered to produce positive experimental results. Consequently when considered with the assay up scaling developed in this thesis, future research is primed to carry out large-scale screens of cancer implicated genes in planarians with the potential to produce high impact research.

7.3.1 Oncomine Dataset

The remaining 200+ Oncomine genes with planarians orthologs should be tested for phenotypes. Researchers working in pairs could aim to inject 50 genes per round, and ultimately aim to have the brightfield live imaging observations of all 200+ genes within a matter of months. Expansion of this process to include FISH investigations of cell behaviour will result in the production of potentially useful list of cancer-implicated genes, validating *in vivo* using the planarian model. The ability to carry out screens relatively inexpensively, and quickly in planarians are key caveats in the promotion of planarians as a model organism for cancer research. Ultimately this work if completed could

be staged as a viable intermediary step between *in vitro* cell studies and expensive vertebrate ones.

7.3.2 RNA-Seq & Proteomics (See Figure 7.1)

Focusing on the SMG-1 accelerated migration/tumour phenotype to produce RNA-seq transcriptome data is another potentially lucrative avenue for the future of this research. I believe current projects in the Aboobaker lab aim to compare the transcript expression profiles of different RNAi profiles post shielded irradiation with specific focus on the migration field. The migration field is ~1mm of tissue that sits between the shielded stem cell niche and the anterior wound site. Upon wounding, migrating stem cells disperse directionally toward the wound and transiently repopulate the area. Isolating tissues from animals across conditions and comparing their transcript expression profiles will help identify genes for functional testing. Transcript expressions, which are unique to the migrating stem cell niche, and are stem cell expressed, will be interesting. By subtracting commonalities in expression between animals with and without migrating cell populations (wounded and unwounded respectively) a list of transcripts that are associated with *de novo* synthesized progeny and stem cells will be generated. This list of potential migration-associated genes will be compared to the expression profiles seen in

homeostatic animals. Identifying which of the genes are significantly differentially expressed between the two conditions will generate a second stage list of potential functional candidates, which can be additionally cross-referenced with *H2B* RNAi (stem cell RNAi) to provide insight as to whether the expression of any stem cell specific genes are gained or lost in the migration enriched tissues. Once candidates are selected, then functional testing using FISH and 3D spatial image analysis (Imaris Bitplane and R 'spatstat' software) can be used to test the hypothesis that these genes may regulate migration *in vivo.* For key molecule changes, which may not be detectable at the transcript level, proteomic investigations can be carried out. Proteomics will require the optimization of fractionation, digestion and dimethyl-labeling conditions to maximise protein detection. The approach selected involves the di-methyl labeling of 3 experimental conditions to identify differentially express proteins. This work can be carried out in collaboration with The Proteomics Facility, Oxford. The facility can provide expert advice on the use of isotopically labeled formaldehyde for di-methyl labeling and can perform fractionation procedures and LC MSMS for us to analyse the protein levels.

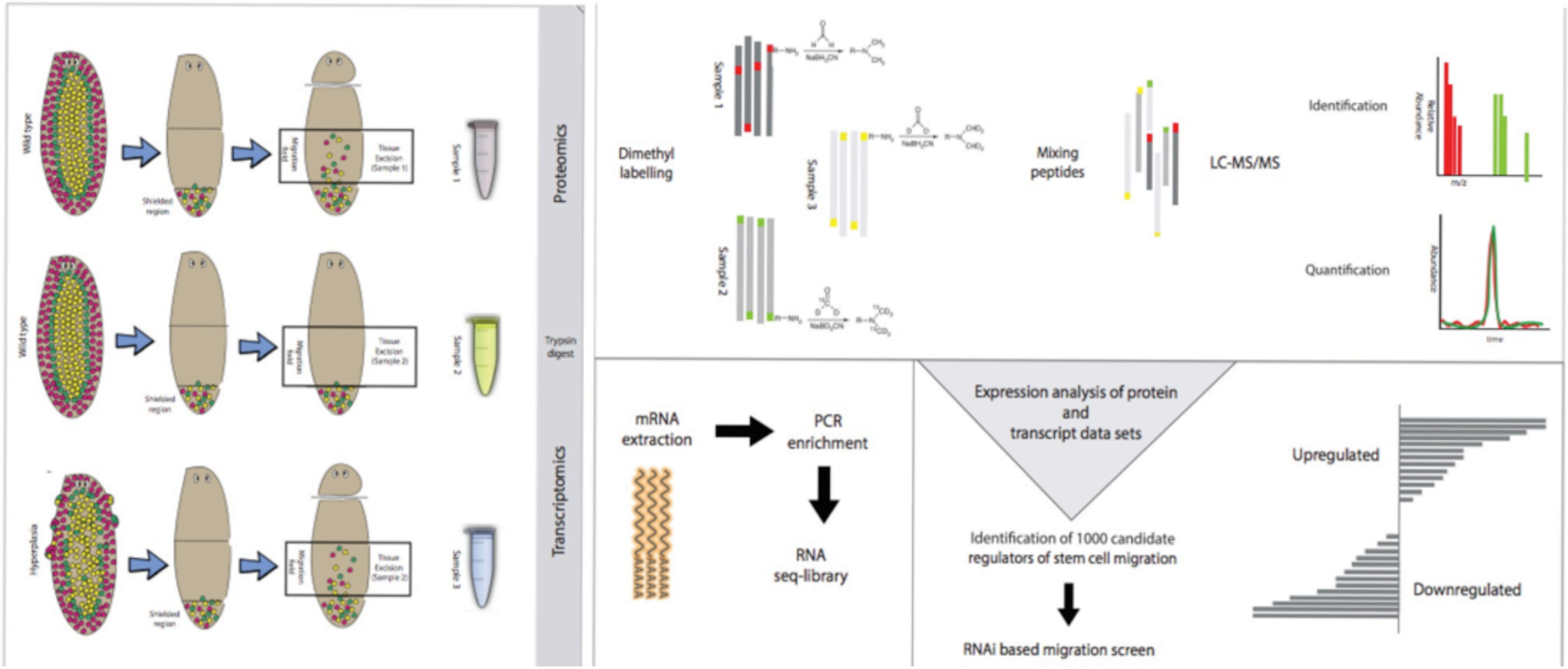

Figure 7.1 Diagrammatic representation of an expression based RNAi screen to identify key regulators of stem cell behaviour.

(a) We will prepare tissues from 'blank', 'migrating' and 'hyperplasic' 9smg-1 RNAi) tissues at key time points (b) These will be used to perform a dimethyl labelling based approach to assess protein expression levels and (c) an RNA-seq approach to express transcript expression levels. (d) these data will be analysed to identify candidate genes showing differential expression between samples and with conservation to mammalian genes. We will focus on conserved genes without known functions or only poorly described physiological functions. These genes will then be screened by RNAi to identify genes with roles in stem cell behaviour.

8. References

1. Jaber F. Epigenetics and Stem Cell Differentiation in Schmidtea mediterranea : The Role of a Methyl-CpG Binding Domain Gene. 2013(July).
2. Reddien PW, Bermange AL, Murfitt KJ, Jennings JR, Sánchez Alvarado A. Identification of genes needed for regeneration, stem cell function, and tissue homeostasis by systematic gene perturbation in planaria. *Dev Cell.* 2005;8(5):635-649.
3. Adoutte a, Balavoine G, Lartillot N, Lespinet O, Prud'homme B, de Rosa R. The new animal phylogeny: reliability and implications. *Proceedings of the National Academy of Sciences of the United States of America.* 2000;97(9):4453-4456.
4. Egger B, Gschwentner R, Rieger R. Free-living flatworms under the knife: past and present. *Development genes and evolution.* 2007;217(2):89-104.
5. Álvarez-Presas M, Baguñà J, Riutort M. Molecular phylogeny of land and freshwater planarians (Tricladida, Platyhelminthes): From freshwater to land and back. *Molecular Phylogenetics and Evolution.* 2008;47(2):555-568.
6. Lázaro EM, Harrath AH, Stocchino Ga, Pala M, Baguñà J, Riutort M. Schmidtea mediterranea phylogeography: an old species surviving on a few Mediterranean islands? *BMC evolutionary biology.* 2011;11:274-274.
7. Cebrià F, Newmark Pa. Morphogenesis defects are associated with abnormal nervous system regeneration following roboA RNAi in planarians. *Development (Cambridge, England).* 2007;134(5):833-837.
8. Cebrià F, Kudome T, Nakazawa M, et al. The expression of neural-specific genes reveals the structural and molecular complexity of the planarian central nervous system. *Mechanisms of development.* 2002;116(1-2):199-204.
9. MacRae EK. The fine structure of sensory receptor processes in the auricular epithelium of the planarian, Dugesia tigrina. *Zeitschrift für Zellforschung und mikroskopische Anatomie (Vienna, Austria : 1948).* 1967;82(4):479-494.
10. Carpenter KS, Morita M, Best JB. Ultrastructure of the photoreceptor of the planarian Dugesia dorotocephala. *Cell and tissue research.* 1974;148(2).
11. Hyman LH. *The Invertebrates: Platyhelminthes And Rhynchocoela The Acoelomate Bilateria vol II*: McGraw-Hill; 1951.
12. Rink JC, Vu HT-K, Sánchez Alvarado A. The maintenance and regeneration of the planarian excretory system are regulated by EGFR signaling. *Development (Cambridge, England).* 2011;138(17):3769-3780.
13. Scimone ML, Srivastava M, Bell GW, Reddien PW. A regulatory program for excretory system regeneration in planarians. *Development (Cambridge, England).* 2011;138(20):4387-4398.
14. Elliott SA, Sánchez Alvarado A. The history and enduring contributions of planarians to the study of animal regeneration. *Wiley interdisciplinary reviews Developmental biology.* 2013;2(3):301-326.
15. Reddien PW, Sánchez Alvarado A. Fundamentals of planarian regeneration. *Annual review of cell and developmental biology.* 2004;20:725-757.
16. Sánchez Alvarado A. Q&A: what is regeneration, and why look to planarians for answers? *BMC biology.* 2012;10:88-88.
17. Morgan TH. Experimental studies of the regeneration of Planaria maculata. *Archiv für Entwickelungsmechanik der Organismen.* 1898;7(2-3):364-397.
18. Newmark PA, Sa A. Regeneration in Planaria. 2001:1-7.
19. Baguna J. Regeneration and pattern formation in planarians formation. 1984;80:63-80.

20. Sanchez Alvarado A, Newmark PA. The use of planarians to dissect the molecular basis of metazoan regeneration 0 Hour. 1998:413-420.
21. Aboobaker A. Planarian stem cells: a simple paradigm for regeneration. *Trends in cell biology.* 2011;21(5):304-311.
22. Rink JC. Stem cell systems and regeneration in planaria. *Development genes and evolution.* 2013;223(1-2):67-84.
23. Baguñà J. The planarian neoblast: the rambling history of its origin and some current black boxes. *The International journal of developmental biology.* 2012;56(1-3):19-37.
24. Wagner DE, Wang IE, Reddien PW. Clonogenic Neoblasts Are Pluripotent Adult Stem Cells That Underlie Planarian Regeneration. *Science.* 2011;332(6031):811-816.
25. Eisenhoffer GT, Kang H, Sánchez Alvarado A. Molecular analysis of stem cells and their descendants during cell turnover and regeneration in the planarian Schmidtea mediterranea. *Cell Stem Cell.* 2008;3(3):327-339.
26. Galloni M. Global irradiation effects, stem cell genes and rare transcripts in the planarian transcriptome. *The International journal of developmental biology.* 2012;56(1-3):103-116.
27. Solana J, Kao D, Mihaylova Y, et al. Defining the molecular profile of planarian pluripotent stem cells using a combinatorial RNAseq, RNA interference and irradiation approach. *Genome biology.* 2012;13(3):R19-R19.
28. Hayashi T, Asami M, Higuchi S, Shibata N, Agata K. Isolation of planarian X-ray-sensitive stem cells by fluorescence-activated cell sorting. *Development, growth & differentiation.* 2006;48(6):371-380.
29. Onal P, Grün D, Adamidi C, et al. Gene expression of pluripotency determinants is conserved between mammalian and planarian stem cells. *The EMBO journal.* 2012;31(12):2755-2769.
30. Aboobaker AA, Kao D. A lack of commitment for over 500 million years: conserved animal stem cell pluripotency. *The EMBO journal.* 2012;31(12):2747-2749.
31. Reddien PW. Specialized progenitors and regeneration. *Development (Cambridge, England).* 2013;140(5):951-957.
32. Lapan SW, Reddien PW. dlx and sp6-9 Control optic cup regeneration in a prototypic eye. *PLoS genetics.* 2011;7(8):e1002226-e1002226.
33. Currie KW, Pearson BJ. Transcription factors lhx1/5-1 and pitx are required for the maintenance and regeneration of serotonergic neurons in planarians. *Development (Cambridge, England).* 2013;140(17):3577-3588.
34. van Wolfswinkel JC WD, Reddien PW. Single-Cell Analysis Reveals Functionally Distinct Classes within the Planarian Stem Cell Compartment. *Cell stem cell.* 2014;S1934-5909(14)00255-0. doi: 10.1016/j.stem.2014.06.007.
35. Forsthoefel DJ, James NP, Escobar DJ, et al. An RNAi screen reveals intestinal regulators of branching morphogenesis, differentiation, and stem cell proliferation in planarians. *Developmental cell.* Oct 16 2012;23(4):691-704.
36. Lehmann R, Nüsslein-Volhard C. The maternal gene nanos has a central role in posterior pattern formation of the Drosophila embryo. *Development (Cambridge, England).* 1991;112(3):679-691.
37. Wang Y, Zayas RM, Guo T, Newmark PA. nanos function is essential for development and regeneration of planarian germ cells. 2007;2007(32):1-6.
38. Reddien PW, Bermange AL, Murfitt KJ, Jennings JR, Sánchez Alvarado A. Identification of genes needed for regeneration, stem cell function, and tissue homeostasis by systematic gene perturbation in planaria. *Developmental cell.* 2005;8(5):635-649.

39. Wenemoser D, Lapan SW, Wilkinson AW, Bell GW, Reddien PW. A molecular wound response program associated with regeneration initiation in planarians. *Genes & Development.* 2012;26(9):988-1002.
40. Pearson BJ, Sánchez Alvarado A. A planarian p53 homolog regulates proliferation and self-renewal in adult stem cell lineages. *Development (Cambridge, England).* 2010;137(2):213-221.
41. González-Estévez C, Felix Da, Smith MD, et al. SMG-1 and mTORC1 act antagonistically to regulate response to injury and growth in planarians. *PLoS genetics.* 2012;8(3):e1002619-e1002619.
42. Oviedo NJ, Pearson BJ, Levin M, Sánchez Alvarado A. Planarian PTEN homologs regulate stem cells and regeneration through TOR signaling. *Disease models & mechanisms.* 2008;1(2-3):131-143; discussion 141.
43. Peiris TH, Weckerle F, Ozamoto E, et al. TOR signaling regulates planarian stem cells and controls localized and organismal growth. *Journal of cell science.* 2012;125(Pt 7):1657-1665.
44. Caron E, Ghosh S, Matsuoka Y, et al. A comprehensive map of the mTOR signaling network. *Molecular systems biology.* 2010;6:453-453.
45. Masse I, Molin L, Mouchiroud L, et al. A novel role for the SMG-1 kinase in lifespan and oxidative stress resistance in Caenorhabditis elegans. *PloS one.* 2008;3(10):e3354-e3354.
46. Brumbaugh KM, Otterness DM, Geisen C, et al. The mRNA surveillance protein hSMG-1 functions in genotoxic stress response pathways in mammalian cells. *Molecular cell.* 2004;14(5):585-598.
47. González-Estévez C, Felix DA, Rodríguez-Esteban G, Aboobaker AA. Decreased neoblast progeny and increased cell death during starvation-induced planarian degrowth. *The International journal of developmental biology.* 2012;56(1-3):83-91.
48. Fernandez-Taboada E, Moritz S, Zeuschner D, et al. Smed-SmB, a member of the LSm protein superfamily, is essential for chromatoid body organization and planarian stem cell proliferation. *Development.* 2010;137(9):1583-1583.
49. Guo T, Peters AHFM, Newmark PA. A Bruno-like gene is required for stem cell maintenance in planarians. *Developmental cell.* 2006;11(2):159-169.
50. Oviedo J, Jennings JR, Reddien PW, Jenkin JC, Sa A. SMEDWI-2 Is a PIWI-Like Protein That Regulates Planarian Stem Cells. 2005;310(November).
51. Palakodeti D, Smielewska M, Lu YC, Yeo GW, Graveley BR. The PIWI proteins SMEDWI-2 and SMEDWI-3 are required for stem cell function and piRNA expression in planarians. *RNA.* Jun 2008;14(6):1174-1186.
52. Solana J. Closing the circle of germline and stem cells: the Primordial Stem Cell hypothesis. *EvoDevo.* 2013;4(1):2-2.
53. Bonuccelli L, Rossi L, Lena A, et al. An RbAp48-like gene regulates adult stem cells in planarians. *Journal of cell science.* 2010;123(Pt 5):690-698.
54. Jaber-Hijazi F, Lo PJKP, Mihaylova Y, et al. Planarian MBD2/3 is required for adult stem cell pluripotency independently of DNA methylation. *Developmental biology.* 2013.
55. Scimone ML, Meisel J, Reddien PW. The Mi-2-like Smed-CHD4 gene is required for stem cell differentiation in the planarian Schmidtea mediterranea. *Development (Cambridge, England).* 2010;137(8):1231-1241.
56. Coward SJ. Chromatoid bodies in somatic cells of the planarian: observations on their behavior during mitosis. *The Anatomical record.* 1974;180(3):533-545.
57. Rouhana L, Vieira AP, Roberts-Galbraith RH, Newmark Pa. PRMT5 and the role of symmetrical dimethylarginine in chromatoid bodies of planarian stem cells. *Development (Cambridge, England).* 2012;139(6):1083-1094.
58. Kandul NP, Noor MaF. Large introns in relation to alternative splicing and gene evolution: a case study of Drosophila bruno-3. *BMC genetics.* 2009;10:67-67.

59. Tharun S. Chapter 4 Roles of Eukaryotic Lsm Proteins in the Regulation of mRNA Function. In: Jeon KW, ed. Vol 272: Academic Press; 2008: 149-189.
60. Quenault T, Lithgow T, Traven A. {PUF} proteins: repression, activation and mRNA localization. *Trends in cell biology.* 2011;21(2):104-112.
61. Salvetti A, Rossi L, Lena A, et al. DjPum, a homologue of Drosophila Pumilio, is essential to planarian stem cell maintenance. *Development (Cambridge, England).* 2005;132(8):1863-1874.
62. Wang Y, Stary JM, Wilhelm JE, Newmark Pa. A functional genomic screen in planarians identifies novel regulators of germ cell development. *Genes & Development.* 2010;24(18):2081-2092.
63. Aboobaker aA. Planarian stem cells: a simple paradigm for regeneration. *Trends in cell biology.* 2011;21(5):304-311.
64. Bonifer C, Hoogenkamp M, Krysinska H, Tagoh H. How transcription factors program chromatin—Lessons from studies of the regulation of myeloid-specific genes. *Seminars in Immunology.* 2008;20(4):257-263.
65. Fisher CL, Fisher AG. Chromatin states in pluripotent, differentiated, and reprogrammed cells. *Current Opinion in Genetics & Development.* 2011;21(2):140-146.
66. Meshorer E, Gruenbaum Y. NURD keeps chromatin young. *Nature cell biology.* 2009;11(10):1176-1177.
67. Schwartz YB, Pirrotta V. Polycomb complexes and epigenetic states. *Current Opinion in Cell Biology.* 2008;20(3):266-273.
68. Jaber-Hijazi F, Lo PJKP, Mihaylova Y, et al. Planarian MBD2/3 is required for adult stem cell pluripotency independently of DNA methylation. *Dev Biol.* 2013.
69. Geyer KK, Chalmers IW, Mackintosh N, et al. Cytosine methylation is a conserved epigenetic feature found throughout the phylum Platyhelminthes. *BMC genomics.* 2013;14:462-462.
70. Guedelhoefer OCt, Sanchez Alvarado A. Amputation induces stem cell mobilization to sites of injury during planarian regeneration. *Development.* Oct 2012;139(19):3510-3520.
71. King RS, Newmark PA. In situ hybridization protocol for enhanced detection of gene expression in the planarian Schmidtea mediterranea. *BMC developmental biology.* 2013;13:8-8.
72. Robb SM, Ross E, Sanchez Alvarado A. SmedGD: the Schmidtea mediterranea genome database. *Nucleic acids research.* Jan 2008;36(Database issue):D599-606.
73. Thompson JD, Higgins DG, Gibson TJ. CLUSTAL W: improving the sensitivity of progressive multiple sequence alignment through sequence weighting, position-specific gap penalties and weight matrix choice. *Nucleic acids research.* Nov 11 1994;22(22):4673-4680.
74. Hanahan D, Weinberg RA. Hallmarks of cancer: the next generation. *Cell.* 2011;144(5):646-674.
75. Guedelhoefer OCt, Sanchez Alvarado A. Planarian immobilization, partial irradiation, and tissue transplantation. *Journal of visualized experiments : JoVE.* 2012(66).
76. Pellettieri J, Fitzgerald P, Watanabe S, Mancuso J, Green DR, Sanchez Alvarado A. Cell death and tissue remodeling in planarian regeneration. *Developmental biology.* Feb 1 2010;338(1):76-85.
77. Isolani ME, Abril JF, Saló E, Deri P, Bianucci AM, Batistoni R. Planarians as a model to assess in vivo the role of matrix metalloproteinase genes during homeostasis and regeneration. *PloS one.* 2013;8(2):e55649-e55649.
78. Hanahan D, Weinberg RA. The hallmarks of cancer. *Cell.* Jan 7 2000;100(1):57-70.

79. Yamaguchi N, Mizutani T, Kawabata K, Haga H. Leader cells regulate collective cell migration via Rac activation in the downstream signaling of integrin beta1 and PI3K. *Scientific reports.* 2015;5:7656.
80. Nieto MA. The snail superfamily of zinc-finger transcription factors. *Nature reviews Molecular cell biology.* Mar 2002;3(3):155-166.
81. del Barrio MG, Nieto MA. Overexpression of Snail family members highlights their ability to promote chick neural crest formation. *Development.* Apr 2002;129(7):1583-1593.
82. Lin Y, Dong C, Zhou BP. Epigenetic regulation of EMT: the Snail story. *Current pharmaceutical design.* 2014;20(11):1698-1705.
83. Gras B, Jacqueroud L, Wierinckx A, et al. Snail family members unequally trigger EMT and thereby differ in their ability to promote the neoplastic transformation of mammary epithelial cells. *PloS one.* 2014;9(3):e92254.
84. Wu Y, Zhou BP. Snail: More than EMT. *Cell adhesion & migration.* Apr-Jun 2010;4(2):199-203.
85. Wang Y, Shi J, Chai K, Ying X, Zhou BP. The Role of Snail in EMT and Tumorigenesis. *Current cancer drug targets.* Nov 2013;13(9):963-972.
86. Liu ZC, Chen XH, Song HX, et al. Snail regulated by PKC/GSK-3beta pathway is crucial for EGF-induced epithelial-mesenchymal transition (EMT) of cancer cells. *Cell and tissue research.* Nov 2014;358(2):491-502.
87. Maseki S, Ijichi K, Tanaka H, et al. Acquisition of EMT phenotype in the gefitinib-resistant cells of a head and neck squamous cell carcinoma cell line through Akt/GSK-3beta/snail signalling pathway. *British journal of cancer.* Mar 13 2012;106(6):1196-1204.
88. Bonavida B, Baritaki S. Inhibition of Epithelial-to-Mesenchymal Transition (EMT) in Cancer by Nitric Oxide: Pivotal Roles of Nitrosylation of NF-kappaB, YY1 and Snail. *Forum on immunopathological diseases and therapeutics.* 2012;3(2):125-133.
89. Kudo-Saito C, Shirako H, Takeuchi T, Kawakami Y. Cancer metastasis is accelerated through immunosuppression during Snail-induced EMT of cancer cells. *Cancer cell.* Mar 3 2009;15(3):195-206.
90. Cavallo F, De Giovanni C, Nanni P, Forni G, Lollini P-L. 2011: the immune hallmarks of cancer. *Cell.* 2011;60(3):319-326.
91. Rowe RG, Li XY, Hu Y, et al. Mesenchymal cells reactivate Snail1 expression to drive three-dimensional invasion programs. *The Journal of cell biology.* Feb 9 2009;184(3):399-408.
92. Peinado H, Ballestar E, Esteller M, Cano A. Snail mediates E-cadherin repression by the recruitment of the Sin3A/histone deacetylase 1 (HDAC1)/HDAC2 complex. *Molecular and cellular biology.* Jan 2004;24(1):306-319.
93. Peinado H, Marin F, Cubillo E, et al. Snail and E47 repressors of E-cadherin induce distinct invasive and angiogenic properties in vivo. *Journal of cell science.* Jun 1 2004;117(Pt 13):2827-2839.
94. Martin TA, Goyal A, Watkins G, Jiang WG. Expression of the transcription factors snail, slug, and twist and their clinical significance in human breast cancer. *Annals of surgical oncology.* Jun 2005;12(6):488-496.
95. Rhodes DR, Kalyana-Sundaram S, Mahavisno V, et al. Oncomine 3.0: genes, pathways, and networks in a collection of 18,000 cancer gene expression profiles. *Neoplasia.* Feb 2007;9(2):166-180.
96. Rhodes DR, Yu J, Shanker K, et al. ONCOMINE: a cancer microarray database and integrated data-mining platform. *Neoplasia.* Jan-Feb 2004;6(1):1-6.
97. Guo T, Peters AHFM, Newmark PA. A Bruno-like gene is required for stem cell maintenance in planarians. *Dev Cell.* 2006;11(2):159-169.

98. Itkonen HM, Engedal N, Babaie E, et al. UAP1 is overexpressed in prostate cancer and is protective against inhibitors of N-linked glycosylation. *Oncogene.* Sep 22 2014.
99. Bektas M, Rubenstein DS. The role of intracellular protein O-glycosylation in cell adhesion and disease. *Journal of biomedical research.* Jul 2011;25(4):227-236.
100. Rohrmoser M, Holzel M, Grimm T, et al. Interdependence of Pes1, Bop1, and WDR12 controls nucleolar localization and assembly of the PeBoW complex required for maturation of the 60S ribosomal subunit. *Molecular and cellular biology.* May 2007;27(10):3682-3694.
101. Banerjee R, Russo N, Liu M, et al. TRIP13 promotes error-prone nonhomologous end joining and induces chemoresistance in head and neck cancer. *Nature communications.* 2014;5:4527.
102. Wang H, Xiao W, Zhou Q, et al. Bystin-like protein is upregulated in hepatocellular carcinoma and required for nucleologenesis in cancer cell proliferation. *Cell research.* Oct 2009;19(10):1150-1164.